

**FABRICATION AND CHARACTERIZATION OF SYNTHESIZED
NANO- / MICRO-SIZE POROUS HOLLOW SILICATE PARTICLES**

ナノ-/マイクロ-サイズ多孔質シリカ中空粒子の作製とその特性評価

by

RAYMOND V.RIVERA VIRTUDAZO

MARCH 2012

DOCTOR OF ENGINEERING

in

FRONTIER MATERIAL ENGINEERING



NAGOYA INSTITUTE OF TECHNOLOGY

NAGOYA 466 8555

JAPAN

**FABRICATION AND CHARACTERIZATION OF SYNTHESIZED
NANO- / MICRO-SIZE POROUS HOLLOW SILICATE PARTICLES**

ナノ・マイクロ・サイズ多孔質シリカ中空粒子の作製とその特性評価

MARCH 2012

RAYMOND V.RIVERA VIRTUDAZO

ABSTRACT

Hollow silicate particles have been attractive for the past decade especially from the chemist and material scientists because of their low density, large specific area, and high chemical with thermal stability. These unique characteristics can be potential applications in fillers, catalysis, separation, controlled release and photonic band gap materials which could be good for various industrial fields especially for nano-science application. So far, a variety of chemical and physical methods have been exploited to fabricate hollow silica particles. Such as, template synthesis and double emulsion method are extensively used. Hence, this dissertation only make used of two processes (template and double emulsion method) to fabricate, investigate, develop and innovate a more eco-friendlier approach in producing nano- and micro-size hollow silicate particles. This research work is particularly followed the principle of Fuji's (CRL, processing group) and Fujiwara's works in fabricating hollow silicate particles by template and double emulsion approach respectively. The study is mainly organized as follows

Chapter 1 is dedicated to a brief and general background of inorganic hollow particles especially hollow silicate particles including some conventional techniques and their various applications. Accordingly, established sets of delimitations for an eco-friendly approached in forming and achieving nano- and micro-size hollow silicate particles. Based on this delimitation, the goal of this study was conceptualized.

Chapter 2 describes a facile route in synthesizing nano- and micro-size hollow silicate particles with tunable shell thickness with unique anisotropic hollow shape by employing inorganic particles as template in conjunction via the sol gel method. The inorganic templates used were calcium rich-hydroxyapatite (CaHAp) nanoparticles (for

nano-size hollow) and calcium carbonate (CaCO_3) micro particles (for micro-size hollow) in fabricating hollow silicate particles. The physico-chemical properties of the hollow particles were characterized by scanning electron microscope (SEM), transmission electron microscopy (TEM), powder x-ray diffraction (PXRD), thermal gravimetric-differential thermal analysis (TG-DTA) and nitrogen adsorption/desorption analysis. The hollow silicate particles showed relatively stable anisotropic hollow shape with uniform shell wall thickness of silicate layers. In addition, the shell thickness and surface roughness have tendency to increase with the increase concentration of tetraethyl orthosilicate (TEOS) precursor in ethanol solution. As expected, unique anisotropic shape and size of the hollow silicate particles depend on the inorganic template used.

Chapter 3 describes the fabrication of hollow silicate particles with micro, meso and macroporous amorphous silicate shell wall. Here, two processes were used such as double template method for nano-size hollow silicate particles with micro/mesoporous shell wall (NSHPMSs) and double emulsion method for micro-size hollow silicate particles with meso/macroporous shell wall (PHSM). For NSHPMSs, CaCO_3 (nano-size:60 nm) were used as core-template and cetyltrimethylammonium bromide (CTAB) for silicate network template. While for PHSM, sodium polymethacrylate (water soluble polymer; Na-PA) was added into the aqueous solution of water₁/oil/water₂ (w_1ow_2) emulsion system with controlled parameters (emulsification rotational speed constant, fixed volume ratio and fixed surfactant ratio), modified (set-up) pressurized N_2 filtration and calcinations. Then, controlled hollow silicate microspheres with meso/macroporous shell were successfully prepared

Chapter 4 an initial investigation on the adsorption of cationic (CTAB,

cetyltrimethylammonium bromide) from aqueous solution onto nano-cube CaCO_3 particles under alkaline condition was studied. A series of batch experiment were performed to determine the sorption graph of CTAB to nano-cube CaCO_3 particles. The experimental studies were analyzed by TG-DTA weight loss (200°C to 400°C). The experimental data coincide to the reference model of typical adsorption isotherm of surfactant on solid oxide surfaces.

Chapter 5 investigates the fabrication of stable hollow calcium-silicate hydrate nanoparticles by template ammonia-hydrothermal approached using CaCO_3 nano-size particles as core-template. This simple process for the formation of a unique hollow calcium silicate (< 100 nm) nano-size particles, which was successfully prepared via the hydrolysis and condensation of tetraethylorthosilicate (TEOS), ammonia water (NH_4OH) and inorganic calcium silicate (CaCO_3) as template and then ammonia-hydrothermally treated. To understand the formation of hollow calcium-silicate hydrate nanoparticles the temperature reaction was varied at room temperature (RT), 90°C and 120°C . Then each reaction temperature was varied in aging time for 3 h, 9 h, 24 h and 10 d. This approached for the formation of new nano-size hollow calcium-silicates hydrates particles can be a good alternative for the application on nano-bioactive materials.

Finally, Chapter 6 furnishes the overall concluding remarks of the present work and the future directions for research. The technique presented in this study provides a good foundation for the various future applications of the hollow silicate particles especially for template and double emulsion approached.

TABLE OF CONTENTS

LIST OF FIGURES	xii
LIST OF TABLES	xxvii

CHAPTER 1 INTRODUCTION

1.1 Fabrication and application techniques of hollow inorganic particles.....	2
1.1.1 Sol-gel process	
1.1.2 Solid-core Template Method	
1.1.3 Soft-Template Method	
1.1.4 Ammonia-Hydrothermal-Template Method	
1.2 Common applications of hollow inorganic particles	12
1.3 Developing a facile route and innovative way in forming a hollow silicate particles	14
1.4 Thesis statement, organization and delimitation	15
References.....	18

CHAPTER 2 PREPARATION OF NANO – and MICRO-SIZE HOLLOW SILICATE PARTICLES (TEMPLATE METHOD)

2.1 Innovative template approach using Colloidal-Calcium rich-Hydroxyapatite nanoparticles (CaHAp) in fabricating unique shape nano-size hollow silicate particles	
2.1.1. Introduction.....	24

2.1.2. Starting materials and schematic outline	
2.1.2.1 Materials	
2.1.2.2 Preparations of spindle-shape hollow silicate nanoparticles	
2.1.2.3 Physico-chemical characterization	
2.1.3. Results and discussion	27
2.1.3.1. Crystallographic properties	
2.1.3.2. Morphological observation	
2.1.3.3. Thermal properties	
2.1.3.4. N ₂ adsorption / desorption properties	
2.1.3.5 Mechanism for the formation of unique nano-size hollow silicate particles	
2.1.4. Conclusion.....	36
References	38
Supporting information	41
2.2 Innovative template approach using Calcium Carbonate microparticles (CaCO ₃) in fabricating anisotropic shape micro-size hollow silicate particles	
2.2.1. Introduction.....	50
2.2.2. Starting materials and schematic outline	
2.2.2.1 Materials	
2.2.2.2 Synthesis of anisotropic micro-size hollow silicate particles	
2.2.2.3 Physico-chemical characterization	
2.2.3. Results and discussion	53

2.2.3.1. Crystallographic and Morphological properties	
2.2.3.2. Morphological observation at increasing TEOS and NH ₄ OH concentration	
2.2.3.3 Thermal properties	
2.2.3.4. N ₂ adsorption / desorption properties	
2.2.3.5 Mechanism for the formation of micro-size hollow silicate particles	
2.2.4. Conclusion.....	61
References.....	62
Supporting information.....	65

**CHAPTER 3 FABRICATION OF POROUS (MICRO, MESO and
MACROPOROUS) AMORPHOUS SHELL HOLLOW SILICATE
PARTICLES**

3.1 Nano-size hollow silicate particles with micro/mesoporous amorphous shell by double template approach using CaCO ₃ nanoparticles and Cetyltrimethylammonium bromide (CTAB) surfactant molecules	
3.1.1.Introduction.....	72
3.1.2. Starting Materials and schematic outline	
3.1.2.1 Materials	
3.1.2.2 Preparation of CaCO ₃ /CTAB/SiO ₂ with micro/mesostructure shell wall	
3.1.2.3 Fabrication of hollow silicate nano-size particles with micro/mesostructure shell wall (NSHPMSs)	
3.1.2.4 Physicochemical characterization	

3.1.3. Results and discussion	78
3.1.3.1. Morphological observation and thermal properties	
3.1.3.2. Small-angle X-ray pattern and N ₂ adsorption / desorption isotherm	
3.1.3.3. Possible scheme upon increasing TEOS, CTAB concentration and Temperature reaction	
3.1.3.4. General Plausible mechanism for the formation of wormhole pattern in NSHPMSs	
3.1.4. Conclusion.....	85
References.....	86
Supporting information.....	91
3.2 Micro-size hollow silicate particles with meso/macroporous shell wall by double emulsion approach with addition of sodium polymethacrylate (Na-PA) (water-soluble polymer).	
3.2.1. Introduction.....	105
3.2.2. Starting Materials and schematic outline	
3.2.2.1 Materials	
3.2.2.2 Synthesis of microsphere hollow silicate particles	
3.2.2.3 Physicochemical characterization	
3.2.3. Results and discussion	109
3.2.3.1 Morphological observation and Particle size distribution (PSD) analysis	
3.2.3.2. Crystallographic properties and Thermal properties	
3.2.3.3. N ₂ adsorption / desorption isotherm	

3.2.3.4. Probable mechanism for the formation of hierarchical porous hollow silicate micro-size sphere via double emulsion method	
3.2.4 Conclusion.....	116
References.....	117
Supporting information.....	119

**CHAPTER 4 INITIAL INVESTIGATION ON THE PRECIPITATE SAMPLE
FOR THE ADSORPTION OF CETYLTRIMETHYLAMMONIUM
BROMIDE ONTO CALCIUM CARBONATE NANO-CUBE
PARTICLES UNDER ALKALINE-AQUEOUS SOLUTION**

4.1 Introduction.....	125
4.2 Starting Materials and schematic outline	
4.2.1 Materials	
4.2.2 Preparation process for the adsorption of CTAB molecules onto CaCO ₃ nanoparticles under alkaline-aqueous solution	
4.2.3 Physicochemical characterization	
4.3 Results and discussion.....	132
4.3.1 Crystallographic and Morphological properties	
4.3.2 Raman and GCMS Analysis	
4.3.3 Thermal Analysis	
4.3.4 Relationship between heat change enthalpy of dehydration of CTAB and actual adsorption isotherm of the dried precipitate sample CTAB/CaCO ₃	
4.3.5 Plausible mechanism for the adsorption of CTAB molecules onto hydrophilic CaCO ₃ nanoparticles then form wormhole mesoporous pattern	

4.4 Conclusion	149
References.....	151
Supporting information.....	155

**CHAPTER 5 FACILE ROUTE IN FABRICATING STABLE AND COMPOSITE
SHELL HOLLOW SILICATE NANOPARTICLES BY
AMMONIA-HYDROTHERMAL PROCESS**

5.1 Introduction.....	159
5.2 Starting Materials and schematic outline	
5.2.1 Materials	
5.2.2 Synthesis of hollow calcium-silicate hydrate nanoparticles	
5.2.3 Physicochemical characterization	
5.3 Results and discussion.....	162
5.3.1 Structural analysis by X-ray diffraction pattern (XRD)	
5.3.2 Morphological observation	
5.3.3 Thermogravimetric analysis	
5.3.4 N ₂ adsorption / desorption isotherm and cavity space (pore size) distribution	
5.3.5 Mechanism of the hollow calcium-silicate hydrate nanoparticles	
5.4 Conclusion	173
References.....	174
Supporting information.....	177

CHAPTER 6 CONCLUDING REMARKS AND POTENTIAL

DIRECTION FOR FUTURE RESEARCH

6.1 Concluding remarks..... 181

6.2 Advantages and disadvantages of these approaches..... 183

6.3 Potential directions for future research..... 185

LIST OF PUBLICATIONS 188

ACKNOWLEDGEMENTS.....

LIST OF FIGURES

CHAPTER 1

- Figure 1.1 Typical Sol gel reaction Scheme.....3
- Figure 1.2 General schematic illustrations of anisotropic hollow particles using inorganic template approach..... 7
- Figure 1.3 A conceptual scheme of microcapsule formation by double emulsion ($w_1/o/w_2$) interfacial reactions9
- Figure 1.4 General illustration for the stabilization of hollow silicate particles by ammonia-hydrothermal template process..... 11

CHAPTER 2.1

- Figure 2.1.1 Process flow for the preparation/fabrication of the unique shape/nano-size hollow silicate particles using CaHAp nanoparticles (1.75 Ca/P slurry type) as template core.....26
- Figure 2.1.2 XRD pattern of (RAW) dried CaHAp powder as well as nano-size CaHAp powder encapsulated by (0.1 mL TEOS) SiO₂, (0.25 mL TEOS) SiO₂, (0.50 mL TEOS) SiO₂, (1.0 mL TEOS) SiO₂27
- Figure 2.1.3 Amorphous XRD pattern of synthesized samples with concentration (0.1 mL TEOS) SiO₂, (0.25 mL TEOS) SiO₂, (0.50 mL TEOS) SiO₂, (1.0 mL TEOS) SiO₂ after acid treatment..... 28
- Figure 2.1.4 XRD pattern of (a) raw CaHAp nanoparticles, (b) nano-size spindle –shape CaHAp encapsulated by (0.5 mL), (c) nano-size spindle shape hollow SiO₂..... 28

Figure 2.1.5 SEM images of nano-rod (spindle) shape CaHAp raw powder (a), and hollow SiO ₂ nanoparticles (b) with TEM images (c and d)	30
Figure 2.1.6 SEM (a) and TEM (b) images: Acid treated samples of nano-size hollow (0.5 mL TEOS) SiO ₂	30
Figure 2.1.7 Thermogravimetric analysis (TG) of (a) raw CaHAp nanoparticles, (b) nano-size spindle shape CaHAp encapsulated by (0.5 mL) SiO ₂ , (c) nano-size spindle shape hollow SiO ₂ nanoparticles	32
Figure 2.1.8 N ₂ adsorption and desorption isotherm and (inset) cavity (pore) size distribution (BJH method) of nano-rod (spindle) shape hollow (0.5 mL TEOS) SiO ₂ particles.....	33
Figure 2.1.9 Schematic illustration of the procedure for the synthesis of nano-size spindle-shape hollow SiO ₂ template with CaHAp nanoparticles	35
CHAPTER 2.1 Supporting information	
Figure 2.1S.1 XRD pattern of: (a) CaHAp standard reflection pattern [Ca ₁₀ (PO ₄) ₆ (OH) ₂], (b) CaHAp solution (dried), (c) CaHAp powder (standard sample).....	41
Figure 2.1S.2 XRD pattern after acid treatment exhibits amorphous phase (0.50 mL TEOS (●)) and (1.0 mL TEOS, (■))	42
Figure 2.1S.3 Particle size distribution of CaHAp`s solution (specific gravity of 1.001 – 0.999) at different ultrasonic time interval. Inset is the zeta potential of the CaHAp nanoparticles	43

Figure 2.1S.4 SEM images (bar line 100 nm): Acid treated samples of nano-size hollow (0.1 mL TEOS) (a), (0.25 mL TEOS) (b), (0.5 mL TEOS) (c), and (1 mL TEOS) (d)	44
Figure 2.1S.5 SEM images (bar line 100 nm): Acid treated samples of nano-size hollow (0.5 mL TEOS) magnified at (a) X100000, (b)X120000, (c) X140000 and (d) X230000	45
Figure 2.1S.6 STEM images (line bar 100 nm [a,b,c], while in [d] 10 nm): acid treated samples of nano-size hollow (0.5 mL TEOS) magnified at (a) X160000, (b)X45000, (c)X190000 and (d) X300000	46
Figure 2.1S.7 SEM (a) and TEM (b) images: Acid treated samples of nano-size hollow (0.5 mL TEOS) SiO ₂	47
Figure 2.1S.8 TEM images: Acid treated samples of nano-size hollow (0.5 mL TEOS) SiO ₂	47
Figure 2.1S.9 Nitrogen adsorption-desorption of nano-rod (spindles) shape CaHAp nanoparticles raw powder (■), core-shell CaHAp/SiO ₂ nanoparticles (●) and spindle-shape (rod) nano-size hollow silica particles (▲) synthesized at ambient temperature.....	48
Figure 2.1S.10 BJH differential pore size distribution nano-rod (spindles) shape CaHAp nanoparticles raw powder (■), core-shell CaHAp/SiO ₂ nanoparticles (●) and spindle-shape (rod) nano-size hollow silica particles (▲) synthesized at ambient temperature	49

CHAPTER 2.2

Figure 2.2.1 Process flow for the preparation/fabrication of the anisotropic micro-size hollow silicate particles using CaCO_3 microparticles as template core.....	52
Figure 2.2.2 XRD pattern of (a) CaCO_3 –raw, (b) as-synthesized CaCO_3 - SiO_2 and (c) amorphous anisotropic micro-size hollow SiO_2 particles (AMSHP)	54
Figure 2.2.3 SEM images of (a) micro-size CaCO_3 –raw and anisotropic micro-size hollow SiO_2 in (b) X300, (c) X800 and X1700 magnification	54
Figure 2.2.4 SEM images of anisotropic micro-size hollow SiO_2 particles at increasing TEOS & NH_4OH concentration (broken box: ideal formula for AMSHP)	55
Figure 2.2.5 TG (a)-DTA (b) monograph (ideal formula) of the synthesized anisotropic micro-size CaCO_3 - SiO_2 particles and hollow anisotropic SiO_2 microparticles	58
Figure 2.2.6 N_2 adsorption/desorption isotherm, inset is the corresponding pore-holes size distribution of the amorphous anisotropic micro-size hollow SiO_2	59
Figure 2.2.7 Schematic formation of anisotropic micro-size hollow silicate particles.....	60

CHAPTER 2.2 Supporting information

Figure 2.2S.1 SEM images of the anisotropic core-shell $\text{CaCO}_3\text{-SiO}_2$ particles with excess silica nanoparticles deposited in the amorphous SiO_2 shell wall.....	65
Figure 2.2S.2 SEM images of anisotropic hollow SiO_2 particles at X22000 (a), X2000 (b), X500 (c) and magnification with laser optical microscope image (d).....	66
Figure 2.2S.3 SEM images of anisotropic hollow SiO_2 particles at X450, X8500, X350, X2500 magnification showing the shell thickness of the amorphous shell	67
Figure 2.2S.4 SEM images of anisotropic hollow SiO_2 particles at (a) low ammonia concentration and (b) high concentration of ammonia showing the shell thickness of the amorphous shell with excess silica nanoparticles deposited on the surface shell.....	68
Figure 2.2S.5 SEM images of anisotropic hollow SiO_2 particles at increasing TEOS concentration and showing the shell thickness of the amorphous shell with excess silica nanoparticles deposited on the surface shell.....	69
Figure 2.2S.6 SEM images of a typical ideal anisotropic hollow SiO_2 particles and showing the shell thickness of the amorphous shell.....	70
Figure 2.2S.7 SEM images of a typical ideal anisotropic hollow SiO_2 particles and showing the thickness of the amorphous shell at increasing TEOS but low in ammonia concentration	71

CHAPTER 3.1

Figure 3.1.1 Process flow for the fabrication of micro/mesoporous shell wall hollow silicate nanoparticles by double template method (CaCO_3 nanoparticles/CTAB).....	76
Figure 3.1.2 (e) STEM, (f) Thermogravimetric data (TGA, weight loss %) and TEM images of (a) CSNSMSs (as synthesized); (b,c,d) NSHPMSs-T1 (acid fluxing); (d, inset) amorphous diffraction ring	78
Figure 3.1.3 (a) Small angle XRD pattern and (b) N_2 adsorption-desorption isotherm with pore size distribution (BJH method, inset) of NSHPMSs-T1 (acid fluxing)	81
Figure 3.1.4 Schematic illustration for the possible effect upon additional increase of TEOS (A), CTAB concentration (B) and higher temperature reaction (C).....	83
Figure 3.1.5 Schematic illustration for the formation of NSHPMSs.....	84

CHAPTER 3.1 Supporting information

Figure 3.1S.1 SEM images: (a) Nano-size CaCO_3 particles (raw), (b) (X100000) CaCO_3 coated with SiO_2 @CTAB as-synthesized (CSNSMSs) and nano-size hollow silicate micro/mesoporous shell (NSHPMSs) with different magnification at (c) X100000, (d) X200000.....	91
---	----

Figure 3.1S.2 (a) SEM images of CaCO_3 coated with $\text{SiO}_2@CTAB$ as synthesized (CSNSMSs) and STEM images of nano-size hollow silicate with micro/mesoporous shell (NSHPMSs) at increasing TEOS (vol) namely (b)NSHPMSs-T1;1 mL TEOS, (c) NSHPMSs-T2; 2mL TEOS and (c) NSHPMSs-T4;4 mL TEOS..... 92

Figure 3.1S.3 STEM images: After acid reflux, hollow silicate with micro/mesoporous shell (NSHPMSs) at increasing CTAB (wt.) (a) NSHPMSs- C0.12; 0.12 g, (b) NSHPMSs-C0.32; 0.32 g, (c) NSHPMSs –C0.42; 0.42 g and (d) NSHPMSs-C0.82; 0.82 g..... 93

Figure 3.1S.4 TEM images (a) CaCO_3 coated with $\text{SiO}_2 @CTAB$ as synthesized (CSNSMSs) and after acid reflux, hollow silicate with micro/mesoporous shell (NSHPMSs) at increasing TEOS (vol) (b) NSHPMSs-T1 , (c) NSHPMSs-T2 and (c) NSHPMSs-T4. 94

Figure 3.1S.5 TEM images: (a) CaCO_3 coated with $\text{SiO}_2 @ CTAB$ as-synthesized (CSNSMSs) and after acid reflux, hollow silicate with micro/mesoporous shell (NSHPMSs) at increasing CTAB (wt.) (b)NSHPMSs –C0.12, (c) NSHPMSs–C0.42 and (d) NSHPMSs –C0.82..... 95

Figure 3.1S.6 STEM/TEM images: hollow silicate with micro/mesoporous shell (NSHPMSs) at increasing temperature reaction (A) NSHPMSs-RT, (B) NSHPMSs-50 °C and (c) NSHPMSs-120°C (82°C). 96

Figure 3.1S.7 Thermogram (TG) and Differential Thermal Analysis (DTA) data of as-synthesized MESOEW (CSNSMSs; ■ TG; ● DTA) with acid-reflux hollow silicate with micro/mesoporous shell MESOEW (NSHPMSs; ▲ TG; ▼ DTA)	97
Figure 3.1S.8 Powder XRD pattern of as-synthesized CSNSMS (■; inset SEM image of CSNSMS-encapsulation of CaCO ₃ /SiO ₂ with CTAB) with acid-reflux hollow silicate with micro/mesoporous shell NSHPMSs (●; inset SEM image of amorphous NSHPMSs.)	98
Figure 3.1S.9 Powder Small angle XRD pattern of acid-reflux hollow silicate with micro/mesoporous shell (NSHPMSs); (a) increasing TEOS concentration (NSHPMSs-T1, NSHPMSs-T2 and NSHPMSs-T4); (b) increasing CTAB concentration (NSHPMSs C0.12, NSHPMSs-C0.52 and NSHPMSs-C0.82); (c) elevate temperature reaction (NSHPMSs-RT, NSHPMSs-75°C and NSHPMSs-120°C (82°C)).....	99
Figure 3.1S.10 Nitrogen adsorption-desorption isotherms (with enlarge view), hollow silicate with micro/mesoporous shell (NSHPMSs) at increasing TEOS (vol) (NSHPMSs-T1, NSHPMSs-T2 and NSHPMSs-T4).....	100
Figure 3.1S.11 Nitrogen adsorption-desorption isotherms (with enlarge view), hollow silicate with micro/mesoporous shell (NSHPMSs) at increasing CTAB concentration (NSHPMSs-C0.12, NSHPMSs-C0.52 and NSHPMSs-C0.82).....	101

Figure 3.1S.12 Nitrogen adsorption-desorption isotherms (with enlarge view), hollow silicate with micro/mesoporous shell (NSHPMSs) at increasing temperature reaction (NSHPMSs-RT, NSHPMSs-75°C and NSHPMSs-120°C (82°C)	102
---	-----

Figure 3.1S.13 Pore size distribution (PSD) curves of acid-reflux hollow silicate with micro/mesoporous shell (NSHPMSs); (a) increasing TEOS concentration (NSHPMSs-T1, NSHPMSs-T2 and NSHPMSs-T4); (b) increasing CTAB concentration (NSHPMSs-C0.12, NSHPMSs-C0.52 and NSHPMSs-C0.82); (c) elevate temperature reaction (NSHPMSs-RT, NSHPMSs-75°C and NSHPMSs-120°C (82°C)	103
---	-----

CHAPTER 3.2

Figure 3.2.1 Process flow for the preparation/fabrication of the meso/macroporous shell wall by double emulsion method with the addition of sodium polymethacrylate (Na-PA)	108
Figure 3.2.2 (a) ODM images, (b) SEM images calcined PSHM prepared by W ₁ P-X/O/W ₂ at increasing Na-PA.....	110
Figure 3.2.3 PSD graph with inset SEM images of calcined PSHM prepared by W ₁ P-X/O/W ₂ at increasing Na-PA.....	111
Figure 3.2.4 (a) Amorphous XRD pattern and (b) TG traces calcined PHSM prepared by W ₁ P-X/O/W ₂ method at increasing Na-PA	112

Figure 3.2.5 (a) N ₂ adsorption- desorption isotherms and (b) pore size distribution calculated by BJH method of calcined PHSM prepared by W ₁ P-X/O/W ₂ method at increasing Na-PA	113
--	-----

Figure 3.2.6 Conceptual scheme of the porous hollow silicate microsphere by W ₁ P-X/O/W ₂ interfacial reaction upon addition of Na-PA and calcinations. Inset: SEM images of the hierarchical surface structure hollow microsphere particles (W ₁ P-12/O/W ₂)	115
--	-----

CHAPTER 3.2 Supporting information

Figure 3.2S.1 Optical microscope images of calcined (w1P-0/O/w2) PHSM.....	119
Figure 3.2S.2 Optical microscope images of calcined (w1P-8/O/w2) PHSM.....	120
Figure 3.2S.3 Optical microscope images of calcined (w1P-12/O/w2) PHSM.....	120
Figure 3.2S.4 Optical microscope images of calcined (w1P-13/O/w2) PHSM.....	121
Figure 3.2S.5 SEM images of uncalcined and calcined (w1P-0/O/w2) PHSM.....	121
Figure 3.2S.6 SEM images of uncalcined and calcined (w1P-8/O/w2) PHSM.....	122
Figure 3.2S.7 SEM images of uncalcined and calcined (w1P-12/O/w2) PHSM.....	122
Figure 3.2S.8 SEM images of uncalcined and calcined (w1P-13/O/w2) PHSM.....	123
Figure 3.2S.9 TG/DTA micrograph of uncalcined (a,b) and calcined (c,d) PHSM samples NSHPMSs-120°C (82°C).....	124

CHAPTER 4

Figure 4.1 Process flow in preparing for the adsorption of CTAB molecules onto CaCO ₃ nanoparticles under alkaline condition.....	130
Figure 4.2 XRD pattern of raw CaCO ₃ nanoparticles with different CTAB concentration adsorp onto CaCO ₃ nanoparticles	132

Figure 4.3	SEM and TEM images of raw CaCO ₃ nanoparticles (a, e) with different CTAB concentration such as 23 mM CTAB (b), 35 mM CTAB (c), 88 mM CTAB (c and d) sample.	134
Figure 4.4	The C-H stretching region in the Raman spectra of CTAB adsorbed on CaCO ₃ nanoparticles from 0 mM CTAB-CaCO ₃ (raw material), 13.16 mM CTAB-CaCO ₃ and 88 mM CTAB-CaCO ₃	135
Figure 4.5	GC-MS analysis of ([a] 0.04 mM and [b] 5.67mM) CTAB/CaCO ₃ samples degradation temperature at (a.1 &b.1) 150 °C and (a.2 &b.2) 300 °C.....	137
Figure 4.6	Complete TG-DTA analysis of the CTAB adsorption at increasing concentration (mM) onto CaCO ₃ nanoparticles under alkaline condition.....	139
Figure 4.7	DTA (b) and TG (a) analysis at 25°C to 500°C CTAB adsorption at increasing concentration (mM) onto CaCO ₃ nanoparticles under alkaline condition	142

Figure 4.8 Relationship between (a) heat change of enthalpy of dehydration of CTAB, peaks (using DTA) vs adsorbed content of CTAB onto nano-cube CaCO₃ particles (using TGA). (inset (a), adsorption isotherm (general) and molecular model for four step adsorption models [22]. Then (b), relationship between weight loss of CTAB adsorp onto nanocube CaCO₃ nanoparticles vs original (NH₄⁺) -CTAB concentration with TEM/SEM images based on the previous results in Chapter 3. (inset (b) green mark is the assume calculated percentage amount of CTAB monolayer coated /adsorbed onto nanocube CaCO₃ nanoparticles and assume to be in region III marked at inset (a)). 144

Figure 4.9 Schematic illustration displaying morphologies that may form /occur during the adsorption of soluble cationic surfactant to a hydrophilic CaCO₃ nano-cube particle (substrate) (1d) and the formation of micro/mesoporous wormhole pattern on the surface of hydrophilic CaCO₃ nano-cube particle 146

CHAPTER 4 Supporting information

Figure 4.S 1 The Raman spectra (1800 – 200 cm⁻¹) of CTAB adsorbed on CaCO₃ nanoparticles from 0mM CTAB-CaCO₃ (raw material), 13.16mM CTAB-CaCO₃ and 88 mM CTAB-CaCO₃..... 155

Figure 4.S 2 GC-MS analysis of pure CTAB powder degradation product; (a) 150 °C and (b) 300 °C 156

Figure 4.S 3 DTA (b) and TG (a) analysis at 25°C to 500°C CTAB adsorption at increasing concentration (mM) onto CaCO₃ nanoparticles under alkaline condition 157

Figure 4.S 4 Theoretical calculation of full monolayer coverage of CTAB on CaCO₃ nanoparticles 158

CHAPTER 5

Figure 5. 1 Process flow for the synthesis of nano-size hollow calcium-silicate hydrate particles using CaCO₃ nanoparticles as template core.....162

Figure 5. 2 XRD pattern measured for (a) raw cubic calcite (CaCO₃) [RMHA]; (b) silica coated CaCO₃ nanoparticles without acid treatment [HS0dAH0]; (c) silica coated CaCO₃ nanoparticles hydrothermally treated for 10 d agitation at 90 °C [HS10d90H1] and (d) 120 °C without acid treatment [CS10d120H2].....163

Figure 5. 3 XRD pattern measured for (a) hollow silica nanoparticles after acid treatment [HS0dAH0ac]; (b) hollow silica nanoparticles process at 90 °C after acid treatment [HS10d90H1ac] and (c) hollow calcium-silicate hydrate nanoparticles process at 120 °C after acid treatment [CS10d120H2ac]. Inset, an image showing the reflection pattern of Ca(OH)₂ [Portlandite, (001)] and Ca₂SiO₄ [Larnite,(-101)].....164

Figure 5. 4 SEM images : (a) CaCO₃ raw (cubic) [RMHA] , (b) CaCO₃ coated with SiO₂ without hydrothermal [HS0dAH0] , (c) CaCO₃ coated with SiO₂ by hydrothermal at 90 °C for 10 d [HS10d90H1], (d) CaCO₃ coated with SiO₂ by hydrothermal at 120 °C for 10 d [CS10d120H2].....165

Figure 5. 5 SEM and TEM images: (a) [RMHA] CaCO₃ raw (cubic); Acid treated samples (b & e) [HS0dAH0ac] nano-size hollow SiO₂ without hydrothermal, (c & f) [HS10d90H1ac] nano-size hollow SiO₂ by hydrothermal at 90 °C for 10 d (d & g) [CS10d120H2ac] nano size hollow Ca(OH)₂-SiO₂ with hydrothermal at 120°C for 10 d.....167

Figure 5. 6 TG thermogram of the nano size hollow particles after acid treatment (a) hollow particles synthesized at ambient temperature [HS0dAH0ac], (b) hollow particles hydrothermally treated at 90 °C for 10 days [HS10d90H1ac], (c) hollow calcium-silicate hydrate nano particles hydrothermally treated at 120 °C for 10 d [CS10d120H2ac].....168

Figure 5. 7 Nitrogen adsorption-desorption isotherms (a to c) and BJH differential pore size distribution (d to f) of hollow particles synthesized at ambient temperature (HS0dAH0ac), hollow particles hydrothermally treated at 90 °C for 10 d (HS10d90H1ac) and hollow calcium-silicate hydrate nanoparticles hydrothermally treated at 120 °C for 10 d (CS10d120H2ac). (inset are the TEM images of the respective hollow particles)..... 170

Figure 5. 8 Schematic Illustration for the formation of Hollow Calcium-Silicate hydrate Nanoparticles..... 172

CHAPTER 5 Supporting information

Figure 5.S 1 TEM images: Acid treated samples (a) [HS0dAH0ac] nano-size hollow SiO₂ without hydrothermal, (b) [CS10d120H2ac] nano-sized hollow Ca(OH)₂-SiO₂ with hydrothermal at 120 °C for 10 d. 177

Figure 5.S 2 Nitrogen adsorption-desorption isotherms (a to c) and BJH differential pore size distribution (d to f) of hollow particles synthesized at ambient temperature (HS0dAH0ac), hollow particles hydrothermally treated at 90 °C for 10 d (HS10d90H1ac) and hollow calcium-silicate hydrate nano particles hydrothermally treated at 120 °C for 10 d (CS10d120H2ac).....	178
Figure 5.S 3 Enlarge XRD of hollow calcium-silicate hydrate nano particles hydrothermally treated at 120 °C for 10 d (CS10d120H2ac) ranging from (17.0 to 20.0) 2 θ	179
Figure 5.S 4 ²⁹ Si NMR spectra. The C-S-H peaks have chemical shifts approximately -78.9 ppm and -87.6 ppm [19].....	180

LIST OF TABLES

CHAPTER 2

Table 2.1.1 Characterization of the Nanostructure CaHAp/SiO ₂ particles and hollow SiO ₂ nanoparticles	34
--	----

CHAPTER 3.1 Supporting information

Table 3.1.S1 Characterization of NSHPMSs	104
--	-----

CHAPTER 4

TABLE 4.1 Concentration of CTAB, Surface adsorption amount, Enthalpy change and thermal transition temperatures of the CTAB coating/adsorption onto CaCO ₃ nanoparticles.	140
---	-----

CHAPTER 1

INTRODUCTION

CHAPTER 1

INTRODUCTION

Particles suspensions in liquid medium are mostly the basis for having surprising array of materials processes and applications in scientific with technological importance. The introduction of micro/nanostructure composite materials has extended the impact of particles by incorporating their functionality with the facile processing of synthetic polymer materials. Though in many cases, particles play the role of fillers or rheological modifiers and influence can be quantified thru features such as size density, volume fraction and shape

With the discovery of fullerenes and carbon nano-tubes, much of the research works in the last decade has been devoted for the preparation of micro/nanostructure hollow particles.[1-4]. In addition to dimensionality, hollow void interior structure deemed as second –generation two-level structural micro/nonmaterial's which may exhibits complex chemical composition but relatively simple structures and hierarchically constructed that may exhibit superior physico-chemical properties for various nano- science application[3, 4]. While the third-generation hollow micro/nano-materials with multilevel interior structures, having a complex interior architecture, spurred interest in the field of material science applications.

In this chapter, introduce the basic foundation and preparation for the fabrication of hollow micro/nanostructure particles. So far, several excellent articles have reviewed/published the progress of inorganic hollow micro/nano size particles with respect to architectural design and synthesis, layer-by-layer assembly, fabrication and bio-related applications, drug release [5-7]. The researcher overviewed some recent

developments in preparation and properties from inorganic materials hollow spheres and focusing on the materials preparation methodology.

1.1 Fabrication and common approaches in forming hollow inorganic particles

Hollow structure with nano/micro-size particles have attracted tremendous interest as a unique class of materials compared to other solid counterparts, due to their higher specific surface area, lower density and better permeation/penetration. Aided by modern technology, scientists have found that unique properties by downsizing from micro to nano-size structure of the hollow materials without changing their chemical composition but notably influence the performance of the materials.[7] Extensive researches have been done to evaluate an ideal and convenient synthesis procedure of hollow micro/nano-size particles under mild conditions. Common aspects are basically discuss provided with the following subject headlines: sol gel processing, solid template and soft template

1.1.1 Sol-gel process

The sol-gel process is a wet-chemical technique used for the fabrication of both glassy and ceramic materials. In this process, the sol (or solution) evolves gradually towards the formation of a gel-like network containing both a liquid phase and a solid phase. The precursors used in sol-gel processing consist of a metal or metalloid element surrounded by various reactive ligands. Metal alkoxides, such as aluminates, titanates and zirconates, are the most popular precursors because of their high reactivity towards water. The most widely used non-metal alkoxides are alkoxy silanes, such as tetramethoxysilane (TMOS) and tetraethoxysilane (TEOS). Although ethyl groups are the most common alkoxy groups, methoxy, propoxy, butoxy and other long-chain hydrocarbon alkoxy groups are also used in alkoxy silanes. Metal alkoxides

(organometallic compounds) are commonly used in the sol-gel process either alone or in combination with non-metal alkoxides such as TEOS or alkoxyborates. The basic structure or morphology of the solid phase can range anywhere from discrete colloidal particles to continuous chain-like polymer network.[8, 9]

A well studied alkoxide is silicon tetraethoxide, or tetraethyl orthosilicate (TEOS). The chemical formula for TEOS is given by: $\text{Si}(\text{OC}_2\text{H}_5)_4$, or $\text{Si}(\text{OR})_4$ where the alkyl group $\text{R} = \text{C}_2\text{H}_5$. Alkoxides are ideal chemical precursors for sol-gel synthesis because they react readily with water. The reaction is called hydrolysis, because a hydroxyl ion becomes attached to the silicon atom. [10] The process consists of a series of hydrolysis and condensation reactions of an alkoxide, which proceed according to the reaction scheme shown in Figure 1.1

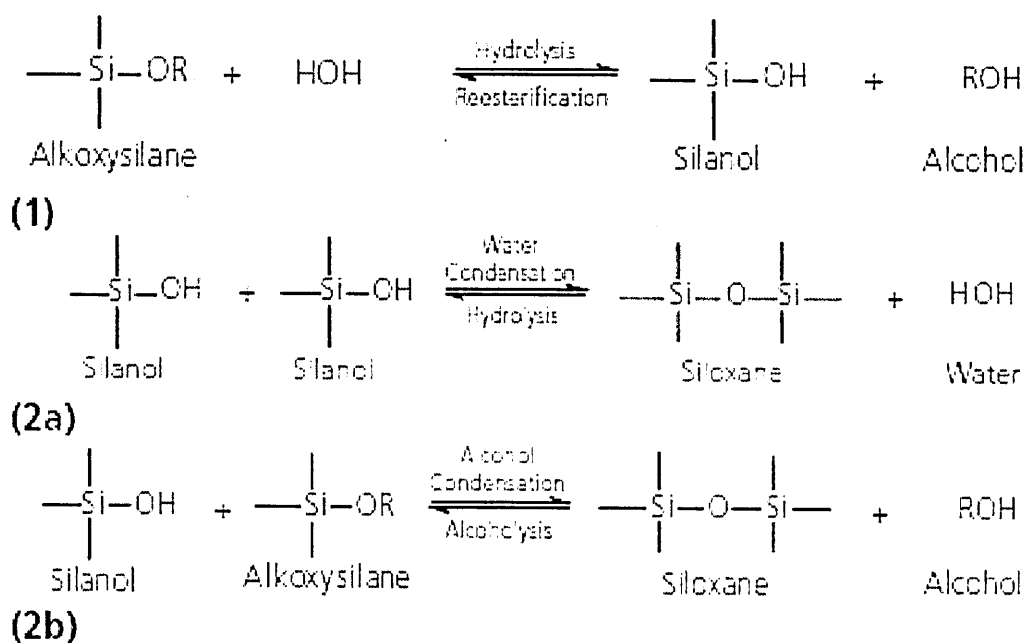


Figure 1. 1 Typical Sol gel Reaction Scheme [10]

Here, alkoxy silanes are used as an example but all of the metal alkoxides react similarly. Wherein hydrolysis and condensation reactions of most metal alkoxides can

be carried out without catalyst because of the extremely fast rates of reaction, alkoxysilanes hydrolyze much more slowly, requiring the addition of either an acidic or basic catalyst. Hydrolysis is initiated by the addition of water to the silane solution under acidic, neutral, or basic conditions. Thus, polymerization is associated with the formation of dimensional network of siloxane [Si–O–Si] bonds accompanied by the production of H-O-H and R-O-H species.

By definition, condensation liberates a small molecule, such as water or alcohol. This type of reaction can continue to build larger and larger silicon-containing molecules by the process of polymerization. Thus, a polymer is a huge molecule (or macromolecule) formed from hundreds or thousands of units called monomers. The number of bonds that a monomer can form is called its functionality. Polymerization of silicon alkoxide, for instance, can lead to complex branching of the polymer, because a fully hydrolyzed monomer $\text{Si}(\text{OH})_4$ is tetra functional (can branch or bond in 4 different directions). Alternatively, under certain conditions (e.g., low water concentration) fewer than 4 of the OR or OH groups (ligands) will be capable of condensation, so relatively little branching will occur. The mechanisms of hydrolysis and condensation, and the factors that bias the structure toward linear or branched structures are the most critical issues of sol-gel science and technology.[8, 9, 11, 12]

Thereby, sol-gel process has been frequently employed in coating the colloidal core-templates followed by forming hollow particles by removing templates. It is a simple reaction that does not require exotic materials, catalysts or expensive deposition equipment. Likewise, sol-gel reactions do not employ extreme reaction conditions. The reactions take place at room temperature and require only moderate temperatures to 'cure' the gel, removing the water/alcohol that the reaction generates. The properties of

the materials prepared using sol gel approaches are easy to modify by utilizing an organically modified alkoxide or a variable arm metalloid (for example, an alkoxyborate instead of an alkoxy silane).

The micro/nano size hollow particles are commonly obtained through self-assembly using surfactants because it provides superior control over nucleation and crystal growth., however is not so popular because of its poor control over phase purity and morphology.

Hence treatment of hollow particles is performed by colloidal-template synthesis.[6, 13] In template route, the inner diameter/shape of hollow particles is only determined by the dimensions of the kind of template (organic[14, 15], inorganic[16-18] and biomolecules[19]) used. Basically, these templates syntheses are divided into two parts namely hard and soft template syntheses in fabricating hollow particles with homogeneous, dense shell wall layers.

In this chapter, an overview of the common preparation and properties from inorganic materials hollow particles. The discussion is focused on the solid-template (known as solid-Cores Template Method) and soft-template (ex. double emulsion Method).

1.1.2 Solid- Core Template Methods

A template in a colloid core-particle is probably mostly effective and universal method for the preparation of hollow particles, especially requiring a narrow size distribution, for example, self-assembly and photonic crystals [6, 20, 21]. In the solid -template assisted synthesis, poly(styreneacrylic acid) (PSA) and polystyrene (PS) latex, silica spheres and CaCO_3 particles are commonly used as colloidal templates for their readily available in a wide range of size.[5, 7, 22] Technically, desired inorganic

precursor is first coated over the core-template either by physical or chemical reaction interaction to provide an intermediate called organic-inorganic hybrid materials containing core shell structure. The core-template particles were subsequently removed by selective dissolution in an appropriate solvent or by calcination at elevated temperature in air to generate hollow particles.[3, 23] Majority of these hollow micro/nanostructures are formed on outer surfaces of templates through sol-gel [24, 25], hydrothermal treatment [26], layer-by-layer [4, 27] and direct chemical deposition[5].

For instance, Tissot et al [28, 29] worked on the synthesis of composite particles with PS as the core and silicate as the shell via an ammonia-catalyzed sol-gel process. A hollow silica spheres were obtained thru a subsequent step by thermal degradation of the PS cores at 600 °C. Similarly, Zhong et al[1, 30, 31] prepared titania coated PS beads by templating the sol-gel precursor solution against crystalline PS beads. This was immersed in toluene to dissolve the PS template to obtain mesoscale titania hollow spheres. While the group of Imhof et al [31] presented a one-step method to coat cationic polystyrene spheres with titania precipitated during the hydrolysis of a titanium alkoxide. This core-shell particle turned into spherical hollow titania shells by dissolution of the polystyrene cores in suspension or by calcination of the dried particles in a furnace. Also by means of a plasma technique, the surfaces of monodisperse PS colloids have been modified with hydroxyl groups. The research works done by Li et al[32] use these surface-modified PS spheres as sacrificial template to fabricate silica-coated PS and titania-coated PS composites by co-condensation between hydroxyl groups with tetraethyl orthosilicate (TEOS) and titanium(IV) isopropoxide (TIPP) in a sol-gel process, respectively. The hollow silica and titania can be generated by the subsequent removal of the PS core using tetrahydrofuran. Although the above

mentioned works were very interesting, the preparation processes seem to be time-consuming, expensive and not eco-friendly approach.

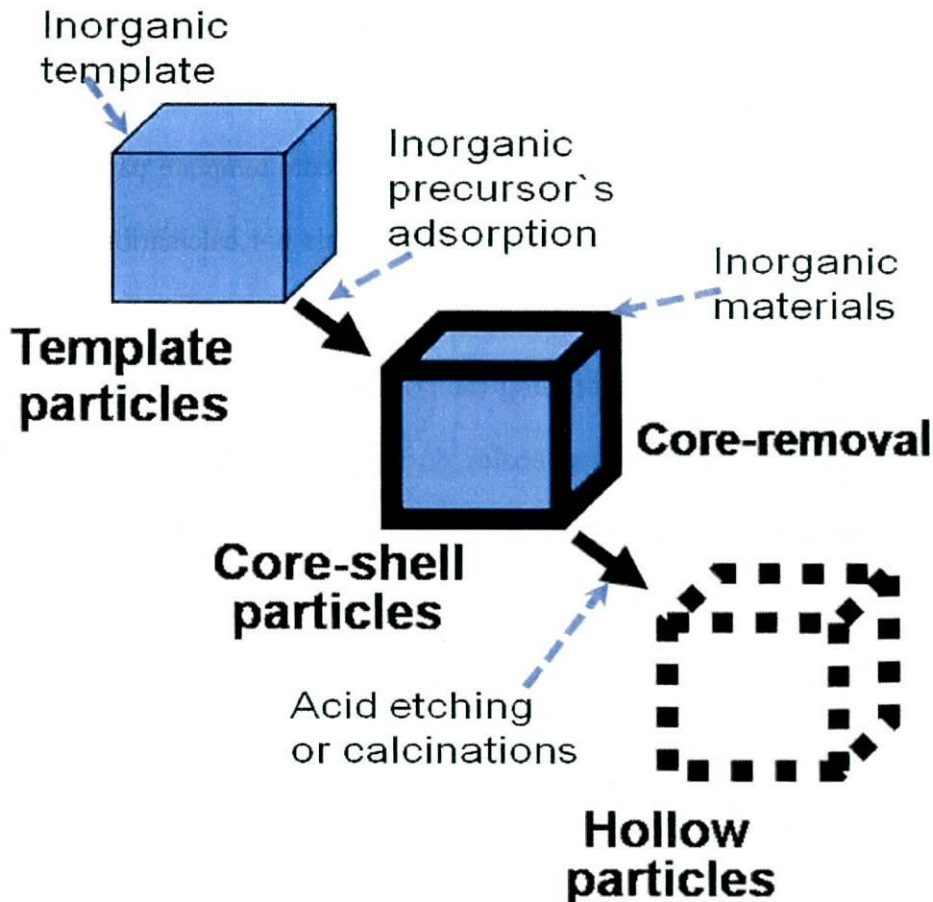


Figure 1. 2 General schematic illustration of anisotropic hollow particles using inorganic template approach.

Simple eco-friendly step processes are needed for the synthesis of hollow particles. Such as the reports done by Fuji et al[33, 34], removing the nano-core CaCO_3 particles by dissolution into acid solvent followed by the formation of nano-size hollow silica particles via template sol-gel process. In this method, aqueous ammonia solution was used as the catalyst and medium. The naturally positively charged CaCO_3 nanoparticles were dispersed into the ethanol (EtOH) solution followed by sonicating for 10 min. In this manner, ensures the generation of silicate sol from the hydrolysis and

the condensation of TEOS. This rapidly captured by CaCO_3 particles via electrostatic interaction in aqueous ammonia solution either in room or elevated temperature. Under acid conditions, CaCO_3 particles were “dissolved” subsequently and even synchronously to directly formed silica hollow particles, as shown in Figure 1.2. The formation of the inorganic shells and the dissolution of core template particle occurred during acid dissolution; neither additional toxic chemicals nor calcination process was used to remove the CaCO_3 cores [34, 35]

With solid template (hard), refilling the hollow interior with functional species or in situ encapsulations of guest molecules during the formation of shells, though possible, is still demanding. Also fabricating a macroporous in the shell wall of hollow microsphere particles is still challenging. These difficulties have prompted to a simpler approaches for producing hollow microsphere with macroporous shell that can easily encapsulate and release guest species. Among these approaches, templating against soft (liquid or gaseous) templates has attracted significant progress especially for emulsion approach. The next section will discuss the essential concept of soft templating and discussed the basic concept of the double emulsion method. These studies established the potential of the soft template method to create an interior space and a functional shell structure through a one-pot synthesis.

1.1.3 Soft Template Method

The soft template synthesis is another simple and general method for obtaining hollow particles. Some hollow particles with nanometer to micrometer diameter have been successfully fabricated using double emulsion process.[36]

Water-in-oil-in-water (W/O/W) double-emulsion system consists of individual oil globules that contain smaller droplets of the internal aqueous phase and are dispersed

in an external aqueous phase. Because of their special internal structure, double emulsions have found significant applications in many areas, such as pharmaceuticals, foods, cosmetics and separations [37-40]. Double emulsions are typically formed through two-emulsification processes, *i.e.*, by first emulsifying the inner droplets in the middle fluid, and then undertaking a second emulsification step for the dispersion [5, 40, 41]

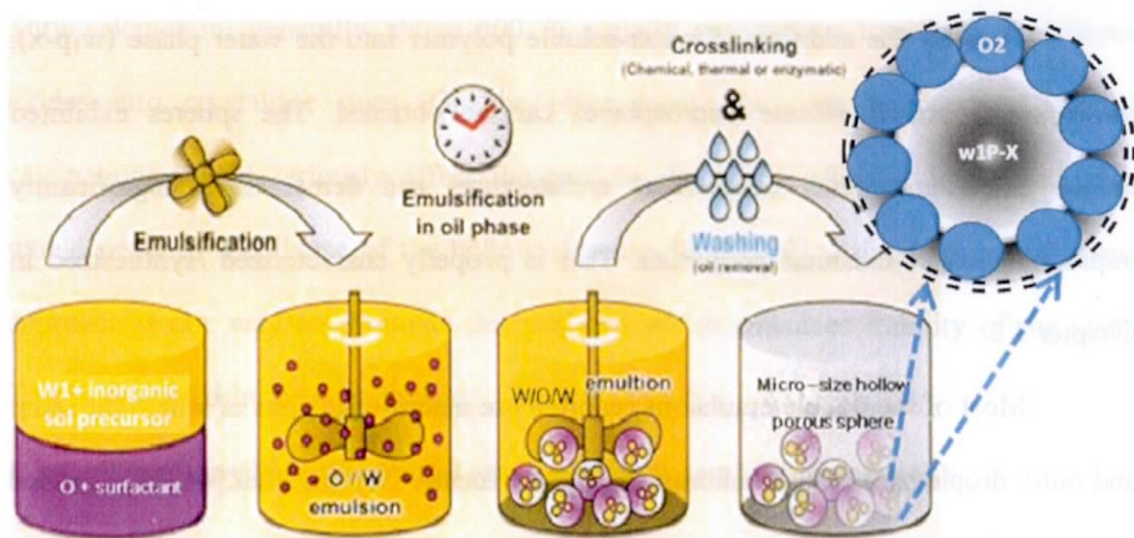


Figure 1. 3 A conceptual scheme of microcapsule formation by double emulsion (w_1Ow_2) interfacial reactions.

Basing from Fujiwara et al. [36, 42, 43], in the case of silica microspheres, the reaction of sodium silicate with a precipitant is utilized. W_1/O emulsion is made of W_1P-X (consist of water and sodium silicate) and O (oil phase) with surfactant for stabilizing emulsion. Then W_1P-X/O is added to another aqueous solution of a precipitant W_2 , forming $w_1p-x/o/w_2$ emulsion system. During the elimination of the oil phase (O) between the two water phases (w_1p-x and w_2), these two aqueous solution are mixed to form silica precipitate along the emulsion interface. The sodium silicate of W_1P-X is providing interfaces forming silicate particles (silicate precipitate). After

complete formation of the precipitate on the interfaces, all sodium silicate is consumed and the inside of the microcapsule is fulfilled with only water. This water is readily removed by drying treatment thru the pores of the silica shell. Finally silica microcapsules (silica hollow sphere) with vacant inside are obtained. In this process no other process to remove the core compound are necessary. This is schematically illustrated as shown in Figure 1.3.

Then by the addition of water-soluble polymer into the water phase (w_1p-x), macroporous hollow silicate microspheres can be obtained. The spheres exhibited unique three-dimensional hierarchical architectures and demonstrated significantly improved physico-chemical properties. This is properly characterized /synthesized in Chapter 3.2.

Most of the double emulsions reported are macro-emulsions of which the inner and outer droplets are both in micron scale. But recently Deming *et al.*[44, 45] reported a nano-scale double emulsion was formed, in which both oil droplet and internal aqueous droplet are in nano-meter size. The ultrasonic and micro-fluidic homogenization was utilized to induce the formation of nano-scale double emulsion, which was stabilized by specially designed amphiphilic diblock copolypeptide surfactants. This opens up the way to prepare double nano-emulsion. Another approach such as micro-fluidic device [46-48] and electric field [49, 50] were also developed to make double emulsions.

To develop simple, effective, controllable, and environmentally benign methods to form hollow microspheres by double emulsions remains challenging and is of great importance. In this thesis, the researcher utilized the works of Fujiwara to fabricate macroporous hollow silicate microspheres with addition of water soluble

polymer and some innovation inters of pressure filtration for faster processing.. This method has some unusual advantages. For example, it is very simple, green, and the formation of double emulsions can be controlled the microsize through emulsion rate speed.

Generally, template sol-gel process involves uncontrollable fast hydrolysis and condensation, and resulted to the formation of amorphous inorganic oxides.[51, 52] Thru calcination, generally above 500 °C usually required to transform amorphous oxides into crystalline ones. On the other hand, the high temperature thermal calcinations would seriously affect the particle size and surface structure and even would result in a collapse of the hollow structure.[5, 13, 22]. Ammonia-hydrothermal approach is one way to eliminate this problem which enhances stability of the shell. This is discussed in the next section.

1.1.4 Ammonia-Hydrothermal-Template (Other template approach)

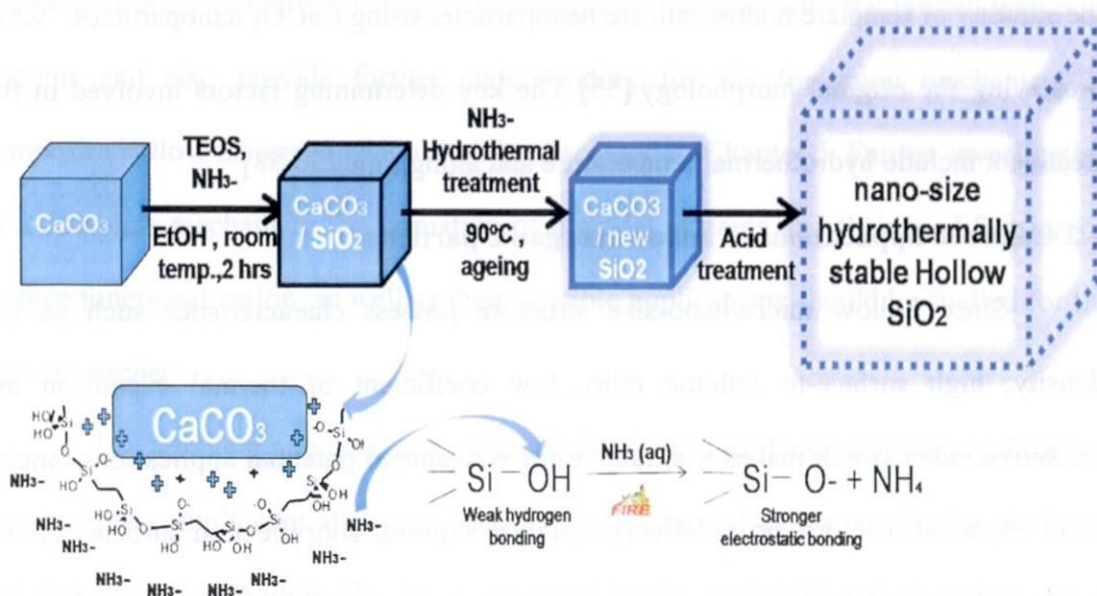


Figure 1. 4 General Illustration of stabilization of hollow silicate particles by ammonia-hydrothermal template process.

Hollow particles of crystalline metal oxides can be synthesized in a simple one-pot synthesis via a hydrothermal approach. Adding metal salts directly to the carbohydrate solutions in water, followed by a hydrothermal treatment and then calcination, hollow particles of various metal oxides, such as Fe_2O_3 , Ni_2O_3 , Co_3O_4 , CeO_2 , MgO , and CuO , were obtained.[53, 54]

By ammonia- hydrothermal treatment provides a facile and convenient method for refining the structural order and pore size uniformity of the acid-made mesoporous silica synthesized from different quaternary ammonium surfactants and acid sources. The post-synthesis treatment provokes transformation of silica wall (S)-interactions within the microstructure from the weaker (X) hydrogen bonding ($\text{S}^+\text{X}^-\text{I}^0$) to the stronger electrostatic (S^+I^-) interactions which is illustrated in Figure 1.4. Such treatment resulted in an increase in both thermal and hydrothermal stability. Recently, the researcher introduced a post-synthesis ammonia hydrothermal treatment to improve the stability of template hollow silicate nanoparticles using CaCO_3 nanoparticles while preserving the original morphology.[55] The key determining factors involved in this treatment include hydrothermal temperature and aging time.[56-58]

1.2 Common applications of hollow inorganic particles

Since hollow micro/nano-size structure possess characteristics such as low density, high surface-to volume ratio, low coefficient of thermal expansion and refractive index which makes it attractive for widespread potential applications ranging from chemical reactors, drug delivery, catalyst support, antireflection surface coating, lightweight materials, for rechargeable batteries and various new application fields.[7, 13, 59] A good example is macro-porous hollow silicates particles good electrode materials for lithium ions [60-62].

With extensive development of hollow particle synthesis, it greatly helps tune the optical properties, catalytic properties and superparamagnetic behaviour [5, 6, 22, 52, 63, 64]. As previously mention, hollow micro/nano-size particles are good for storage and charge carriers [36, 61, 65-69]. For instance, hollow silicates particles has been extensively studied for biomedical applications technically like drug/gene delivery because of its biocompatibility, non-toxicity and well-established in terms of bioconjugation methods using silane chemistry [5, 69-72]. Generally, it has the ability for adsorption and release of sensitive materials such as fluorescent and drug markers aside from well-known catalytic applications [6, 59, 73, 74]. Moreover, drug molecules can be loaded into the cavity and on the surface of the hollow structure and typically release over living cells wherein it can control the amount rate of drugs by altering the pore dimensions and wall structures [5, 22, 37, 74, 75]

In this research, the results briefly provide a new method for an alternative synthetic strategy to fabricate unique hollow silicate particles with stable shell wall pore systems and also provide further understanding for the formation mechanism of composite hollow materials which shall be discussed in Chapter 5. Further investigation of a complete mechanism for formation of bimodal systems and their modification by surface functionalization, as well as their possible applications should be studied for the next researcher.

The template approach can be easily implemented. However, the capability of constructing complicated structure, such as macro-through-holes connecting the inner and outer spaces of hollow structures, is limited by the availability of a template. As an alternative, it is important to develop a range of comprehensive template free methods, hopefully having the same flexibility as the existing template-assisted techniques, to

meet new technological requirements.[5-7, 24] Hopefully based on the different template mechanisms, one could developed and synthesize hollow particles with more complicated structure in a simple approach.

1.3 Developing a facile route and innovative way in forming hollow silicate particles.

A lot of significant achievements have been made in this area, as reviewed in this paper. Nevertheless, there are still some challenges that need to be fulfilled. Syntheses of complicated structure such as controlling the size/shape, sphere-in-ellipsoidal and cage-like surfaces in a hollow particle are just in its initial stage. It is anticipated that solid template and soft template/free template technique will play a greater role in future fabrication of complicated structure. The functional use of hollow structures is closely correlated with their morphological properties such as the exterior shape, the interior space, and the shell structure. To increase the permeability and create the ability to store bio-macromolecules and nanoparticles, it is desirable to build large through-holes on the shells of inorganic hollow structures, which deteriorates the mechanical strength of the hollow spheres. The simultaneous achievement of a robust hollow architecture and improved large molecule permeability in a environmentally friendly approach is still remains a challenge

Hence, micro/nanostructure hollow silicate particles are interesting not only because of their superior interior void structures, but also for a few more important reasons as mentioned previously. Generally, the successful creation of these micro/nano-scopic materials itself is a proud representative of the advancement of modern synthetic technology. Thus, it is very helpful to deepen to understand the mechanism for the formation of micro/nanostructure hollow particles, which will

encourage designing more and more novel structure. Also, compared with bulk micro/nano-material, the micro/nano-scopic hollow interior spaces with multiphase interfaces might cause a number of variations in the physico-chemical properties, reinforce interfacial effects and control the local chemical microenvironment that can bring a lot of potential applications.[5-7, 73, 74, 76]

1.4 Thesis statement, organization and delimitations

The main goal of this thesis is to establish an eco-friendly and innovative way/condition in fabricating nano- and micro-size hollow silicate particles by template core (solid) and double emulsion (soft) approach. Consequently, the parameter conditions are varied such as reaction temperature, aging time, tetraethyl orthosilicate (TEOS) concentration, surfactant concentration and water soluble polymer (sodium polymethacrylate) concentration to optimized the fabrication of hollow silicate particles. As part of this study, the effect of template-ammonia hydrothermal approached is investigated in order to confirmed formation of a novel-type stable hollow calcia-silicate nanoparticles material. This thesis is likely to contribute a facile approach in the area of fabricating hollow particles, which presents a simple, innovate way and an eco-friendly process for the formation of hollow silicate particles.

The thesis is organized as follows:

In Chapter 2, explicates the facile route in synthesizing nano- and micro-size hollow silicate particles with tunable shell thickness and unique anisotropic hollow shape by employing inorganic particles as template in conjunction with the sol gel method. The inorganic templates used were hydroxyapatite (HAp) nanoparticles (for nano-size hollow) and calcium carbonate (CaCO_3) micro particles (for micro-size hollow) in fabricating hollow silicate particles. The hollow silicate particles showed

relatively stable anisotropic hollow shape with uniform shell wall thickness with silicate layers. In addition, the shell thickness and surface roughness have tendency to increase with the increase concentration of tetraethyl orthosilicate (TEOS) precursor in ethanol solution. As expected, unique anisotropic shape and size of the hollow silicate particles depend on the inorganic template used.

In Chapter 3, give details on the fabrication of hollow silicate particles with micro, meso and macroporous amorphous silicate shell wall. Here, two processes were used such as double template method for nano-size hollow silicate particles with micro/mesoporous shell wall (NSHPMSs) and double emulsion method for micro-size hollow silicate particles with meso/macroporous shell wall (PHSM). For NSHPMSs, CaCO_3 (nano-size:60 nm) as core-template and cetyltrimethylammonium bromide (CTAB) for silicate network template were used. While for PHSM, sodium polymethacrylate (water soluble polymer; Na-PA) was added into the aqueous solution of water₁/oil/water₂ (W_1OW_2) emulsion system with controlled parameters (emulsification rotational speed constant, fixed volume ratio and fixed surfactant ratio), modified (set-up) pressurized by N_2 filtration and then calcination. Then, controlled hollow silicate microspheres with meso/macroporous shell were successfully prepared

In Chapter 4, investigate the physic-chemical properties of the precipitate sample cationic cetyltrimethylammonium bromide (CTAB) adsorp onto the nanocube CaCO_3 particle (NcCP) in an aqueous ammonia rich (NH_4^+) solution. Based on the results of Raman Spectroscopy (RS), GC-MS and TGA/DTA analysis, only CTAB molecules was presently absorb onto the NcCP and the increase of surface area confirms the formation of CTAB@ CaCO_3 nanoparticles. Interestingly by TEM images, CTAB layers was partially identified onto the surface of NcCP. Generally, adsorption of CTAB molecules

onto NcCP under aqueous alkaline medium had no effect on the cubic crystal structure, particle size morphology and moderate effect on the surface area. Presently, it confirms the adsorption mechanism of cationic surfactant onto NcCP colloids model and contributes to the better understanding on the sorption and structural arrangement of sorbed surfactant onto the NcCP–aqueous alkaline interface. This investigation is expected to create new, low cost route to produce promising nanopowders and conversion to hollow particles with multicomponent porous surface shell.

In Chapter 5, examine the fabrication of stable hollow calcia-silicate nanoparticles by template ammonia-hydrothermal approached using CaCO_3 nano-size particles as core-template. This simple process for the formation of a unique hollow calcium silicate (< 100 nm) nano-size particles, which was successfully prepared via the hydrolysis and condensation of tetraethylorthosilicate (TEOS), ammonia water (NH_4OH) and inorganic calcium silicate (CaCO_3) as template and then ammonia-hydrothermally treated. To understand the formation of hollow calcia-silicate nanoparticles the temperature reaction was varied at room temperature (RT), 90 and 120 °C. Then each reaction temperature was varied in aging time for 3 h, 9 h, 24 h and 10 d. This approached for the formation of new nano-size hollow calcium-silicates particles can be a good alternative for the application on nano-bioactive materials.

Finally, in Chapter 6, the concluding remarks of the present work were stated and the future directions of this research work were recommended.

References

- [1] Y. Xia, B. Gates, Y. Yin, Y. Lu, Monodispersed Colloidal Spheres: Old Materials with New Applications, *Advanced Materials* 12 (10) (2000) 693-713.
- [2] Y. Xia, P. Yang, Y. Sun, Y. Wu, B. Mayers, B. Gates, Y. Yin, F. Kim, H. Yan, One-Dimensional Nanostructures: Synthesis, Characterization, and Applications, *Advanced Materials* 15 (5) (2003) 353-389.
- [3] F. Caruso, A. Caruso, H. ohwald, Nanoengineering of inorganic and hybrid hollow spheres by colloidal templating, *Science* 282 (1998) 1111 - 1114.
- [4] F. Caruso, Hollow Capsule Processing through Colloidal Templating and Self-Assembly, *Chemistry – A European Journal* 6 (3) (2000) 413-419.
- [5] X.W. Lou, L.A. Archer, Z. Yang, Hollow Micro-/Nanostructures: Synthesis and Applications, *Advanced Materials* 20 (21) (2008) 3987-4019.
- [6] F. Caruso, R.A. Caruso, H. Möhwald, Nanoengineering of Inorganic and Hybrid Hollow Spheres by Colloidal Templating, *Science* 282 (5391) (1998) 1111-1114.
- [7] M.S. Fleming, T.K. Mandal, D.R. Walt, Nanosphere–Microsphere Assembly: Methods for Core–Shell Materials Preparation, *Chemistry of Materials* 13 (6) (2001) 2210-2216.
- [8] L.F. Francis, Sol-Gel Methods for Oxide Coatings, *Materials and Manufacturing Processes* 12 (6) (1997) 963-1015.
- [9] C.J. Brinker, D.R. Tallant, E.P. Roth, C.S. Ashley, Sol-gel transition in simple silicates: III. Structural studies during densification, *Journal of Non-Crystalline Solids* 82 (1-3) (1986) 117-126.
- [10] C.J. Brinker, G.W. Scherer, *Sol-Gel Science: The Physics and Chemistry of Sol-Gel Processing* 1ed., Academic Press; , San Diego CA, USA, 1990.
- [11] W.J. Elferink, B.N. Nair, R.M. de Vos, K. Keizer, H. Verweij, Sol–Gel Synthesis and Characterization of Microporous Silica Membranes: II. Tailor-Making Porosity, *J. Colloid Interface Sci.* 180 (1) (1996) 127-134.
- [12] A.A. Kline, T.N. Rogers, M.E. Mullins, B.C. Cornilsen, L.M. Sokolov, Sol-gel kinetics for the synthesis of multi-component glass materials, *Journal of Sol-Gel Science and Technology* 2 (1) (1994) 269-272.
- [13] Y. Wang, A.S. Angelatos, F. Caruso, Template Synthesis of Nanostructured Materials via Layer-by-Layer Assembly†, *Chemistry of Materials* 20 (3) (2007) 848-858.
- [14] A. Ahmed, R. Clowes, E. Willneff, H. Ritchie, P. Myers, H. Zhang, Synthesis of Uniform Porous Silica Microspheres with Hydrophilic Polymer as Stabilizing Agent,

Industrial & Engineering Chemistry Research 49 (2) (2009) 602-608.

[15] Y. Chen, E.T. Kang, K.G. Neoh, A. Greiner, Preparation of Hollow Silica Nanospheres by Surface-Initiated Atom Transfer Radical Polymerization on Polymer Latex Templates, *Advanced Functional Materials* 15 (1) (2005) 113-117.

[16] J. Andersson, S. Areva, B. Spliethoff, M. Linden, Sol-gel synthesis of a multifunctional, hierarchically porous silica/apatite composite, *Biomaterials* 26 (2003) 6827-6835.

[17] R.M. Anisur, J. Shin, H.H. Choi, K.M. Yeo, E.J. Kang, I.S. Lee, Hollow silica nanosphere having functionalized interior surface with thin manganese oxide layer: nanoreactor framework for size-selective Lewis acid catalysis, *Journal of Materials Chemistry* 20 (47) (2010) 10615-10621.

[18] W. Zhao, M. Lang, Y. Li, L. Li, J. Shi, Fabrication of uniform hollow mesoporous silica spheres and ellipsoids of tunable size through a facile hard-templating route, *Journal of Materials Chemistry* 19 (18) (2009) 2778-2783.

[19] K. Kamalasanan, S. Jhunjunwala, J. Wu, A. Swanson, D. Gao, S.R. Little, Patchy, Anisotropic Microspheres with Soft Protein Islets, *Angewandte Chemie International Edition* (2011) n/a-n/a.

[20] X. Xu, S.A. Asher, Synthesis and Utilization of Monodisperse Hollow Polymeric Particles in Photonic Crystals, *Journal of the American Chemical Society* 126 (25) (2004) 7940-7945.

[21] R.A. Caruso, A. Susa, F. Caruso, Multilayered Titania, Silica, and Laponite Nanoparticle Coatings on Polystyrene Colloidal Templates and Resulting Inorganic Hollow Spheres, *Chemistry of Materials* 13 (2) (2001) 400-409.

[22] Z. Niu, J. He, T.P. Russell, Q. Wang, Synthesis of Nano/Microstructures at Fluid Interfaces, *Angewandte Chemie International Edition* 49 (52) (2010) 10052-10066.

[23] H. Xu, W. Wang, Template Synthesis of Multishelled Cu₂O Hollow Spheres with a Single-Crystalline Shell Wall, *Angewandte Chemie International Edition* 46 (9) (2007) 1489-1492.

[24] M. Darbandi, R. Thomann, T. Nann, Hollow Silica Nanospheres: In situ, Semi-In situ, and Two-Step Synthesis, *Chemistry of Materials* 19 (7) (2007) 1700-1703.

[25] S.-J. Ding, C.-L. Zhang, M. Yang, X.-Z. Qu, Y.-F. Lu, Z.-Z. Yang, Template synthesis of composite hollow spheres using sulfonated polystyrene hollow spheres, *Polymer* 47 (2006) 8360-8366.

[26] R.V.R. Virtudazo, H. Watanabe, M. Fuji, M. Takahashi, A Simple Approach to form Hydrothermally Stable Templated Hollow Silica Nanoparticles, John Wiley & Sons, Inc., 2010.

[27] F. Caruso, Nanoengineering of Particle Surfaces, *Advanced Materials* 13 (1) (2001) 11-22.

- [28] I. Tissot, C. Novat, F. Lefebvre, E. Bourgeat-Lami, Hybrid Latex Particles Coated with Silica, *Macromolecules* 34 (17) (2001) 5737-5739.
- [29] E. Bourgeat-Lami, I. Tissot, F. Lefebvre, Synthesis and Characterization of SiOH-Functionalized Polymer Latexes Using Methacryloxy Propyl Trimethoxysilane in Emulsion Polymerization, *Macromolecules* 35 (16) (2002) 6185-6191.
- [30] Z. Zhong, Y. Yin, B. Gates, Y. Xia, Preparation of Mesoscale Hollow Spheres of TiO₂ and SnO₂ by Templating Against Crystalline Arrays of Polystyrene Beads, *Advanced Materials* 12 (3) (2000) 206-209.
- [31] A. Imhof, Preparation and Characterization of Titania-Coated Polystyrene Spheres and Hollow Titania Shells, *Langmuir* 17 (12) (2001) 3579-3585.
- [32] H. Li, C.-S. Ha, I. Kim, Facile Fabrication of Hollow Silica and Titania Microspheres Using Plasma-Treated Polystyrene Spheres as Sacrificial Templates, *Langmuir* 24 (19) (2008) 10552-10556.
- [33] M. Fujii, C. Takai, Y. Tarutani, T. Takei, M. Takahashi, Surface properties of nanosize hollow silica particles on the molecular level, *Advanced Powder Technology* 18 (2007) 81-91.
- [34] R.V.R. Virtudazo, H. Watanabe, T. Shirai, M. Fujii, M. Takahashi, Direct Template Approach for the Formation of (Anisotropic Shape) Hollow Silicate Microparticles, in: *IOP Conference Series: Materials Science and Engineering*, ICC3, 2011.
- [35] H. Watanabe, M. FUJII, M. TAKAHASHI, Synthesis, characterization and application of nano-sized hollow silica particles, in: *Proceeding 9th Ceramic Materials and Components for Energy and Environmental Application and Lazer Ceramics Symposium Conference*, China, 2008, pp. 145-150.
- [36] M. Fujiwara, K. Shiokawa, I. Sakakura, Y. Nakahara, Silica Hollow Spheres with Nano-Macroholes Like Diatomaceous Earth, *Nano Letters* 6 (12) (2006) 2925-2928.
- [37] P. Tyagi, P.C. Wu, M. Chancellor, N. Yoshimura, L. Huang, Recent advances in intravesical drug/gene delivery, *Molecular pharmaceutics* 3 (4) (2006) 369-379.
- [38] C. Ye, A. Chen, P. Colombo, C. Martinez, Ceramic microparticles and capsules via microfluidic processing of a preceramic polymer, *Journal of The Royal Society Interface* 7 (Suppl 4) (2010) S461-S473.
- [39] M.A. Aravand, M.A. Semsarzadeh, Particle Formation by Emulsion Inversion Method: Effect of the Stirring Speed on Inversion and Formation of Spherical Particles, *Macromolecular Symposia* 274 (1) (2008) 141-147.
- [40] F. Gao, Z.-G. Su, P. Wang, G.-H. Ma, Double Emulsion Templated Microcapsules with Single Hollow Cavities and Thickness-Controllable Shells, *Langmuir* 25 (6) (2009) 3832-3838.
- [41] M. Jafelicci Jr, M. Rosaly Davolos, F. José dos Santos, S. José de Andrade, Hollow silica particles from microemulsion, *Journal of Non-Crystalline Solids* 247 (1-3) (1999)

98-102.

[42] M. Fujiwara, K. Shiokawa, K. Morigaki, Y. Zhu, Y. Nakahara, Calcium carbonate microcapsules encapsulating biomacromolecules, *Chemical Engineering Journal* 137 (1) (2008) 14-22.

[43] M. Fujiwara, K. Shiokawa, I. Sakakura, Y. Nakahara, Preparation of Hierarchical Architectures of Silica Particles with Hollow Structure and Nanoparticle Shells: A Material for the High Reflectivity of UV and Visible Light, *Langmuir* 26 (9) (2010) 6561-6567.

[44] J.A. Hanson, T.J. Deming, Functionalized nanoscale through microscale polypeptide stabilized emulsions for display of biomolecules, *Polymer Chemistry* 2 (7) (2011) 1473-1475.

[45] J.A. Hanson, C.B. Chang, S.M. Graves, Z. Li, T.G. Mason, T.J. Deming, Nanoscale double emulsions stabilized by single-component block copolypeptides, *Nature* 455 (7209) (2008) 85-88.

[46] H.C. Shum, D. Lee, I. Yoon, T. Kodger, D.A. Weitz, Double Emulsion Templated Monodisperse Phospholipid Vesicles, *Langmuir* 24 (15) (2008) 7651-7653.

[47] H.C. Shum, Y.-j. Zhao, S.-H. Kim, D.A. Weitz, Multicompartment Polymersomes from Double Emulsions, *Angewandte Chemie International Edition* 50 (7) (2011) 1648-1651.

[48] H.C. Shum, J.-W. Kim, D.A. Weitz, Microfluidic Fabrication of Monodisperse Biocompatible and Biodegradable Polymersomes with Controlled Permeability, *Journal of the American Chemical Society* 130 (29) (2008) 9543-9549.

[49] A.K. Tucker-Schwartz, Z. Bei, R.L. Garrell, T.B. Jones, Polymerization of Electric Field-Centered Double Emulsion Droplets to Create Polyacrylate Shells, *Langmuir* 26 (24) (2010) 18606-18611.

[50] Z.M. Bei, T.B. Jones, A. Tucker-Schwartz, Forming concentric double-emulsion droplets using electric fields, *Journal of Electrostatics* 67 (2-3) (2009) 173-177.

[51] M. Yang, J. Ma, C. Zhang, Z. Yang, Y. Lu, General Synthetic Route toward Functional Hollow Spheres with Double-Shelled Structures, *Angewandte Chemie* 117 (41) (2005) 6885-6888.

[52] M. Yang, J. Ma, Z. Niu, X. Dong, H. Xu, Z. Meng, Z. Jin, Y. Lu, Z. Hu, Z. Yang, Synthesis of Spheres with Complex Structures Using Hollow Latex Cages as Templates, *Advanced Functional Materials* 15 (9) (2005) 1523-1528.

[53] M.-M. Titirici, M. Antonietti, A. Thomas, A Generalized Synthesis of Metal Oxide Hollow Spheres Using a Hydrothermal Approach, *Chemistry of Materials* 18 (16) (2006) 3808-3812.

[54] J.H. Bang, K.S. Suslick, Sonochemical synthesis of nanosized hollow hematite, *Journal of American Chemical Society* 129 (2007) 2242-2243.

- [55] R. V.Rivera-Virtudazo, H. Watanabe, M. Fuji, M. Takahashi, Hollow Silica Nanoparticles: Simple Template to Stabilize the Amorphous Silica Shell by Hydrothermal-Templated Process, in: The 2nd Thailand-Japan International Academic Conference Integrated Research for Sustainable Development, Thai Students Association in Japan Under Royal Patronage (TSAJ), Kyoto, Japan, 2009, pp. 83-84.
- [56] X.-H. Li, D.-H. Zhang, J.-S. Chen, Synthesis of Amphiphilic Superparamagnetic Ferrite/Block Copolymer Hollow Supmicrospheres, *Journal of American Chemical Society* 128 (2006) 8382-8383.
- [57] J.-H. Sun, M.-O. Coppens, A hydrothermal post-synthesis route for the preparation of high quality MCM-48 with a tailored pore size, *Journal of Materials Chemistry* 12 (2002) 3016-3020.
- [58] H.-P. Lin, C.-Y. Mou, Salt effect in post-synthesis hydrothermal treatment of MCM-41, *Microporous and Mesoporous Materials* 55 (2002) 69-80.
- [59] N.E. Botterhuis, Q. Sun, P.C.M.M. Magusin, R.A. van Santen, N.A.J.M. Sommerdijk, Hollow Silica Spheres with an Ordered Pore Structure and Their Application in Controlled Release Studies, *Chemistry – A European Journal* 12 (5) (2006) 1448-1456.
- [60] M.M. Ashton-Patton, M.M. Hall, J.E. Shelby, Formation of low density polyethylene/hollow glass microspheres composites, *Journal of Non-Crystalline Solids* 352 (6-7) (2006) 615-619.
- [61] S.D. McAllister, S.N. Patankar, I.F. Cheng, D.B. Edwards, Lead dioxide coated hollow glass microspheres as conductive additives for lead acid batteries, *Scripta Materialia* 61 (4) (2009) 375-378.
- [62] J.D. Newell, S.N. Patankar, D.B. Edwards, Porous microspheres as additives in lead-acid batteries, *Journal of Power Sources* 188 (1) (2009) 292-295.
- [63] H.M. Chen, R.-S. Liu, Architecture of Metallic Nanostructures: Synthesis Strategy and Specific Applications, *The Journal of Physical Chemistry C* 115 (9) (2011) 3513-3527.
- [64] B. Wei, S. Wang, H. Song, H. Liu, J. Li, N. Liu, A review of recent progress in preparation of hollow polymer microspheres, *Petroleum Science* 6 (3) (2009) 306-312.
- [65] A.L. Campbell, S.D. Stoyanov, V.N. Paunov, Fabrication of functional anisotropic food-grade micro-rods with micro-particle inclusions with potential application for enhanced stability of food foams, *Soft Matter* 5 (5) (2009) 1019-1023.
- [66] Y. Cheng, J. Guo, X. Liu, A. Sun, G. Xu, P. Cui, Preparation of uniform titania microspheres with good electrorheological performance and their size effect, *Journal of Materials Chemistry* (2011).
- [67] D.B. Edwards, P.W. Appel, Modeling lead/acid batteries that have positive electrodes containing hollow, glass microspheres, *Journal of Power Sources* 46 (1)

(1993) 39-48.

[68] B. Holt, R. Lam, F.C. Meldrum, S.D. Stoyanov, V.N. Paunov, Anisotropic nano-papier mache microcapsules, *Soft Matter* 3 (2) (2007) 188-190.

[69] Z.-Z. Li, L.-X. Wen, L. Shao, J.-F. Chen, Fabrication of porous hollow silica nanoparticles and their applications in drug release control, *Journal of Controlled Release* 98 (2) (2004) 245-254.

[70] B. Neu, A. Voigt, R. Mitlöhner, S. Leporatti, C.Y. Gao, E. Donath, H. Kiesewetter, H. Möhwald, H.J. Meiselman, H. Bäuml, Biological cells as templates for hollow microcapsules, *Journal of Microencapsulation: Micro and Nano Carriers* 18 (3) (2001) 385 - 395.

[71] K. Pays, J. Giermanska-Kahn, B. Pouligny, J. Bibette, F. Leal-Calderon, Double emulsions: how does release occur?, *Journal of Controlled Release* 79 (1-3) (2002) 193-205.

[72] W. Tong, C. Gao, Multilayer microcapsules with tailored structures for bio-related applications, *Journal of Materials Chemistry* 18 (32) (2008) 3799-3812.

[73] K. Hadinoto, P. Phanapavudhikul, Z. Kewu, R.B.H. Tan, Novel Formulation of Large Hollow Nanoparticles Aggregates as Potential Carriers in Inhaled Delivery of Nanoparticulate Drugs, *Industrial & Engineering Chemistry Research* 45 (10) (2006) 3697-3706.

[74] J. Liu, S.Z. Qiao, J.S. Chen, X.W. Lou, X. Xing, G.Q. Lu, Yolk/shell nanoparticles: new platforms for nanoreactors, drug delivery and lithium-ion batteries, *Chemical Communications* (2011).

[75] X.-J. Wu, Y. Jiang, D. Xu, A Unique Transformation Route for Synthesis of Rodlike Hollow Mesoporous Silica Particles, *The Journal of Physical Chemistry C* (2011) null-null.

[76] H.-P. Hentze, S.R. Raghavan, C.A. McKelvey, E.W. Kaler, Silica Hollow Spheres by Templating of Catanionic Vesicles, *Langmuir* 19 (4) (2003) 1069-1074.

CHAPTER 2

PREPARATION OF NANO- and

MICRO-SIZE HOLLOW SILICATE

PARTICLES (TEMPLATE METHOD)

2.1 INNOVATIVE TEMPLATE APPROACH

USING COLLOIDAL-CALCIUM

RICH-HYDROXYAPPATITE

NANOPARTICLES (CaHAp) IN

FABRICATING UNIQUE SHAPE NANO-SIZE

HOLLOW SILICATE PARTICLES

CHAPTER 2

PREPARATION AND FABRICATION OF NANO- and MICRO-SIZE HOLLOW SILICATE PARTICLES (TEMPLATE METHOD)

2.1 Innovative template approach using colloidal-Calcium rich-Hydroxyapatite nanoparticles (CaHAp) in fabricating unique shape nano-size hollow silicate particles

2.1.1 Introduction

There have been notable interests in fabricating hollow nano-particles for a potential application on nano-science for as a catalysts or drug-delivery agent. Nano-scale hollow silicate particles have been processed by various methods such as mini-emulsion[1, 2], spray-drying[3, 4] and template method[5, 6] but producing a less than 100 nm is still a great challenge. In this study, template method is used to fabricate nano-size hollow silicate particles by coating the nano-core-particles calcium rich-hydroxyapatite (CaHAp) with silicate shell followed by acid treatment. Although this template technique has been successfully applied to create hollow particles using core-template particles such as polystyrene[7, 8], Fe₂O₃ [9] and other inorganic materials[10], but still needs improvement for an eco-friendly approach for facet hollow silicate particles. Here in this chapter, two aspects are demonstrated; encapsulation of CaHAp nanoparticles with amorphous silicate shell and produced unique nano-size shape hollow silicate particles. At this point, the concern is developing less than 60 nm-scale hollow silicate particles using calcium rich-hydroxyapatite particles (Ca(OH)₂:H₃PO₄ = 1.75:1, synthesized by Tanaka *et al.*[11, 12]). The advantages in utilizing HAp particles includes the following: easily dissociate at mild

acid concentration[12] and no special equipment to recycle the dissolved HAp particles. There were other studies pertaining to modify/coat the HAp particles [13, 14] but in attempting to utilize as template-colloidal CaHAp solution (1.75 (Ca/P) in creating nano-size hollow silicate particle with less than 60 nm; (as far as we know), the researcher were the primary one to do it successfully.

In this chapter, the optimization of the amount of tetraethoxysilane (TEOS) concentration in order to evaluate the encapsulation of silicate onto CaHAp nanoparticles and formation of hollow silicate nanoparticle using colloidal-CaHAp (1.75 Ca/P) solution were studied..

2.1.2 Starting materials and schematic outline

2.1.2.1 Materials

Nano-size colloidal Calcium rich-Hydroxyapatite solution (1g/L) (specific gravity of 1.001 (HAp; $\text{Ca}_{10}(\text{PO}_4)_6(\text{OH})_2$), provided by Tanaka et al[11, 12])) was used as nano-core particles / template for the formation of hollow nano-size/oblique shape silica particles. Tetraethoxysilane (TEOS, Wako pure chemical) was used as precursor of silica shell. Ammonia water (NH_4OH , 28% Wako pure chemical) used as catalyst and Ethanol (EtOH, Wako pure chemical) used for washing the template reaction.

2.1.2.2 Preparation of Spindle-Shaped Hollow silicate Nanoparticles

This unique shape / nano-size hollow silicate particles were synthesized based on the previous principle done by Prof. Fuji, CRL NIT [15] . In this case, 50 mL of calcium rich-hydroxyapatite solution (1g/L) ($\text{Ca}_{10}(\text{PO}_4)_6(\text{OH})_2$) was dispersed by ultra-sonic for 5 min (2 times), and 0.0197 mol of ammonium aqueous solution ($\text{H}_2\text{O}:\text{NH}_3$) were added to the solution, after then stirred for 30 min. Then 0.00225614 mol (0.5 mL) of tetraethoxysilane (TEOS) was added drop wise to the solution,

followed by stirring for at least 2 h, a core-shell CaHAp / silica particles was prepared. (Note: only the amount of TEOS was varied from 1 mL, 0.5 mL, 0.25 mL and 0.1 mL for optimization). In obtaining hollow silicate particles, after 2 h continuous stirring, the white gel solution were filtered and washed several times (4X or until becomes neutral) by ethanol, then dried in a vacuum oven to 90 °C for 5 h. In removing the CaHAp core, acid treatment (3.0 mol/L, HCl) was done for 8 h stirring. After then, filtered and washed several times (4X or until becomes neutral) with distilled ethanol/water. Finally, vacuum dried the obtained sample to 90 °C for 1 d; oblique nano-size hollow silicate particle was obtained. See Figure 2.1.1 for the process flow for the fabrication of the unique shape / nano-sized hollow silicate particles

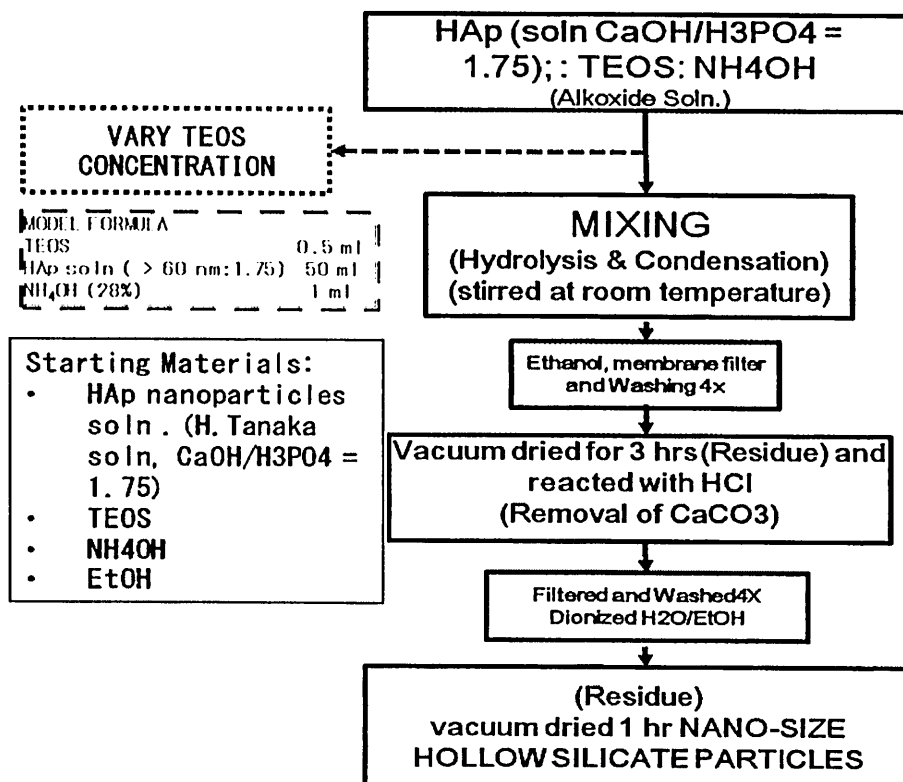


Figure 2.1. 1 Process flow for the preparation/fabrication of the unique shape / nano-size hollow silicate particles using CaHAp nanoparticles (1.75 Ca/P slurry type) as template core.

2.1.2.3 Physico-chemical characterization

The product were characterized by X-ray Diffraction (XRD, Model RINT 1100, Rigaku) with Cu K α radiation ($\lambda= 1.54056 \text{ \AA}$), at a scanning rate of 0.02 $^\circ/\text{s}$ (5° to 60° , 2θ) with an operating voltage of 40 kV and emission current 30 mA. The thermal property of the sample was investigated using the Thermogravimetry (TG, TG-8120, Rigaku, Japan) under oxygen atmosphere. The heating rate of the temperature increase at 10 $^\circ\text{C}/\text{min}$ with temperature ranged from (22 to 1000) $^\circ\text{C}$. Morphology and microstructure of hollow particles were examined using scanning electron microscopy (SEM; JSM-7000F, JEOL) and transmission electron microscopy (TEM, 2000EXII). The specific surface area of the sample was determine by Barrett-Joyner-Halenda (BJH) method via the automatic surface area analyzer (BELSORP-max) with Nitrogen gas adsorption and desorption isotherm recorded at 77K.

2.1.3 Results and discussion

2.1.3.1 Crystallographic properties

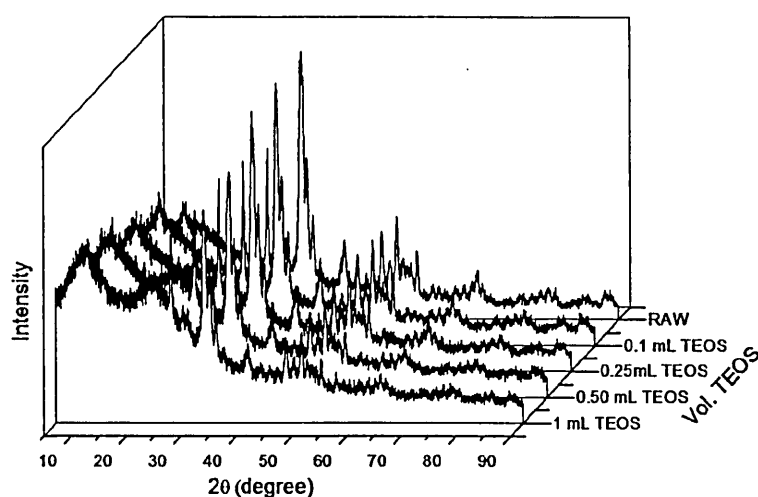


Figure 2.1. 2 XRD pattern of (RAW) dried CaHAp powder as well as nano-size CaHAp powder encapsulated by (0.1 mL TEOS) SiO₂, (0.25 mL TEOS) SiO₂, (0.50 mL TEOS) SiO₂, and (1.0 mL TEOS) SiO₂.

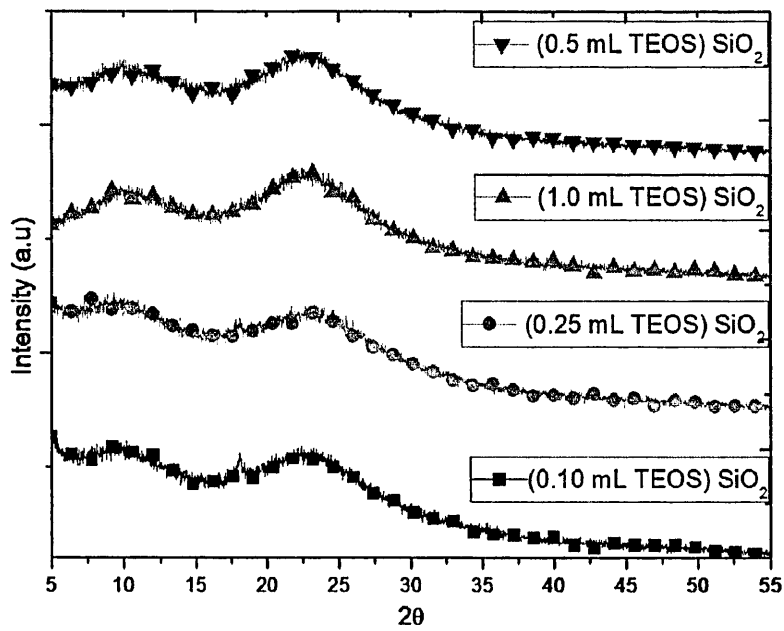


Figure 2.1.3 Amorphous XRD pattern of synthesized samples with concentration of (0.1 mL TEOS) SiO_2 , (0.25 mL TEOS) SiO_2 , (0.50 mL TEOS) SiO_2 , and (1.0 mL TEOS) SiO_2 after acid treatment

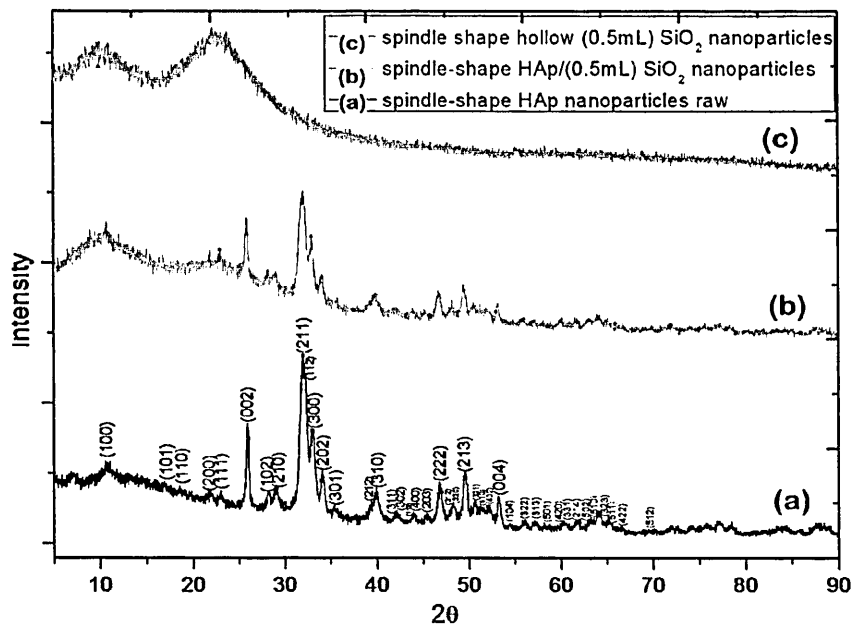


Figure 2.1.4 XRD pattern of (a) raw HAp nanoparticles (b) nano-size spindle-shape CaHAp encapsulated by (0.5 mL) SiO_2 (c) nano-size spindle shape hollow SiO_2 nanoparticles.

As evidence, Figure 2.1.2 shows the XRD patterns of the diffraction angle identified as HAp^[16] (the core particles CaHAp). Theoretically, this indicated that the amorphous silicate covered the core (CaHAp) nanoparticles as shown in Figure 2.1.2 and 2.1.4. Wherein, partially hydrolyzed TEOS molecules were absorbed on the surface of HAp nanoparticles followed by the surface nucleation and growth (encapsulation) mechanism. Surface nucleation and surface charges were mostly the dominant mechanism for the ratio of CaHAp / (0.5ml TEOS) SiO₂ due to a sufficiently enough amount of siloxane (TEOS) concentration to encapsulate HAp nanoparticles. Ideally, as the siloxane-TEOS concentration increases, thickness of shell SiO₂ increased that leads to the increase of amorphous phase concentration. Additionally, it can also reduce the separation distance between siloxane molecules and enhance the probability of the silicate clustering formation and also directly formed as an agglomeration of the nanoparticles [13, 14, 17].

In order to validate that the amorphous shell SiO₂ was coated on the surface of CaHAp (core) nanoparticles; dissolution thru acid treatment was done. As expected, generally no visual peaks (amorphous phase) was observed as shown in Figure 2.1.3 and 2.1.4c. But only (1.0 and 0.5) mL of TEOS amount formed a nano-size hollow silicate particles, this was clearly established and observed in SEM, TEM and STEM images (Figure 2.1.5 to 2.1.6) at section 2.1.3.2.

2.1.3.2 Morphological observation

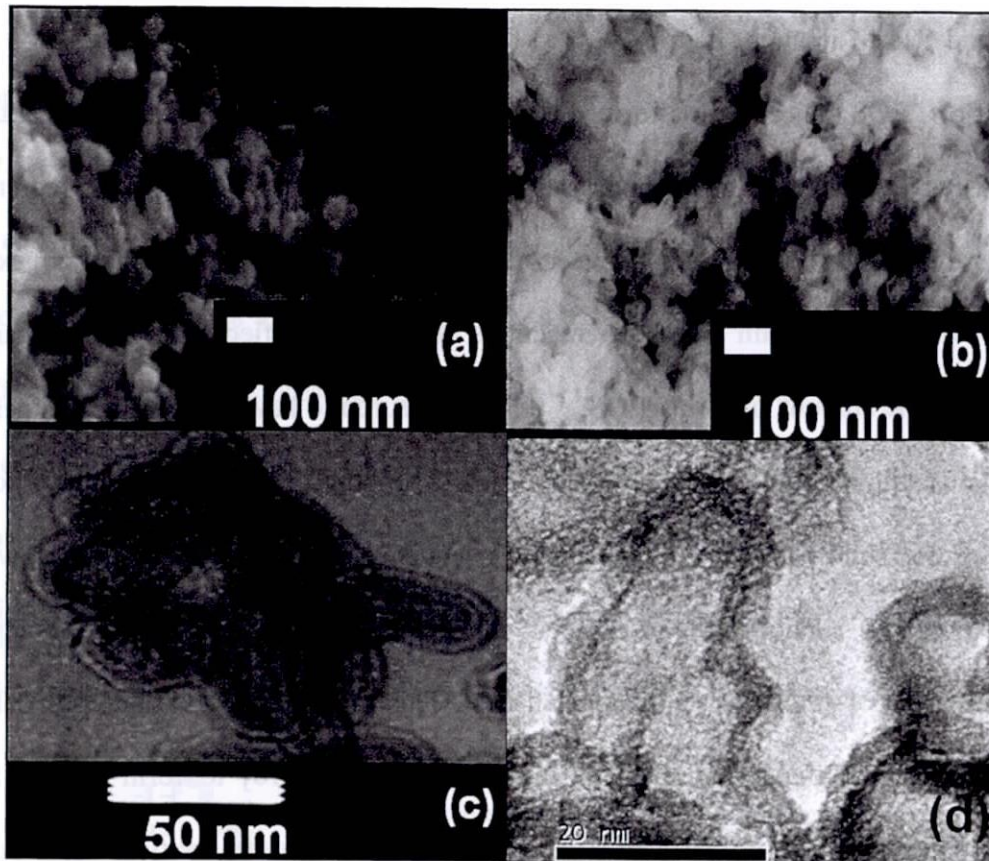


Figure 2.1. 5 SEM images of nano-rod (spindle) shape CaHAp raw powder particles (a) and hollow SiO₂ nanoparticles (b) with TEM images (c and d)

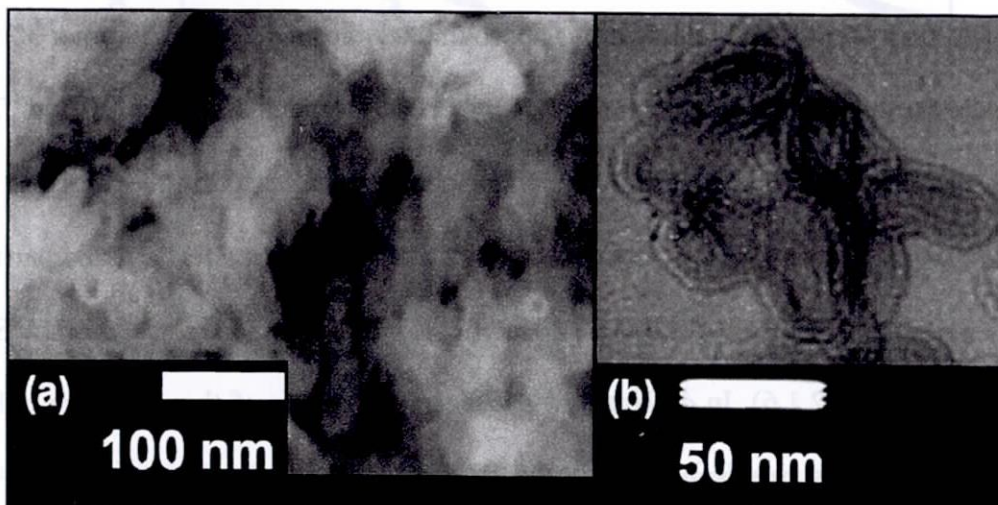


Figure 2.1. 6 SEM (a) and TEM (b) images: Acid treated samples of nano-size hollow (0.5 mL TEOS) SiO₂

Nano-size hollow silicate particles is clearly established and observed in SEM, TEM and STEM images (Figure 2.1.5 to Figure 2.1.6) in which (1.0 mL and 0.5 mL) amount of TEOS concentration formed a nano-rod (spindle) shape hollow SiO₂ particles. Obviously, it showed an amorphous shell SiO₂ after acid dissolution. This requires a suitable thickness relationship between the core and the shell, so that no excess silicates/materials remain after the reactions. Results signified that suitable/careful addition of the amount silanol (TEOS, ~ 0.5 mL) assured to have a uniform thickness of amorphous silicate shell coating. Beyond or lesser amount of silanol, the solution forms excess or one solid particle. This represents a sequence of incomplete reaction in which the amount of silanol less or exceed the required thickness for the complete transformation of amorphous silicate shell wall. This further supports that core-CaHAp nanoparticles completely removed during acid dissolution[18] to form hollow SiO₂ nanoparticles. (see Figure 2.1.5 to Figure 2.1.6). To further substantiate the reported hollow particles, TEM micrograph was investigated as shown in Figure 2.1.6. It visibly showed the morphology of the nano-size rod shape hollow particles at approximately a length less than 60 nm while the width is approximately around 30 nm (50 nm x 30 nm). The thickness of the amorphous wall SiO₂ was nearly around less than 10 nm. This implies that the silica circulate into the CaHAp nanoparticles during hydrolysis and condensation reaction process, consistent with the surface nucleation and surface charges mechanism in coating CaHAp nanoparticles with silicate to formed hollow SiO₂ (Figure 2.1.5d and 2.1.6). In determining the thermal stability of the nano-size hollow silicate nanoparticles, thermogravimetric analysis was done as explain in section 2.1.3.3

2.1.3.3 Thermal properties

Verification regarding the composition and structure of the synthesized nanoparticles is specified by thermogravimetric analysis (TGA) as shown in Figure 2.1.7 (a,b and c). The TGA analysis showed that the total reduction of weight loss of raw CaHAp nanoparticles increased for CaHAp/SiO₂ nanoparticles and hollow SiO₂ particles (7.5 %, 10 % and 14.0%, respectively). This gap implies that the reduction significantly due to the presence of SiO₂ coating[19]; composed of organic solvent, condensation of terminal silanol groups (OH groups) and phase transformation (amorphous silica to quartz)[20], typical for hollow silicate particles. In enhancing the physic-chemical properties of the hollow silicate nanoparticles, surface area and pore distribution of the synthesized particles were analyzed as discussed in section 2.1.3.4.

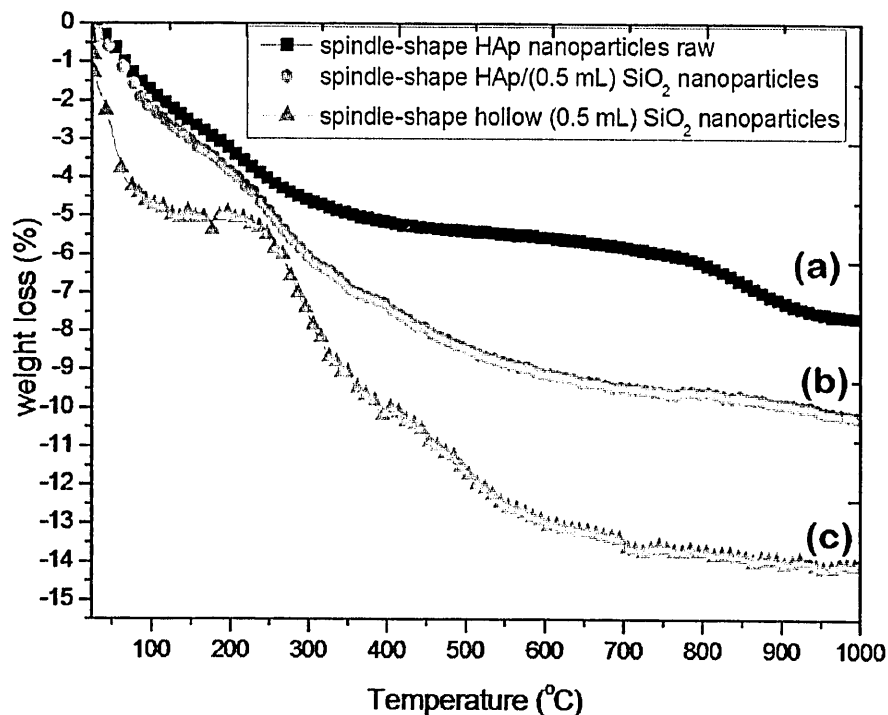


Figure 2.1.7 Thermogravimetric analysis (TG) of (a) raw CaHAp nanoparticles, (b) nano-size spindle-shaped CaHAp encapsulated by (0.5 mL) SiO₂, (c) nano-size spindle shape hollow SiO₂ nanoparticles

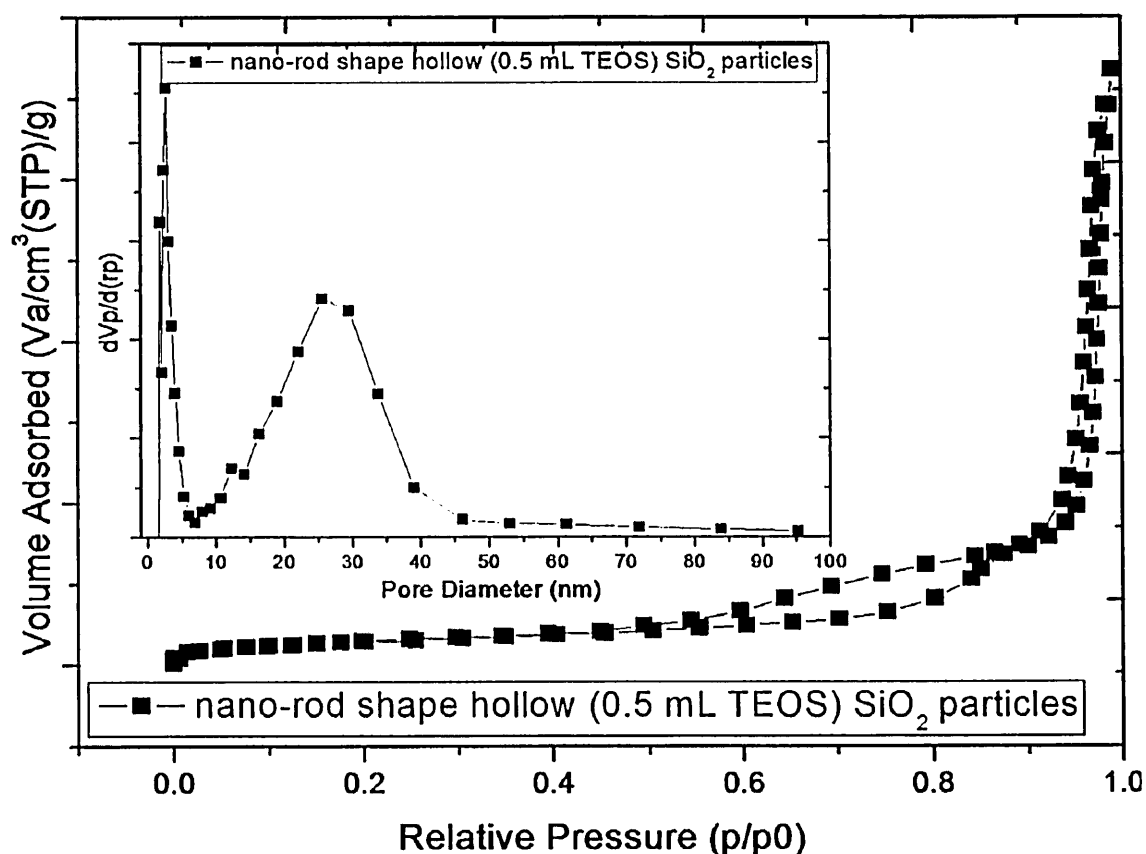


Figure 2.1.8 N₂ adsorption and desorption isotherms and (inset) cavity (pore) size distribution (BJH method) of nano-rod (spindle) shape hollow (0.5 mL TEOS) SiO₂ particles.

2.1.3.4 N₂ adsorption/desorption properties

The nitrogen adsorption isotherm at 77 K was analyzed (shown in Figure 2.1.8) for the nano-rod shape hollow SiO₂ particles that exhibits type IV isotherms with cavity (pore) size distribution (inset) of ~ 10.65 nm. Interestingly, the adsorption isotherm (Figure 2.1.8) of hollow SiO₂ has two hysteresis loops. The first one at the relative pressure ($0.45 < p/p_0 < 0.88$) with type H3 hysteresis loop, characteristic of a cage-like network nanostructure[21]. While, the second loop at relative pressure ($0.9 < p/p_0 < 0.99$), due to the void space among the aggregated hollow nano-rod shape particles^[22] (see supplementary information Figure 2.1S.9 and 2.1S.10). In this case, the

aggregation maybe cause during the aging and filtration process [8, 20, 23, 24]. But, this phenomenon (adsorption desorption pattern, two hysteresis loops) were not observed in raw CaHAp powder and core-shell CaHAp/SiO₂ nanoparticles. The discrepancy of the cage (pore) size calculated from the BJH method and the estimated observation in TEM, mainly due to the fact that the BJH model; not very suitable for determining the pore size with cage network nanostructure [21, 25]. Clearly, the surface area and pore volumes of the hollow nanoparticles (204.03 m²/g and 1.18 cm³/g, respectively) increase compared to raw HAp nanoparticles (111.7m²/g and 0.4912 cm³/g, respectively, Table 2.1.1).

Table 2.1.1 Characterization of the Nanostructure CaHAp/SiO₂ particles and hollow SiO₂ nanopaticles

Material	Pore Volume (cm ³ /g , BET)	Cavity diameter (nm., BJH)	Surface Area (m ² /g, BET)
CaHAp powder (solution dried)	0.4912	10.65	111.7
CaHAp/(0.5 mL TEOS) SiO ₂	0.8981	1.21	108.8
Hollow (0.5 mL TEOS) SiO ₂	1.18	6.06	204.0

2.1.3.5 Mechanism for the formation of unique nano-size hollow silicate particles

In Figure 2.1.9 showed a schematic illustration of encapsulating nano-size Calcium rich-hydroxyapatite (CaHAp) with silica in order to produce nano-size rod shape hollow silicate particles. This facile shape hollow silicate nanoparticles is based on the same principle previously done by Fuji et al[15]. But in this case, colloidal CaHAp solution is used (50 mL; 1.75(Ca/P)); specific gravity of 1.001, average nano-size ~ 45 nm particles; see the supplementary information for the detailed analysis,

Figure 2.1.2, Fig. 2.1S.1, 2.1S.2 and 2.1S.3), ammonium aqueous solution (NH_4OH , 28 %) and tetraethoxysilane (TEOS), mix and stir for at least 2 h at ambient temperature, with molar ratio of 1 TEOS: 11.5 NH_4OH . But before mixing, colloidal HAp solution is ultra-sonicated for 10 min (5 min interval), to assist in dispersing and exposing the surface of the nano-size HAp in order to be coated individually[26] by TEOS (silicate source). (See supplementary information, Figure 2.1S.3).

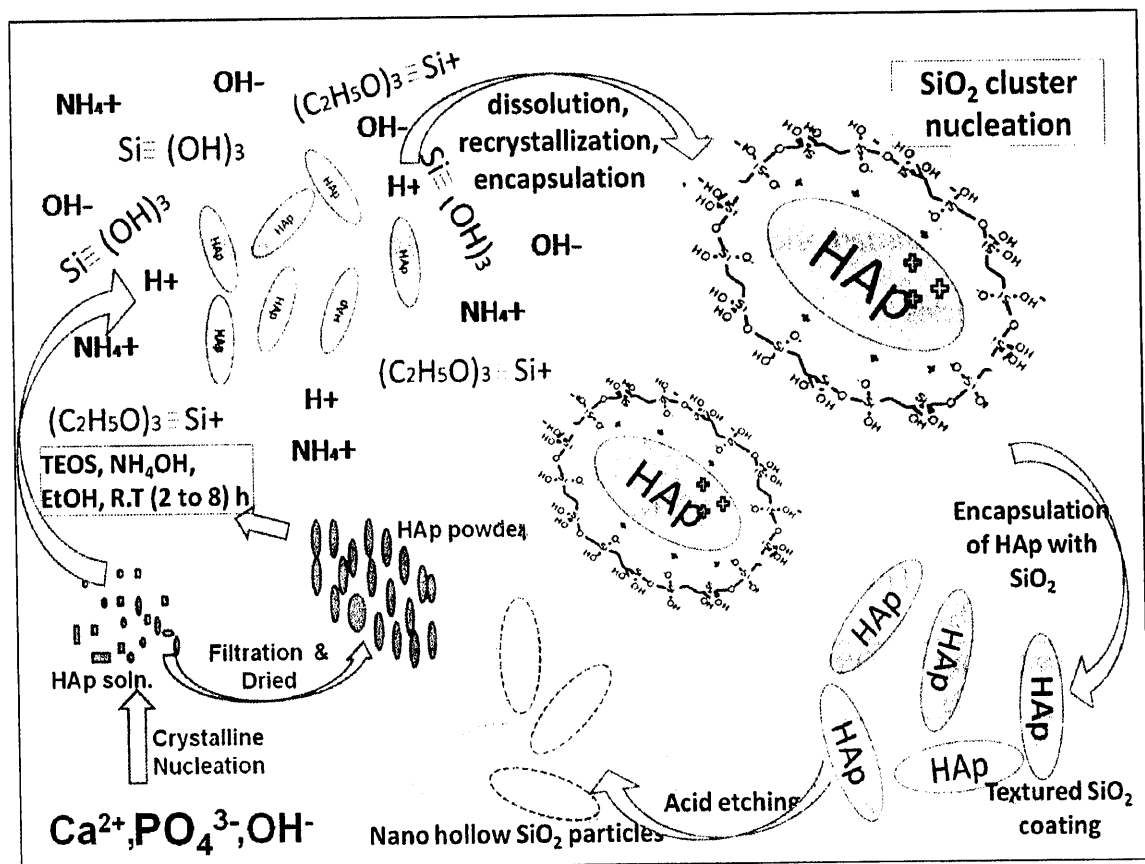


Figure 2.1. 9 Schematic illustration of the procedure for the synthesis of nano-size spindle-shape hollow SiO_2 template with CaHAp nanoparticles.

As illustrated, core-shell nano-size particle is formed during hydrolysis of TEOS and followed by condensation of silica that coats the core CaHAp nanoparticles. For simplicity of this report, the focus is on the formation of nano-size rod shape hollow SiO_2 using CaHAp nanoparticles by template approach. In this manner, the coating

mechanism is based on the heterogeneous nucleation phenomena (surface nucleation) processes [27-29]. The surface nucleation reaction occurs via adsorption of partially hydrolyzed TEOS molecules into the CaHAp surface nanoparticles. Under basic condition (pH 10-11), neighbouring silanol groups react with each other and form siloxane bonds via condensation reaction[30]. The mechanism proceeds via nucleation of silica in solution and the subsequent adsorption onto the surface of CaHAp nanoparticles. Notably, the kinetic reaction and with sufficient amount of siloxane (TEOS) to coat/encapsulate CaHAp nanoparticles followed by acid treatment produced uniquely nano-rod shape hollow SiO₂

2.1.4 Conclusion

Compared with other template process, this eco-friendly template approach is capable of producing large scale nano-silicate hollow particles with lesser toxic acid usage with recyclable core-template. In addition, this method is certainly not limited to binary system, it is also suitable and applicable for ternary-composite system (example: hollow calcium-silicate hydrate and formation of hollow bio-active glass nanoparticles). Although the researcher has demonstrated the fabrication of randomly distributed nano-size hollow silicate particles, in principle, it is also possible to encapsulate CaHAp nanoparticles with amorphous silicate walls functionalized by bio-active compounds or covered with mesoporous organosilicate shell following the same approach. Such fabrication of encapsulation of CaHAp nanoparticles with some hybrid organosilicate shell walls, then form hollow nanoparticles may possess a new field of interest of nano-science application as nano-carriers/containers. The researcher believe that the current results open up research works to create exciting/interesting morphologies of the amorphous shell with hollow interior that are not accessibly done with the present

available approach via template method by utilizing colloidal (1.75 Ca/P) CaHAp nanoparticles.

In summary, this chapter has demonstrated a simple, versatile and general route to coat CaHAp nanoparticles with silicate shells that formed uniquely nano-rod shape hollow SiO₂ nanoparticles. Consequently, CaHAp nanoparticles coated silicate can be furtherly functionalized for the bio-glass application. The present approached for the formation of unique nano-shape hollow SiO₂ could allow for the synthesis of hybrid hollow structures for future imaging, sensing and drug delivery application.

References

- [1] D. Lensen, D.M. Vriezema, J.C.M. van Hest, Polymeric Microcapsules for Synthetic Applications, *Macromolecular Bioscience* 8 (11) (2008) 991-1005.
- [2] Z. Feng, Z. Wang, C. Gao, J. Shen, Template Polymerization to Fabricate Hydrogen-Bonded Poly(acrylic acid)/Poly(vinylpyrrolidone) Hollow Microcapsules with a pH-Mediated Swelling–Deswelling Property, *Chemistry of Materials* 19 (19) (2007) 4648-4657.
- [3] N. Hagura, A.B.D. Nandiyanto, F. Iskandar, K. Okuyama, A role of template surface charge in the preparation of porous and hollow particles using spray-drying, *Chemistry letters* 38 (11) (2009) 1076-1077.
- [4] G.L. Messing, S.C. Zhang, G.V. Jayanthi, Ceramic Powder Synthesis by Spray Pyrolysis, *Journal of the American Ceramic Society* 76 (11) (1993) 2707-2726.
- [5] M.S. Yavuz, Y. Cheng, J. Chen, C.M. Cobley, Q. Zhang, M. Rycenga, J. Xie, C. Kim, K.H. Song, A.G. Schwartz, L.V. Wang, Y. Xia, Gold nanocages covered by smart polymers for controlled release with near-infrared light, *Nat Mater* 8 (12) (2009) 935-939.
- [6] H. Jin fan, M. Knez, R. Scholz, K. Nielsch, E. Pippel, D. Hesse, M. Zacharias, U. Gosele, Monocrystalline spinel nanotube fabrication based on the Kirkendall effect, *Nat Mater* 5 (8) (2006) 627-631.
- [7] S.O. Obare, N.R. Jana, C.J. Murphy, Preparation of Polystyrene- and Silica-Coated Gold Nanorods and Their Use as Templates for the Synthesis of Hollow Nanotubes, *Nano Letters* 1 (11) (2001) 601-603.
- [8] S.J. Ding, C.L. Zhang, M. Yang, X.Z. Qu, Y.F. Lu, Z.Z. Yang, Template synthesis of composite hollow spheres using sulfonated polystyrene hollow spheres, *Polymer* 47 (25) (2006) 8360-8366.
- [9] Y. Piao, J. Kim, H.B. Na, D. Kim, J.S. Baek, M.K. Ko, J.H. Lee, M. Shokouhimehr, T. Hyeon, Wrap-bake-peel process for nanostructural transformation from [beta]-FeOOH nanorods to biocompatible iron oxide nanocapsules, *Nat Mater* 7 (3) (2008) 242-247.

- [10] Y. Sun, B.T. Mayers, Y. Xia, Template-Engaged Replacement Reaction: A One-Step Approach to the Large-Scale Synthesis of Metal Nanostructures with Hollow Interiors, *Nano Letters* 2 (5) (2002) 481-485.
- [11] H. Tanaka, M. Chikazawa, K. Kandori, T. Ishikawa, Influence of thermal treatment on the structure of calcium hydroxyapatite, *Physical Chemistry Chemical Physics* 2 (11) (2000) 2647-2650.
- [12] H. Tanaka, K. Uchida, Preparation and Surface Characterization of Calcium Hydroxyapatite Grafting of Phosphoethanolamine, *Phosphorus Research Bulletin* 24 (2010) 38-42.
- [13] M. Vallet-Regi, D. Arcos, Silicon substituted hydroxyapatites. A method to upgrade calcium phosphate based implants, *Journal of Materials Chemistry* 15 (15) (2005) 1509-1516.
- [14] L. Borum, O.C. Wilson, Surface modification of hydroxyapatite. Part II. Silica, *Biomaterials* 24 (21) (2003) 3681-3688.
- [15] M. Fuji, C. Takai, Y. Tarutani, T. Takei, M. Takahashi, Surface properties of nanosize hollow silica particles on the molecular level, *Advanced Powder Technology* 18 (2007) 81-91.
- [16] S. Bose, S.K. Saha, Synthesis and Characterization of Hydroxyapatite Nanopowders by Emulsion Technique, *Chemistry of Materials* 15 (23) (2003) 4464-4469.
- [17] C. Shaoqiang, Z. Ziqiang, Z. Jianzhong, Z. Jian, S. Yanling, Y. Ke, W. Weiming, W. Xiaohua, F. Xiao, L. Laiqiang, S. Li, Hydroxyapatite coating on porous silicon substrate obtained by precipitation process, *Applied Surface Science* 230 (1-4) (2004) 418-424.
- [18] A. Ludwig, S.C. Dave, W.I. Higuchi, J.L. Fox, A. Katdare, Dissolution rate of apatite powders in acidic fluoride solutions and the relationship to hydroxyapatite disk and bovine enamel behavior, *International Journal of Pharmaceutics* 16 (1) (1983) 1-10.
- [19] X. Jiang, T.L. Ward, Y.-S. cheng, J. Liu, J. Brinker, Aerosol fabrication of hollow mesoporous silica nanoparticles and encapsulation of L-methionine as a candidate drug cargo, *Chem. Commun.* 46 (2010) 3019-3021.

- [20] W.G. Fan, L. Gao, Synthesis of silica hollow spheres assisted by ultrasound, *J. Colloid Interface Sci.* 297 (1) (2006) 157-160.
- [21] J. Liu, S. Bai, H. Zhong, C. Li, Q. Yang, Tunable Assembly of Organosilica Hollow Nanospheres, *The Journal of Physical Chemistry C* 114 (2) (2009) 953-961.
- [22] J.-F. Chen, J.-X. Wang, R.-J. Liu, L. Shao, L.-X. Wen, Synthesis of porous silica structures with hollow interiors by templating nanosized calcium carbonate, *Inorganic Chemistry Communications* 7 (3) (2004) 447-449.
- [23] B. Tan, S.E. Rankin, Dual Latex/Surfactant Templating of Hollow Spherical Silica Particles with Ordered Mesoporous Shells, *Langmuir* 21 (18) (2005) 8180-8187.
- [24] F. Caruso, Hollow Capsule Processing through Colloidal Templating and Self-Assembly, *Chemistry – A European Journal* 6 (3) (2000) 413-419.
- [25] J.C. Groen, L.A.A. Peffer, J. Pérez-Ramírez, Pore size determination in modified micro- and mesoporous materials. Pitfalls and limitations in gas adsorption data analysis, *Microporous and Mesoporous Materials* 60 (1-3) (2003) 1-17.
- [26] Y. Han, S. Li, X. Wang, I. Bauer, M. Yin, Sonochemical preparation of hydroxyapatite nanoparticles stabilized by glycosaminoglycans, *Ultrasonics Sonochemistry* 14 (3) (2007) 286-290.
- [27] D. Li, R.B. Kaner, How nucleation affects the aggregation of nanoparticles, *Journal of Materials Chemistry* 17 (22) (2007) 2279-2282.
- [28] M.-Y. Ma, Y.-J. Zhu, L. Li, S.-W. Cao, Nanostructured porous hollow ellipsoidal capsules of hydroxyapatite and calcium silicate: preparation and application in drug delivery, *Journal of Materials Chemistry* 18 (23) (2008) 2722-2727.
- [29] Q. Chen, C. Boothroyd, G.H. Tan, N. Sutanto, A.M. Soutar, Silica Coating of Nanoparticles by the Sonogel Process, *Langmuir* 24 (3) (2008) 650-653.
- [30] H. Zou, S. Wu, Q. Ran, J. Shen, A Simple and Low-Cost Method for the Preparation of Monodisperse Hollow Silica Spheres, *The Journal of Physical Chemistry C* 112 (31) (2008) 11623-11629.

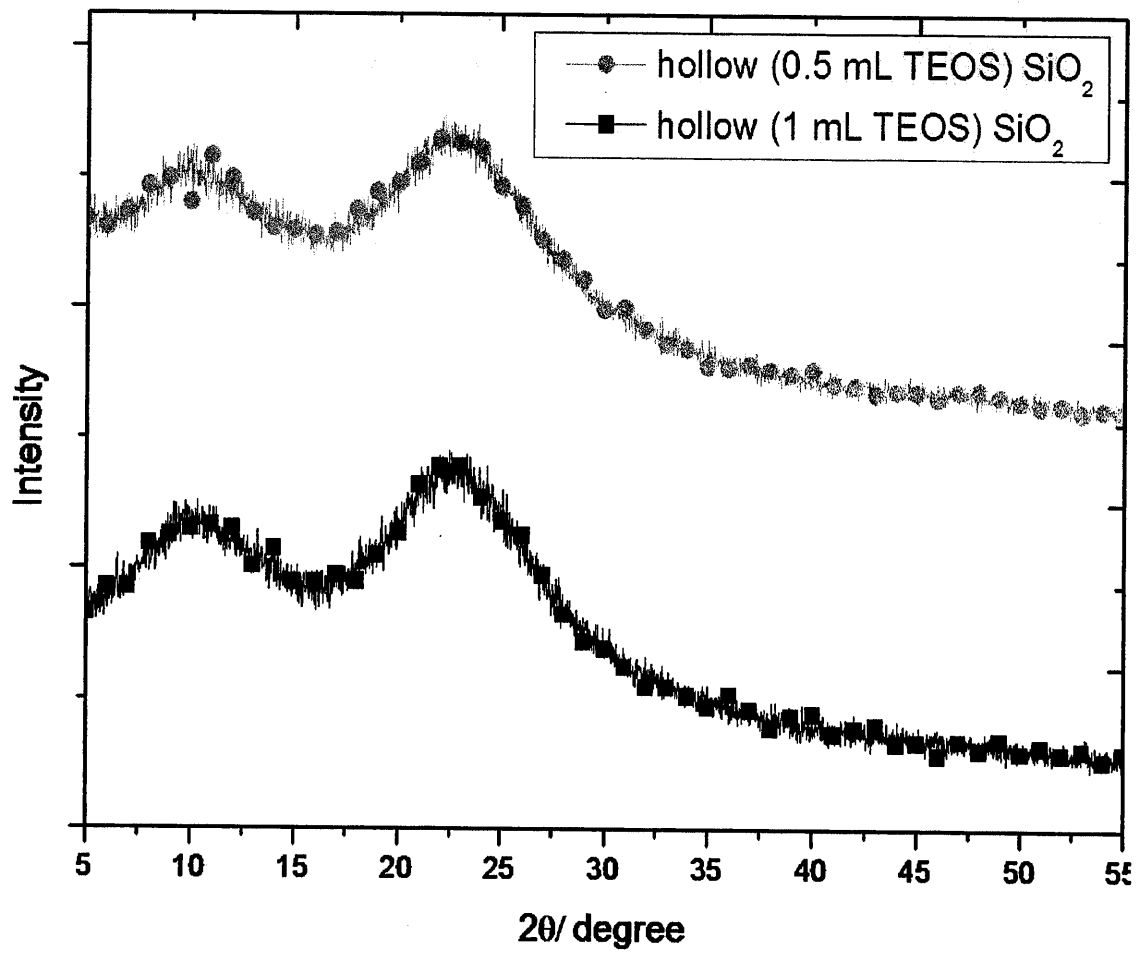


Figure 2.1S. 2 XRD pattern after Acid treatment exhibit amorphous phase (0.50 mL TEOS, (●)) SiO₂, and (1.0 mL TEOS, (■)) SiO₂.

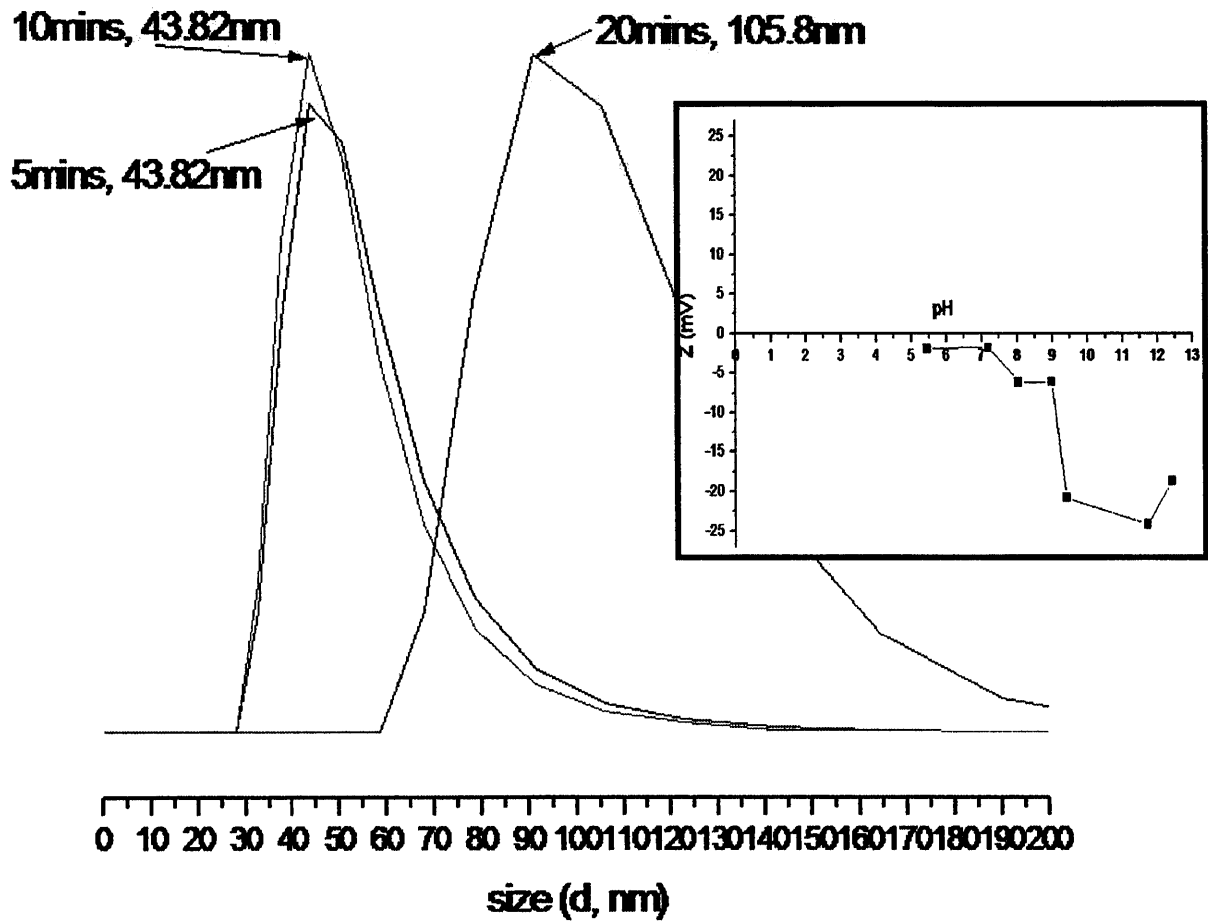


Figure 2.1S. 3 Particle size distribution of CaHAp's solution (specific gravity of 1.001-0.999) at different ultrasonic time interval. Inset is the zeta potential of the CaHAp nanoparticles.

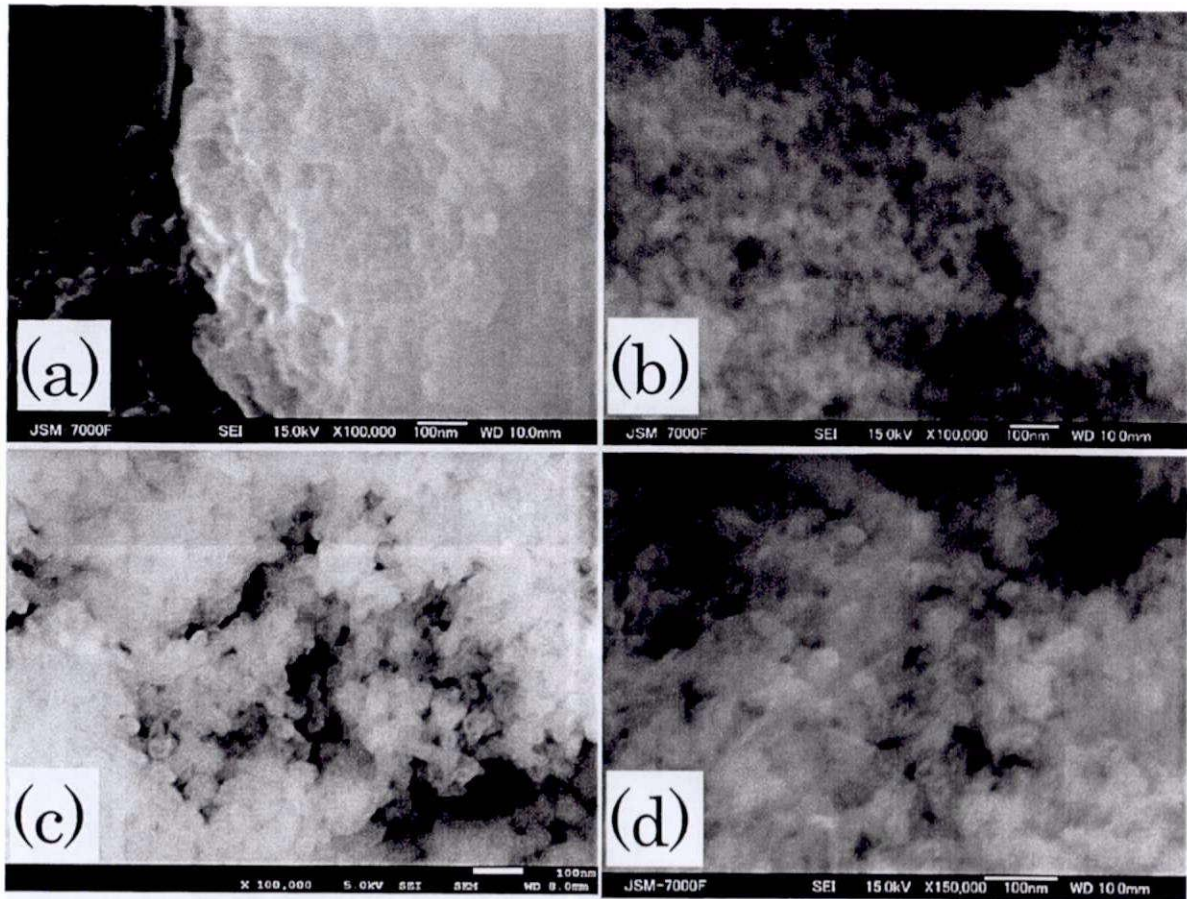


Figure 2.1S. 4 SEM images (bar line 100 nm): Acid treated samples of nano-sized hollow (0.1 mL TEOS) (a), (0.25 mL TEOS) (b), (0.5 mL TEOS) (c), and (1 mL TEOS) (d).

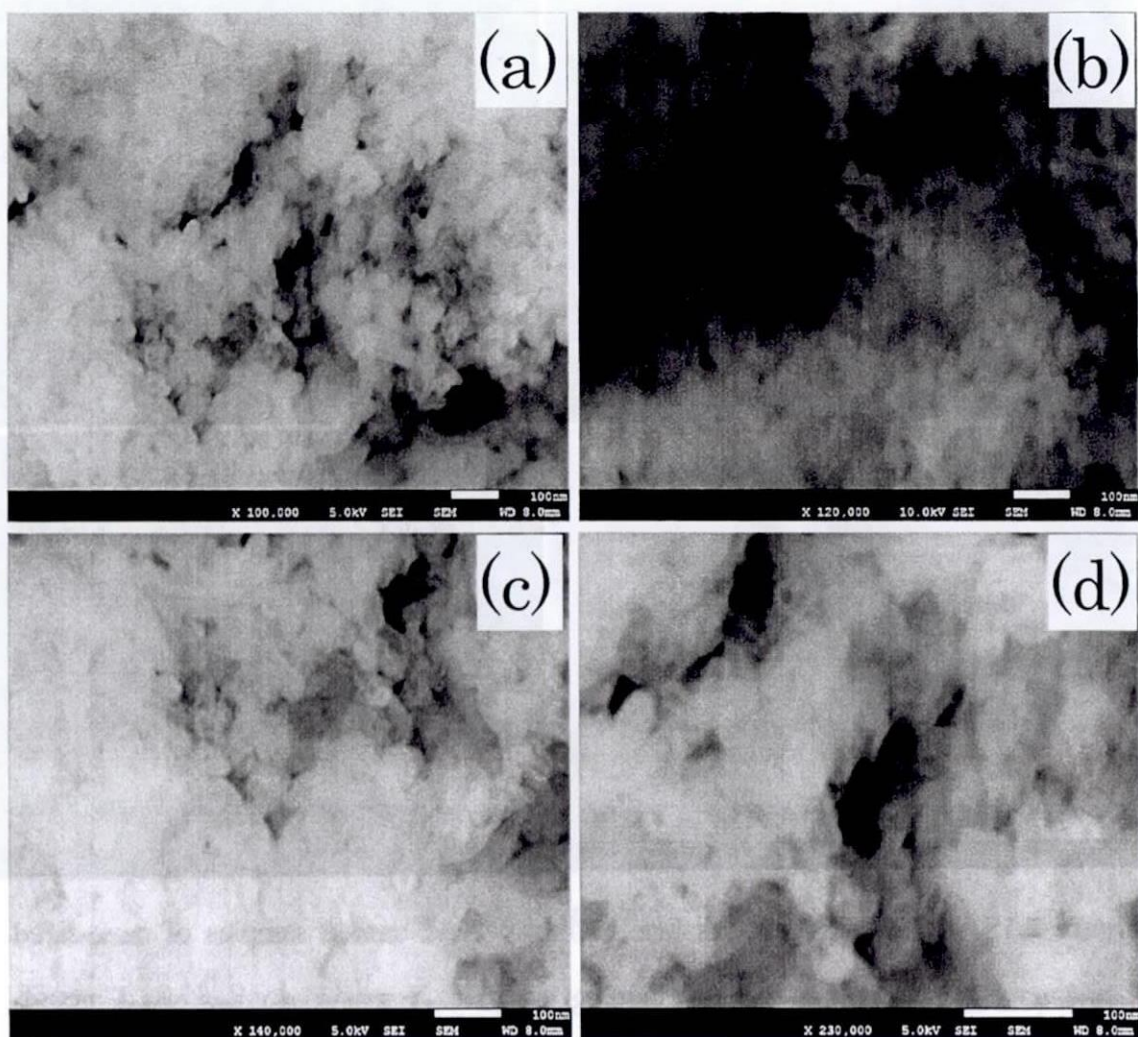


Figure 2.1S. 5 SEM images (bar line 100 nm) : Acid treated samples of nano-size hollow (0.5 mL TEOS) magnified at (a) X100000, (b) X 120000 (c) X 140000 and (d) X230000

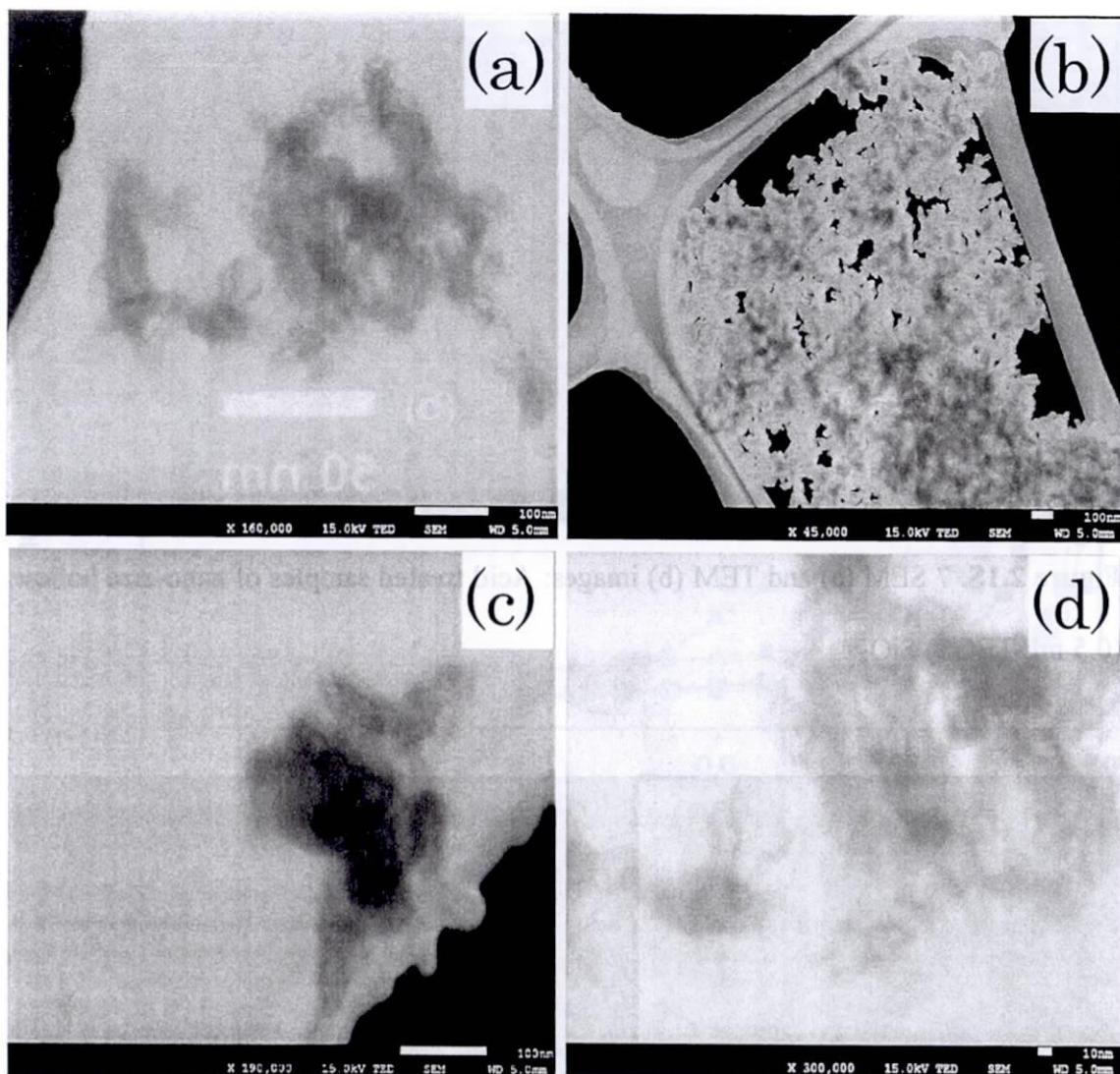


Figure 2.1S. 6 STEM images (line bar 100 nm [a,b,c] while in [d] 10 nm) : Acid treated samples of nano-size hollow (0.5 mL TEOS) magnified at (a) X160000, (b) X 45000 (c) X 190000 and (d) X300000.

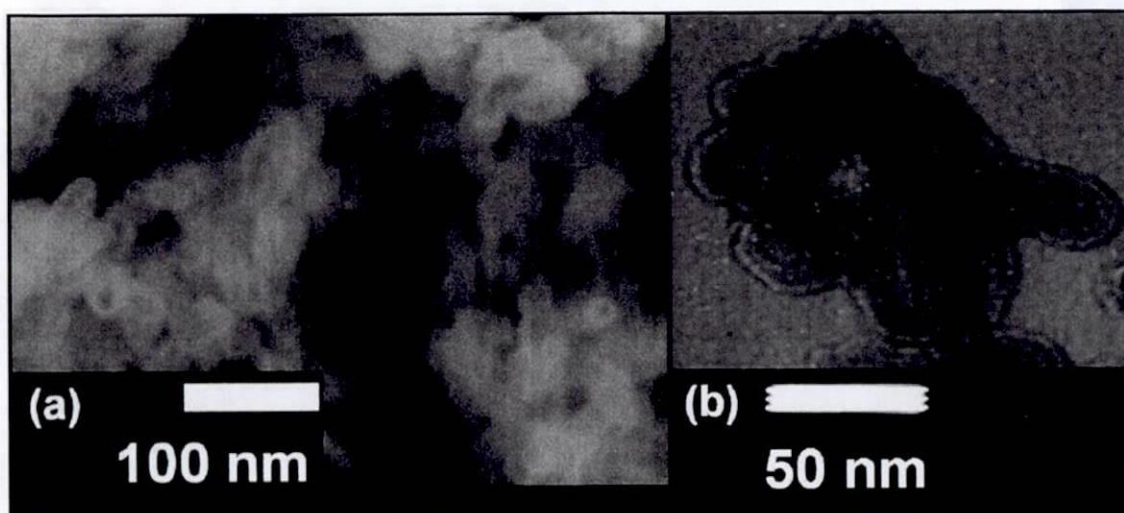


Figure 2.1S. 7 SEM (a) and TEM (b) images: Acid treated samples of nano-size hollow (0.5 mL TEOS) SiO_2

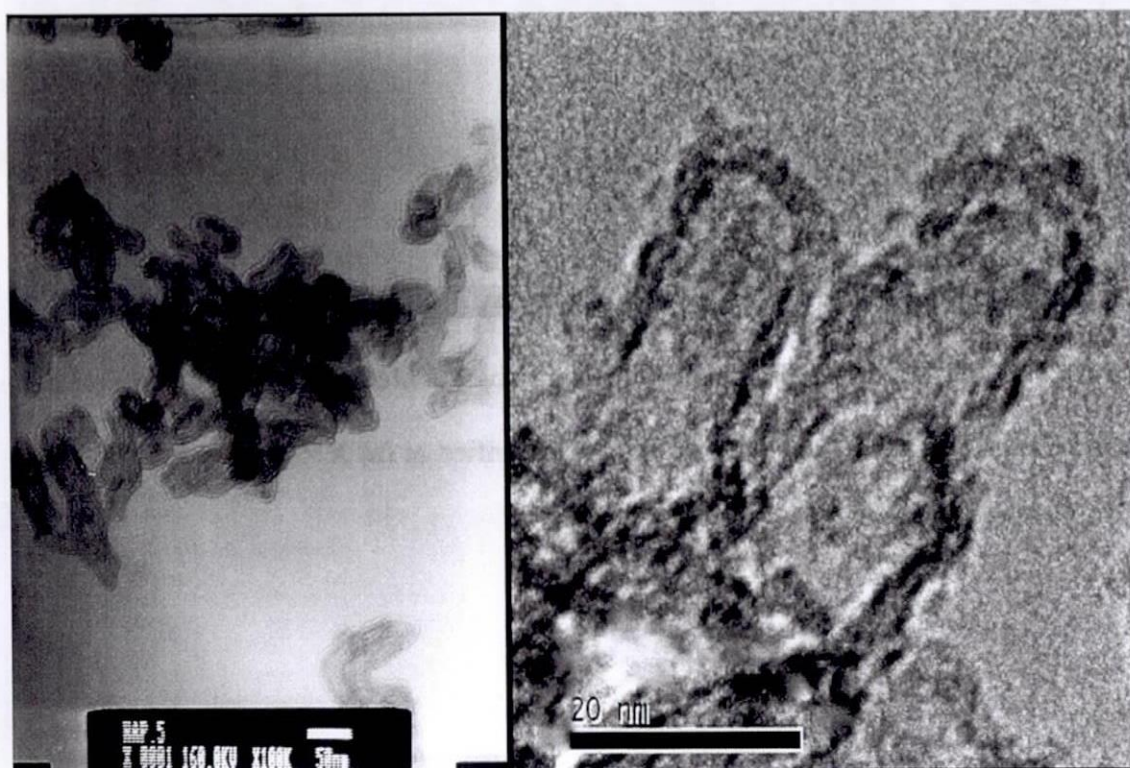


Figure 2.1S. 8 TEM images: Acid treated samples of nano-size hollow (0.5 mL TEOS) SiO_2

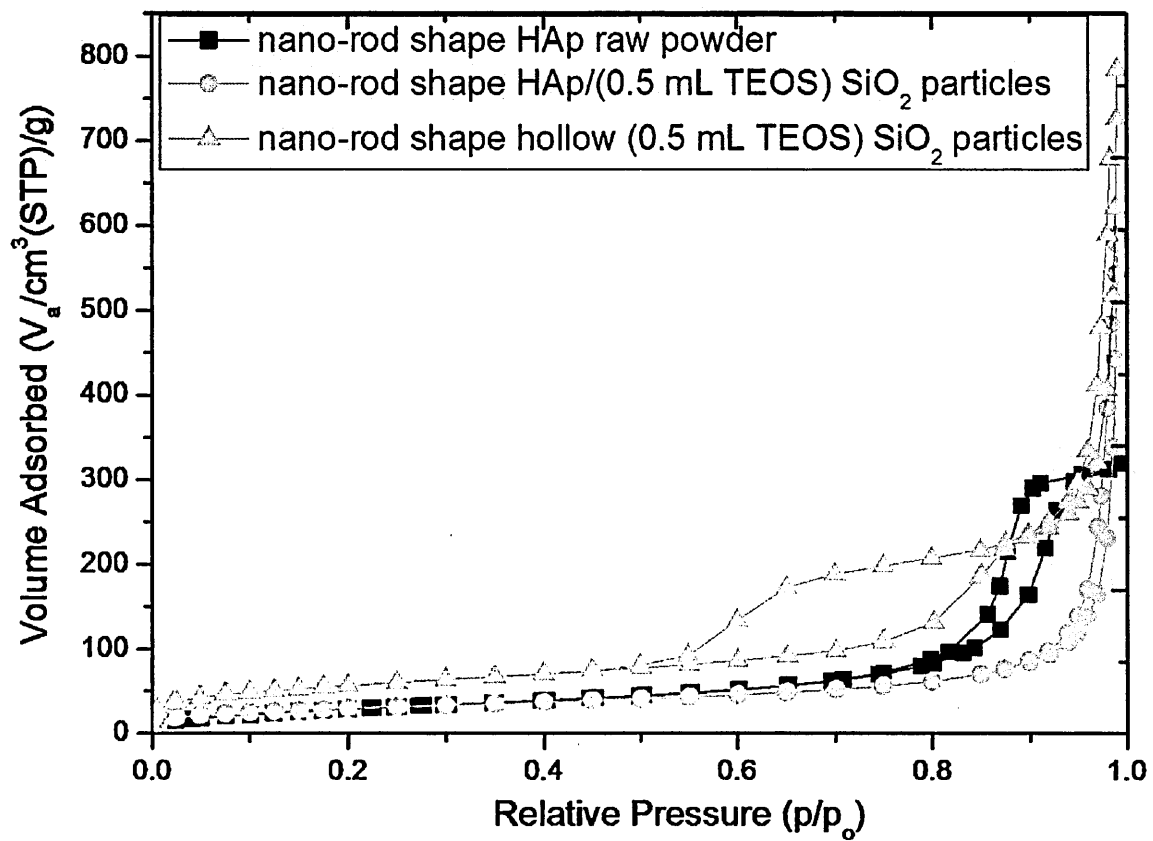


Figure 2.1S. 9 Nitrogen adsorption-desorption isotherms of nano-rod (spindles) shape CaHAp nanoparticles raw powder (■), core-shell CaHAp/ SiO₂ nanoparticles (●) and spindle-shape (rod) nano-size hollow silica particles (▲) synthesized at ambient temperature.

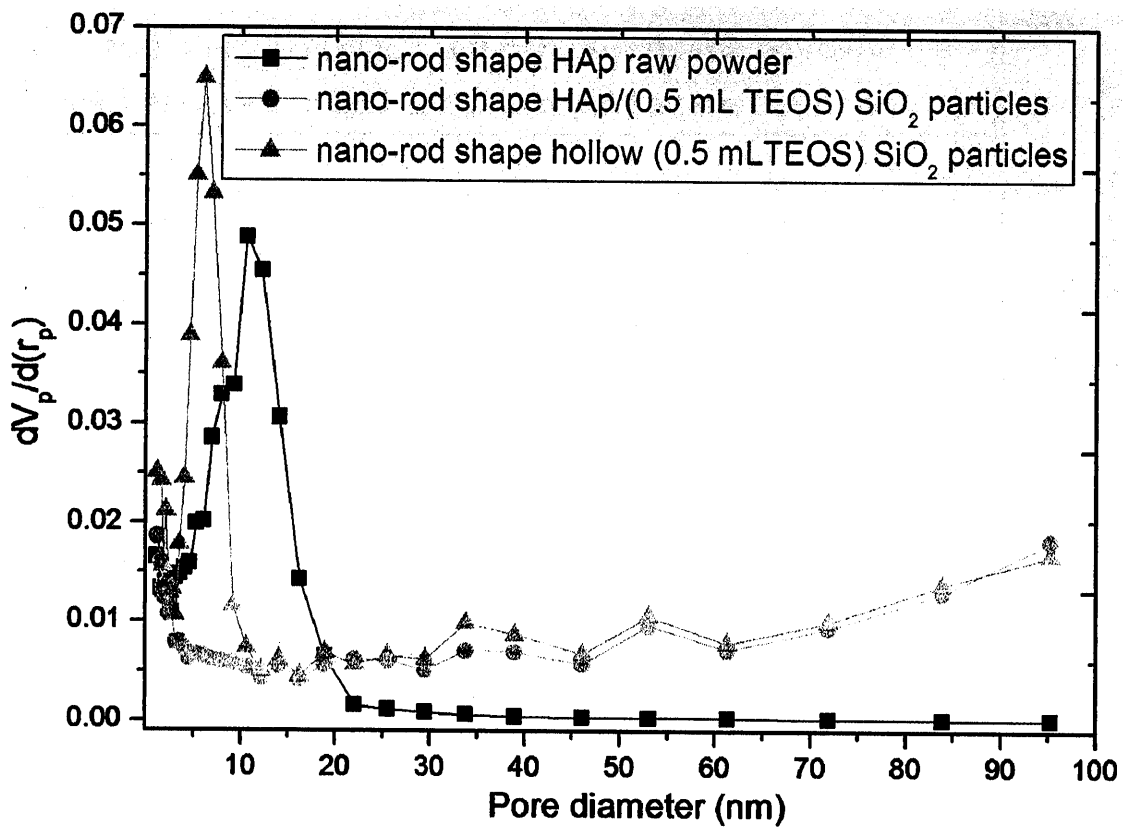


Figure 2.1S. 10 BJH differential pore size distribution of nano-rod (spindle) shape CaHAp nanoparticles raw powder (■), core-shell CaHAp/ SiO₂ nanoparticles (●) and spindle-shape (rod) nano-size hollow silica particles (▲) synthesized at ambient temperature.

CHAPTER 2

PREPARATION OF NANO- and MICRO-SIZE HOLLOW SILICATE PARTICLES (TEMPLATE METHOD)

2.2 INNOVATIVE TEMPLATE APPROACH

USING CALCIUM CARBONATE MICROPARTICLES (CaCO₃) IN FABRICATING ANISOTROPIC SHAPE MICRO-SIZE HOLLOW SILICATE PARTICLES

2.2 Innovative template approach using Calcium carbonate microparticles (CaCO₃) in fabricating anisotropic shape micro-size hollow silicate particles

2.2.1 Introduction

Most synthesized particles tend to compel for a spherical (interfaces) shape; somehow this designate that to create/fabricate anisotropic particles directly is fairly challenging. Basically, anisotropic particles are non-spherical shape, non-homogenous bulk composition with multiple compartments [1]. Specifically, hollow anisotropic particles with multiple compartments/holes have earned great interest in recent years. There had been reports that micro-scale with anisotropic hollow particles exhibited interaction direct-dependent with target surfaces and has non-uniform release profiles for biological drug delivery or environmental field application for studying the bacterial migration in soil/water surroundings [2].

Several techniques have been reported to fabricate anisotropic hollow particles[3] but the easily/mostly/directly used was template approached. This process can generate most complicated structures with good structural control of various sizes and shapes wherein the colloidal templates coated with different materials by means of sol-gel process[4], layer by layer approach[5] or chemical deposition[6], after then by calcinations or acid dissolution, hollow particles formed. Also, different anisotropic templates (such as inorganic {gold, hematites, silica, bimetallic}[7, 8], organic [9] [10, 11] and biotemplates {cellulose, collagen/silk, and DNA/virus}[12, 13]) had been utilized in fabricating anisotropic hollow particles.

However, most of the process/approach/materials (core-template) mention (above) required a lot of toxic (harmful) chemicals, elevated (high) temperature/pressure, and obscure with intricate post-treatment in removing core (metals, polymers

or organic materials) sacrificial template to form hollow particles. For these reasons, there is a need to explore other alternative and possibilities in producing anisotropic micro-scale hollow particles (AMSHP) under environmental friendly conditions and preserve morphology with disperse particles.

Herein in this section presented a simple, direct and flexible alternative to produce anisotropic micro-scale hollow silica particles using CaCO_3 particles as sacrificial template, forming micro-size hollow particles with anisotropic identical to the core (sacrificial) template.

2.2.2 Starting materials and schematic outline

2.2.2.1 Materials

Micro-scale particles calcium carbonate (CaCO_3) (Nittetsu Kogyo) used as core (sacrificial) templates. Tetraethoxysilane (Wako pure chemicals) used as precursor of silica shell. Ammonia water (28% Wako pure chemical) used as catalyst and Ethanol (Wako pure chemical) used as solvent for sol-gel template reaction

2.2.2.2 Synthesis of anisotropic micro-scale hollow silicate particles

Unique micro-scale anisotropic hollow silicate particles were synthesized based on the previous works done by our laboratory (CRL, NIT) using CaCO_3 as template[14]. Calcium carbonate (CaCO_3), ethanol (EtOH), tetraethoxysilane (TEOS) and ammonium aqueous solution (NH_4OH) were mixed and stirred for (least) 2 h at ambient temperature with molar ratio of 1.88:28.85:1:2.85 (CaCO_3 : EtOH: TEOS: NH_4OH), a core-shell (calcium carbonate/ silica) particles was made. (note: only the amount of TEOS and NH_4OH were varied (note: TEOS concentration varied at 1.5 mL, 2 mL, 3 mL and 4 mL accompanied by variation of NH_4OH concentration at 1.5 mL, 2 mL, 2.5 mL and 3 mL respectively)The synthesise product were filtered and washed

several times (4X or until becomes neutral) by ethanol/water, then vacuum dried (90 °C, 5 h). Acid treatment (3.0 mol/L) was done to remove CaCO₃ (core-sacrificial template) for 8 h stirring. After then, filtered and washed (4X) with ethanol/water. Finally, vacuum dried (90 °C, 1 d), anisotropic micro-sized hollow silicate particles was obtained, wherein the process flow schematically shown in Figure 2.2.1.

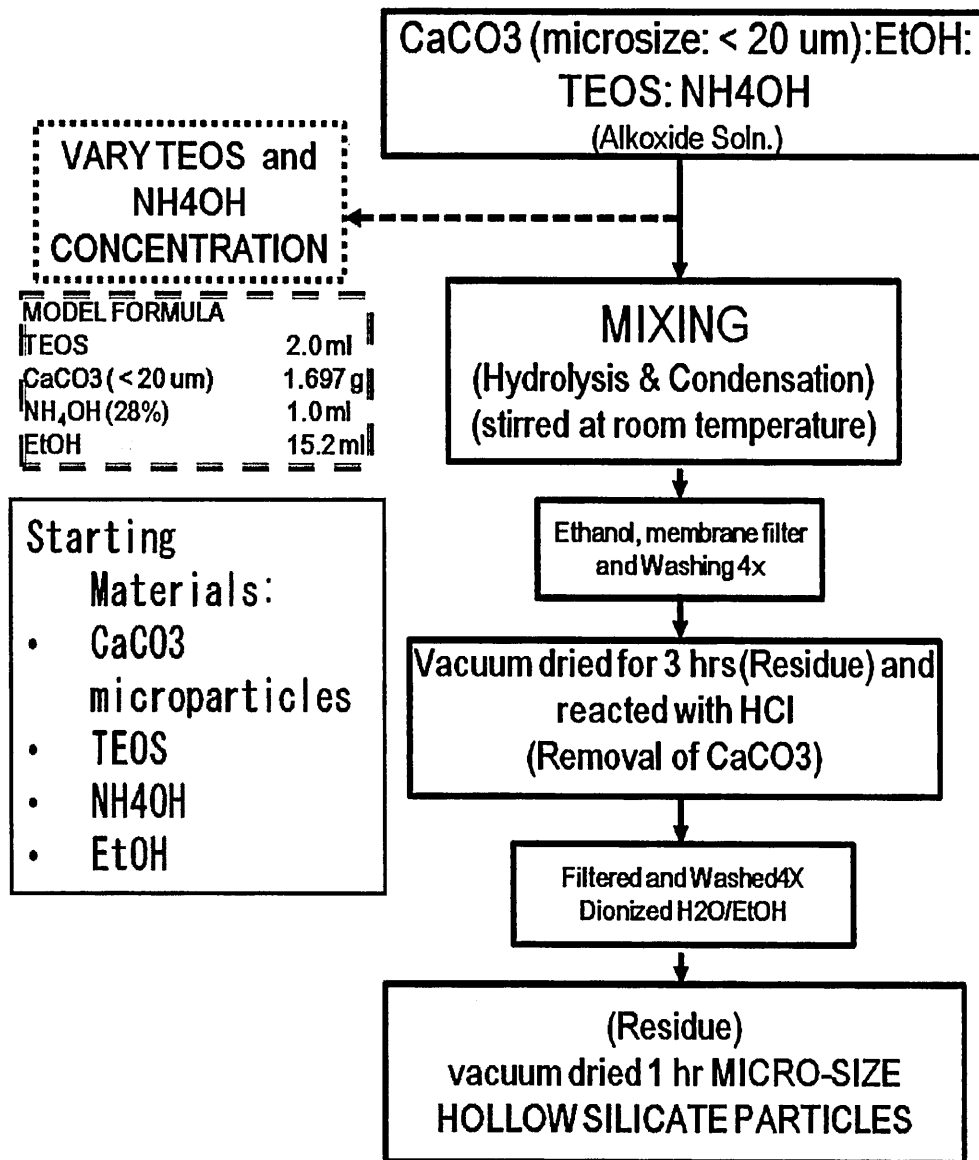


Figure 2.2.1 Process flow for the preparation/fabrication of the anisotropic micro-size hollow silicate particles using CaCO₃ microparticles as template core.

2.2.2.3 Physico-chemical characterization

The product were characterized by X-ray Diffraction (XRD, Model RINT 1100, Rigaku) with Cu K α radiation ($\lambda= 1.54056 \text{ \AA}$), at a scanning rate of of 0.02 $^\circ/\text{s}$ (5 $^\circ$ to 60 $^\circ$, 2 θ) with an operating voltage of 40 kV and emission current 30 mA. The thermal property of the sample was investigated using the Thermogravimetry (TG, TG-8120, Rigaku, Japan) under oxygen atmosphere. The heating rate of the temperature increase at 10 $^\circ\text{C}/\text{min}$ with temperature ranged from (22 to 1000) $^\circ\text{C}$. Morphology and microstructure of hollow particles were examined using scanning electron microscopy (SEM; JSM-7000F, JEOL). The specific surface area of the sample was determine by Barrett-Joyner-Halenda (BJH) method via automatic surface area analyzer (BELSORP-max) with Nitrogen gas adsorption and desorption isotherm recorded at 77K.

2.2.3 Results and discussion

2.2.3.1 Crystallographic and Morphological properties

In this section are results showing evidence of anisotropic micro-size hollow SiO₂ particles. The XRD analysis is shown in Figure 2.2.2. The XRD pattern (sharp peaks) of the as-synthesized micro-sized CaCO₃-SiO₂ (Figure 2.2.2b) is identical to (raw-calcite[15]) CaCO₃ (Figure 2.2.2a). In this case, micro-size CaCO₃ core (sacrificial -template) particles were technically coated by amorphous silica shell network. This was clearly verified thru acid dissolution (for 8 h) of the as-synthesized product (CaCO₃ dissolved) and no visual peaks (amorphous SiO₂ (Figure 2.2.2c)) was observed.

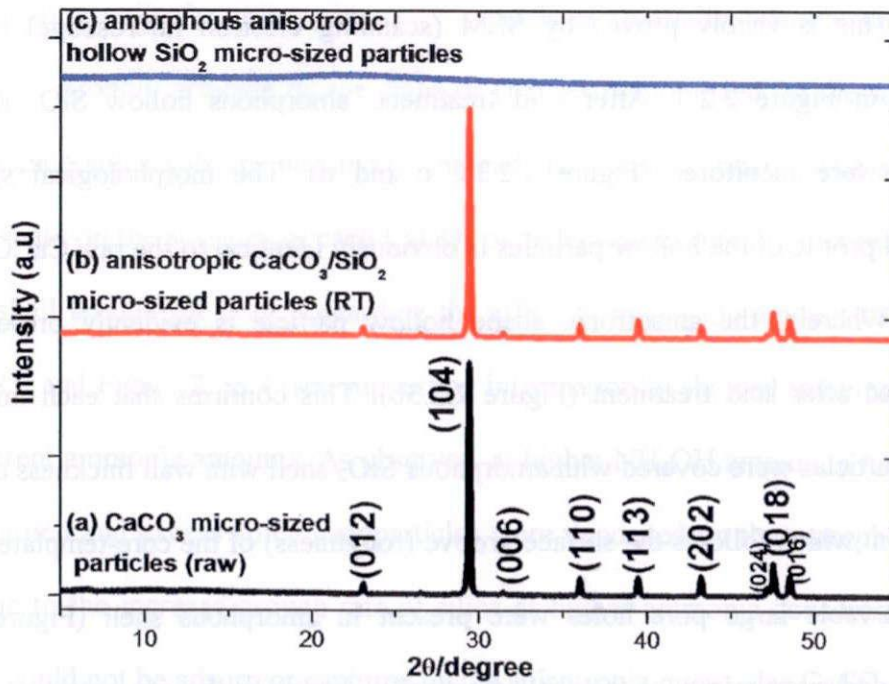


Figure 2.2. 2 XRD pattern of (a) CaCO₃ –raw, (b) as-synthesized CaCO₃-SiO₂ and (c) amorphous anisotropic micro-size hollow SiO₂ particles (AMSHP)

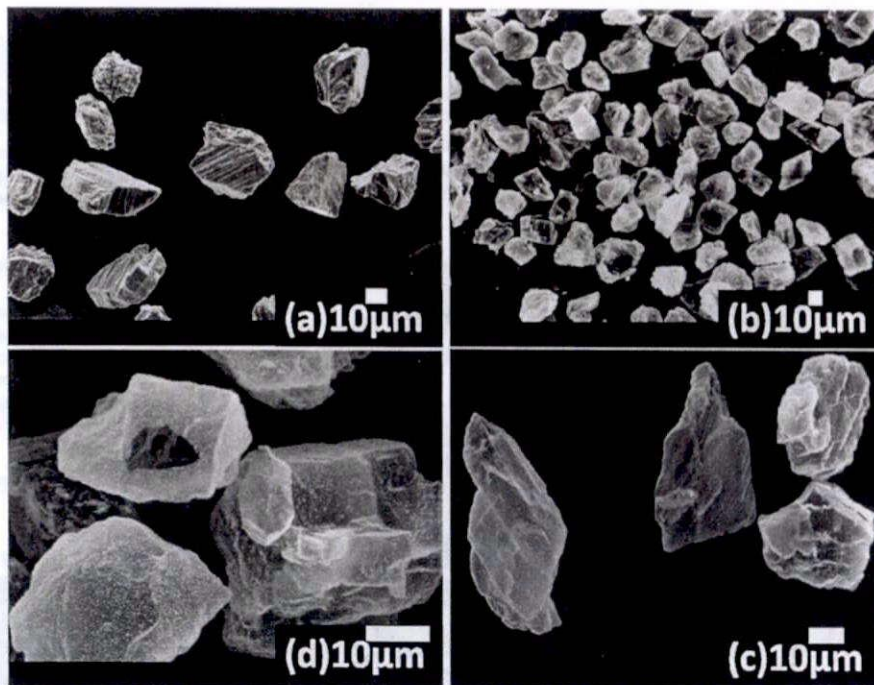


Figure 2.2. 3 SEM images of (a) micro-size CaCO₃ –raw, and anisotropic micro-size hollow SiO₂ in (b) x300, (c) x800 and (d) x1,700 magnification.

This is visibly proven by SEM (scanning electron microscope) images as revealed in Figure 2.2.3. After acid treatment, amorphous hollow SiO_2 micro-size particles were monitored (Figure 2.2.3b, c and d). The morphological shape and structural profile of the hollow particles is obviously identical to the raw CaCO_3 (Figure 2.2.3a). Wherein, the anisotropic shape hollow particle is evidently preserved and maintained after acid treatment (Figure 2.2.3b). This confirms that each micro-sized CaCO_3 particles were covered with amorphous SiO_2 shell with wall thickness appears to be uniform which follows the surface groove (roughness) of the core-template (CaCO_3) and observable large pore holes were present in amorphous shell (Figure 2.2.3d). Stability and morphology of the shell drastically change as the concentration of TEOS and NH_4OH concentration varied. The next section discussed these effects.

2.2.3.2 Morphological observation at increasing TEOS and NH_4OH concentration

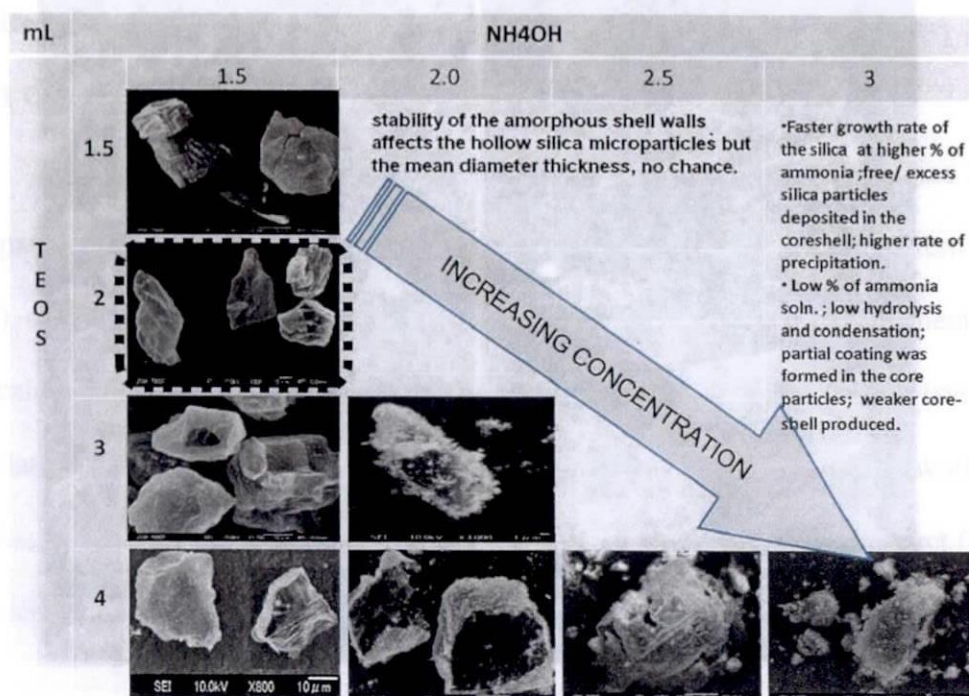


Figure 2.2. 4 SEM images of anisotropic micro-size hollow SiO_2 particles at increasing TEOS & NH_4OH concentration (broken box: ideal formula for AMSHP)

Coating colloidal micro-size CaCO_3 particles (partially positive charge[16]) with silica is strongly affected by the signs of charges immobilized on the surfaces of the cores since silica sols are negatively charged. In this case, many silica sols could easily nucleate on the surfaces of each CaCO_3 particles and eventually merge and grow into thin shell around the core. Regarding the effect of increasing amount of NH_4OH , Figure 2.2.4 and Figure 2.2S.4 (see supporting information's) showed samples obtained from different ammonia amounts. As observed, at higher NH_4OH amount, a rough silica coating formed and excess silica nanoparticles were deposited on the amorphous shell. This is due to the increase growth rate of silica at higher ammonia concentration [17, 18] that it could not be adsorbed or captured by the anisotropic micro-size CaCO_3 particles and free (excess) silica nanoparticles were more prevalently produced as seen in Figure 2.2.4 and Figure 2.2S.1. It was also noted that the system became less stable with high ammonia concentration and complete precipitation occurred immediately[17]. While at low concentration of ammonia, unstable hollow particles or no hollow formed as shown in Figure 2.2.4 and Figure 2.2S.4. Thereby, hydrolysis rate of TEOS is so slow that any deposition of silica on the CaCO_3 could not proceed. Hence the concentration of catalysis is very low and the shell formation did not proceed within the reaction time produced no hollow particles especially lower than 2.85 ratio of NH_4OH (> 1.5 mL).

Basically, the thickness of the coating layer could be conveniently controlled by adjusting the amount of TEOS solutions over a certain range. However as seen, thickness of the silica shell was maintained at 15 nm to 20 nm wherein an increasing (surplus) TEOS concentration generate more excess silica nanoparticles deposited on the amorphous shell as seen in Figure 2.2.4 and Figure 2.2S3, 2.2S.6, 2.2S.7. Similar to the amount of NH_4OH , the amount of TEOS also had an important effect on the

appearance of the hollow silicate particles since more TEOS amount implied a longer duration of etching according to the fixed dripping rate of the TEOS solution (see Figure 2.2S.5)

From the above discussion, it was interesting and necessary to have control over the formation of anisotropic hollow silicate micro-size particles (AMSHP). (Figure 2.2S.2 and 2.2S.3) In this case at room temperature, the amounts of TEOS and NH₄OH have been regarded as two important factors to decide whether AMSHP were obtained. However, some studies reported that both of them were not ideal to control over the formation of hollow particles for instance temperature and amount of core particles also affects the thickness and morphology of the hollow particles [17-19].

2.2.3.3 Thermal properties

From the ideal formula of the synthesized sample (core-shell composite and anisotropic micro-sized hollow SiO₂ particles), thermogravimetric (TG) and differential thermal analysis (DTA) were furtherly investigated as shown in Figure 2.2.5a (TG) and 2.2.5b (DTA) respectively. As projected in Figure 2.2.5, there are three significant temperature region detected for weight loss, which is mostly true for synthesized core-shell composite CaCO₃-SiO₂ microparticles.

Several features were detected: (i) free and bound water molecules was fully lost at < 200 °C; (ii) in the temperature range between 200°C and 360°C, combustion/lost of organic substances and (iii) core-shell CaCO₃-SiO₂ and CaCO₃, calcite crystals begin to decomposed at > 570 °C, the obviously majority occurred by the weight loss of CaCO₃ occurred owing to the thermal decomposing into CaO and CaCO₃-SiO₂ [20, 21]; proven by the weight loss maintain at approximately 50% in all the samples.

While for anisotropic hollow SiO_2 particles; region I (25 °C to 150 °C) was due to the removal of bound water while in region II (200 °C to 500 °C) mainly attributed to organic compounds and some loss of OH^- groups. Lastly, region III (above 520 °C) weight loss in this area is attributed to the structural change of amorphous silica shell network[22].

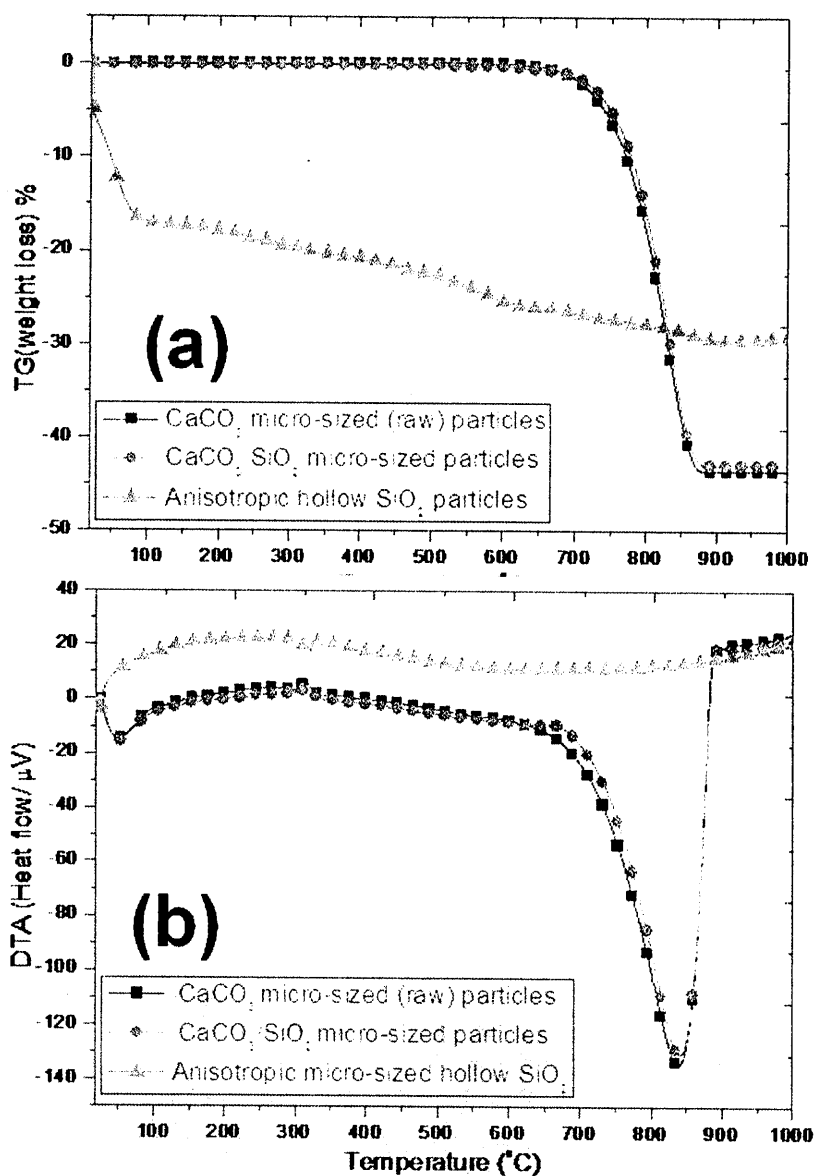


Figure 2.2. 5 TG(a)-DTA (b) monograph (ideal formula) of the synthesized anisotropic micro-size $\text{CaCO}_3\text{-SiO}_2$ particles and hollow anisotropic SiO_2 microparticles

2.2.3.4 N₂ adsorption/desorption properties

The surface area (BJH method) analysis as N₂- adsorption/ desorption isotherm (77K, Figure 4b) of anisotropic micro-sized hollow SiO₂ particles was classified as type II isotherm (*no plateau at high p/p₀*) based on the International Union of Pure and Applied Chemistry (IUPAC) nomenclature [23, 24]. It showed that the shell mainly amorphous with (49.23 to 75.35) m²/g surface area (BJH method) with pore holes larger than (2.0 to 3.6) nm (see the inset, Figure 4b). The results collaborated with the morphology profiles as observed in SEM images of the anisotropic hollow SiO₂ particles, uniform shell wall thickness that follows the surface roughness of the core-templates (CaCO₃) with randomly distributed pore holes in the amorphous shell (see Figure 2.2S.2 and 2.2S.3)

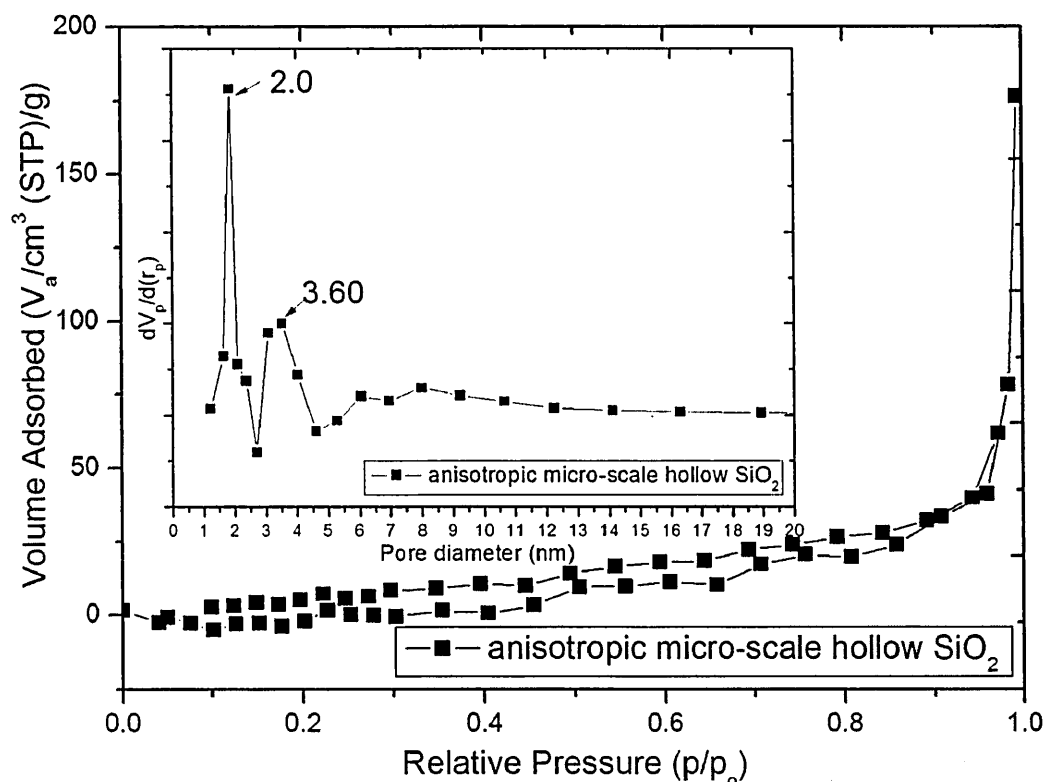


Figure 2.2.6 N₂ adsorption/desorption isotherm, inset is the corresponding pore – holes size distribution of the amorphous anisotropic micro-size hollow SiO₂

2.2.3.5 Mechanism for the formation of unique micro-size hollow silicate particles

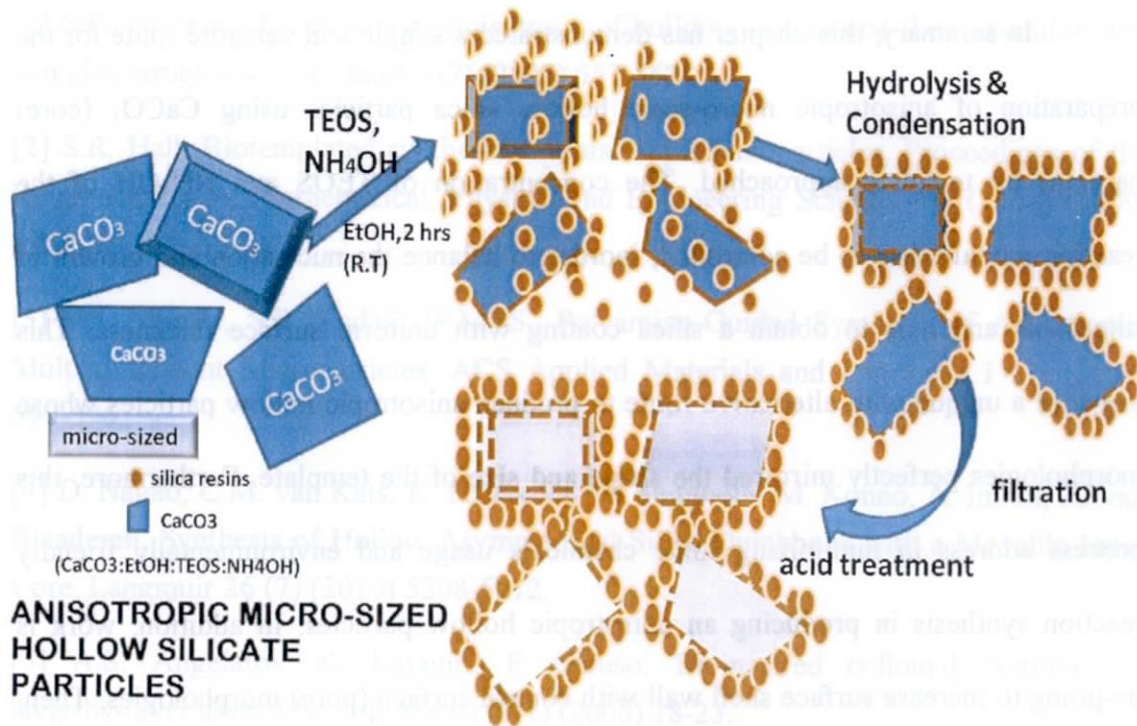


Figure 2.2.7 Schematic formation of anisotropic micro-size hollow silicate particles

In the coating process as illustrated in Figure 2.2.7, TEOS is added to the ammonia-contained CaCO_3 anisotropic micro-sized particles for sol-gel reaction. Under this condition, silica formed as the shell on the core particles via ammonia-catalyzed hydrolysis and condensation of TEOS [14, 17, 25]. Wherein the basic condition (pH 10-11), neighbouring silanol groups react with each other and form siloxane bonds via condensation reaction [17]. The mechanism proceeds via nucleation of silica in solution and the subsequent adsorption onto the surface of CaCO_3 particles. Notably, the kinetic reaction and with sufficient amount of siloxane (TEOS) to coat and encapsulate anisotropic micro-size CaCO_3 particles followed by acid treatment produced uniquely anisotropic micro-sized hollow silicate particles. Note that the AMSHP obtained using this method exhibited no obvious shape-size morphology difference of the core-template particles.

2.2.4 Conclusion

In summary, this chapter has demonstrated a simple and versatile route for the preparation of anisotropic micro-scale hollow silica particles using CaCO_3 (core) particles by template approach. The concentration of TEOS and NH_4OH of the reaction medium has to be controlled, in order to balance the nucleation and growth of silica sols and thus to obtain a silica coating with uniform surface thickness. This provides a unique with alternative route to produce anisotropic hollow particles whose morphologies perfectly mirrored the shape and size of the template. Furthermore, this process address in minimizing toxic chemicals usage and environmentally friendly reaction synthesis in producing an anisotropic hollow particles. In addition, work is on-going to increase surface shell wall with control surface (pore) morphologies. Then, functionalization of these anisotropic hollow silica microparticles for a possible application in targeting large drug delivery (LPP's) or triggering material for a chemical release application and other industrial application such as in ceramic, glass and cement production.

The uses and knowledge gained from this process in fabricating anisotropic hollow silica microparticle seem limitless and the availability of this simple method to make such hollow particles will catalyze many new discoveries and technologies.

References

- [1] S.C. Glotzer, M.J. Solomon, Anisotropy of building blocks and their assembly into complex structures, *Nat Mater* 6 (7) (2007) 557-562.
- [2] S.R. Hall, Biotemplated syntheses of anisotropic nanoparticles, *Proceedings of the Royal Society A: Mathematical, Physical and Engineering Science* 465 (2102) (2009) 335-366.
- [3] V.S. Murthy, S.B. Kadali, W.M. S., Polyamine-Guided Synthesis of Anisotropic, Multicomponent Microparticles, *ACS Applied Materials and Interfaces* 1 (3) (2009) 590-596.
- [4] D. Nagao, C.M. van Kats, K. Hayasaka, M. Sugimoto, M. Konno, A. Imhof, A. van Blaaderen, Synthesis of Hollow Asymmetrical Silica Dumbbells with a Movable Inner Core, *Langmuir* 26 (7) (2010) 5208-5212.
- [5] A.S. Angelatos, K. Katagiri, F. Caruso, Bioinspired colloidal systems via layer-by-layer assembly, *Soft Matter* 2 (1) (2006) 18-23.
- [6] W. Tong, C. Gao, Multilayer microcapsules with tailored structures for bio-related applications, *Journal of Materials Chemistry* 18 (32) (2008) 3799-3812.
- [7] N.C. Bigall, A. Eychmüller, Synthesis of noble metal nanoparticles and their non-ordered superstructures, *Philosophical Transactions of the Royal Society A: Mathematical, Physical and Engineering Sciences* 368 (1915) (2010) 1385-1404.
- [8] Y.B.D.G. Guozhen Shen, Recent developments in single-crystal inorganic nanotubes synthesised from removable templates, in, *Inderscience Publishers*, 2007.
- [9] M.S. Yavuz, Y. Cheng, J. Chen, C.M. Cobley, Q. Zhang, M. Rycenga, J. Xie, C. Kim, K.H. Song, A.G. Schwartz, L.V. Wang, Y. Xia, Gold nanocages covered by smart polymers for controlled release with near-infrared light, *Nat Mater* 8 (12) (2009) 935-939.
- [10] J.A. Champion, Y.K. Katare, S. Mitragotri, Making polymeric micro- and nanoparticles of complex shapes, *Proceedings of the National Academy of Sciences* 104 (29) (2007) 11901-11904.
- [11] K.J.C. van Bommel, A. Friggeri, S. Shinkai, Organic Templates for the Generation of Inorganic Materials, *Angewandte Chemie International Edition* 42 (9) (2003)

980-999.

[12] E. Pouget, E. Dujardin, A. Cavalier, A. Moreac, C. Valery, V. Marchi-Artzner, T. Weiss, A. Renault, M. Paternostre, F. Artzner, Hierarchical architectures by synergy between dynamical template self-assembly and biomineralization, *Nat Mater* 6 (6) (2007) 434-439.

[13] N.F. Steinmetz, D.J. Evans, Utilisation of plant viruses in bionanotechnology, *Organic & Biomolecular Chemistry* 5 (18) (2007) 2891-2902.

[14] M. Fuji, C. Takai, Y. Tarutani, T. Takei, M. Takahashi, Surface properties of nanosize hollow silica particles on the molecular level, *Advanced Powder Technology* 18 (2007) 81-91.

[15] R.V.R. Virtudazo, H. Watanabe, M. Fuji, M. Takahashi, A Simple Approach to form Hydrothermally Stable Templated Hollow Silica Nanoparticles, John Wiley & Sons, Inc., 2010.

[16] G.B. Sukhorukov, D.V. Volodkin, A.M. Gunther, A.I. Petrov, D.B. Shenoy, H. Mohwald, Porous calcium carbonate microparticles as templates for encapsulation of bioactive compounds, *Journal of Materials Chemistry* 14 (14) (2004) 2073-2081.

[17] H. Zou, S. Wu, Q. Ran, J. Shen, A Simple and Low-Cost Method for the Preparation of Monodisperse Hollow Silica Spheres, *The Journal of Physical Chemistry C* 112 (31) (2008) 11623-11629.

[18] Y. Lu, J. McLellan, Y. Xia, Synthesis and Crystallization of Hybrid Spherical Colloids Composed of Polystyrene Cores and Silica Shells, *Langmuir* 20 (8) (2004) 3464-3470.

[19] B. Tan, S.E. Rankin, Dual Latex/Surfactant Templating of Hollow Spherical Silica Particles with Ordered Mesoporous Shells, *Langmuir* 21 (18) (2005) 8180-8187.

[20] N. Yamasaki, T. Weiping, K. Jiajun, Low-temperature sintering of calcium carbonate by hydrothermal hot-pressing technique, *Journal of Materials Science Letters* 11 (1992) 934-936.

[21] E.T. Stepkowska, Z. Sulek, J.L. Perez-Rodriguez, A. Justo, C. Maqueda, Thermal and microstructural studies on mud with additives, *Journal of Thermal Analysis* 37 (1991) 1497-1511.

- [22] J.-A. Kim, J.-K. Suh, S.-Y. Jeong, J.-M. Lee, S.-K. Ryu, Hydration reaction in synthesis of crystalline-layered sodium silicate, *Journal of Industrial and Engineering Chemistry* 6 (4) (2000) 219-225.
- [23] K.S.W. Sing, Physisorption of nitrogen by porous materials, *Journal of Porous Materials* 2 (1995) 5-8.
- [24] K.S.W. Sing, D.H. Everett, R.A.W. Haul, L. Moscou, R.A. Pierotti, J. Rouquerol, T. Siemieniewska, Reporting physisorption data for Gas/Solid systems with Special Reference to the determination of surface area and porosity, *Pure and Appl. Chem.* 57 (4) (1985) 603-619.
- [25] H. Watanabe, M. Fuji, M. Takahashi, Synthesis, characterization and application of nano-sized hollow silica particles, in: *Proceeding 9th Ceramic Materials and Components for Energy and Environmental Application and Lazer Ceramics Symposium Conference, China, 2008*, pp. 145-150.

CHAPTER 2.2

Supporting Information

Innovative template approach using calcium carbonate microparticles (CaCO_3) in fabricating anisotropic shape micro-size hollow silicate particles

Results

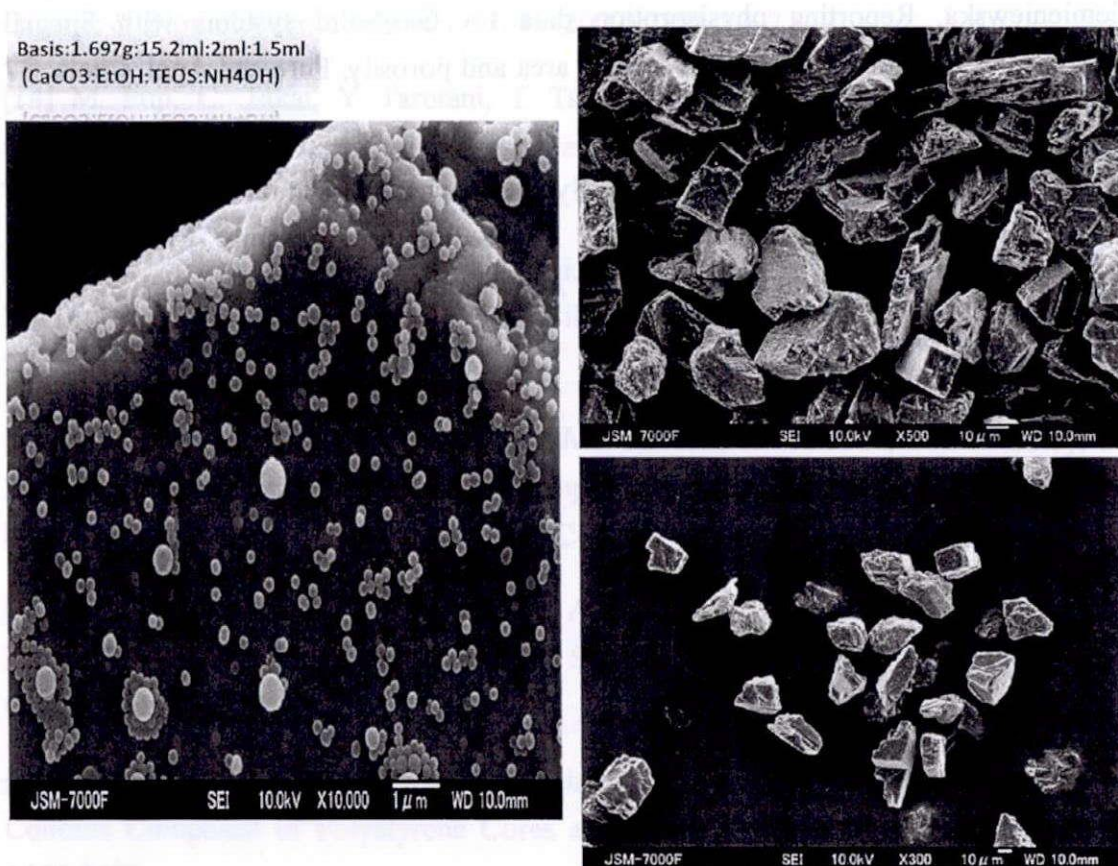


Figure 2.2S. 1. SEM images of the anisotropic core-shell CaCO_3 - SiO_2 particles with excess silica nanoparticles deposited in the amorphous SiO_2 shell wall

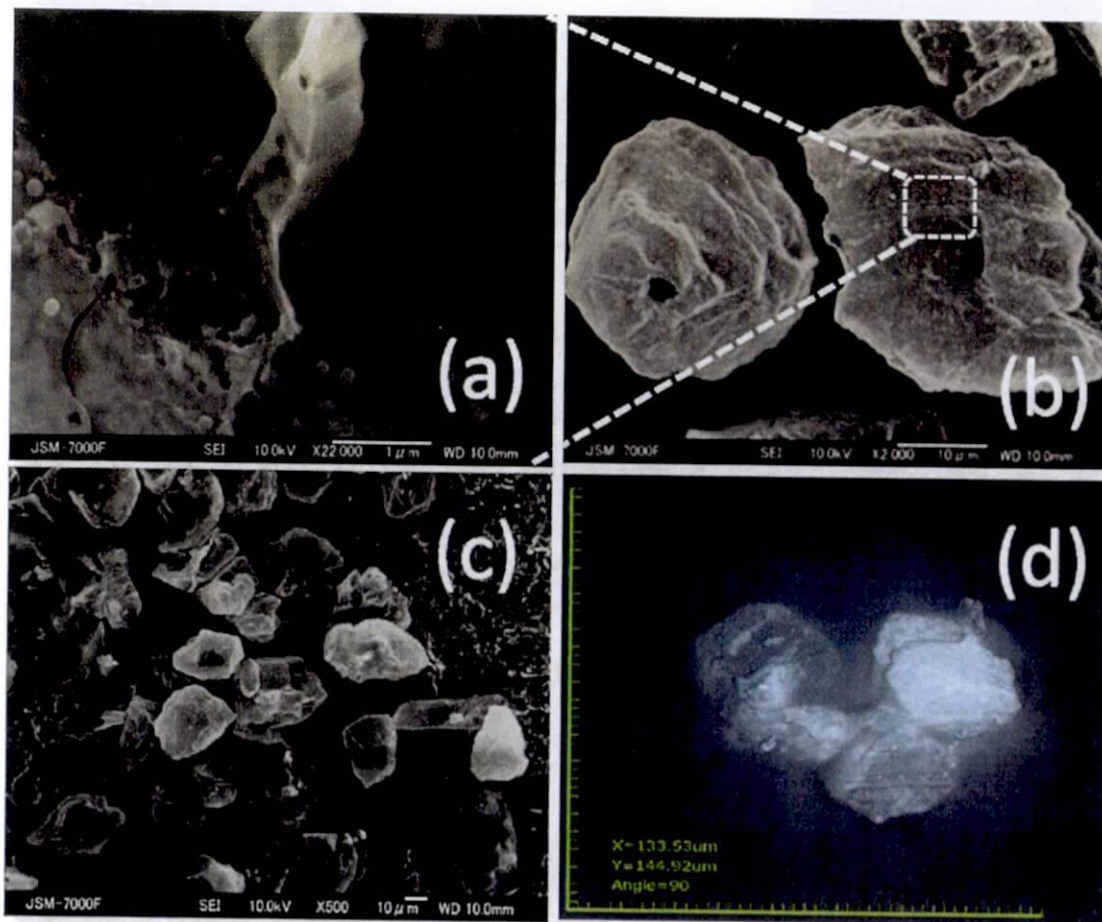


Figure 2.2S. 2 SEM images of anisotropic hollow SiO₂ particles at X22000 (a), X2000(b), X500 (c) magnification with laser optical microscope image (d)

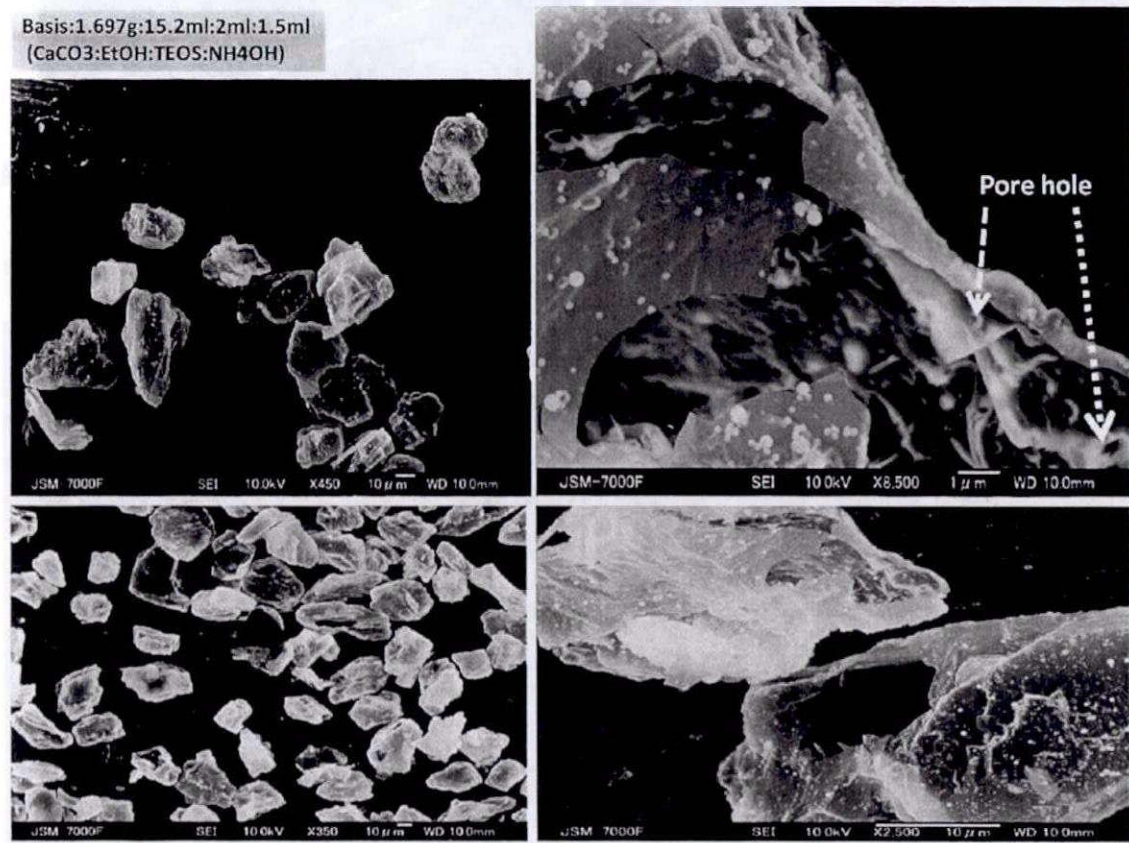


Figure 2.2S. 3 SEM images of anisotropic hollow SiO₂ particles at X450, X8500, X350, X2500 magnification showing the shell thickness of the amorphous shell

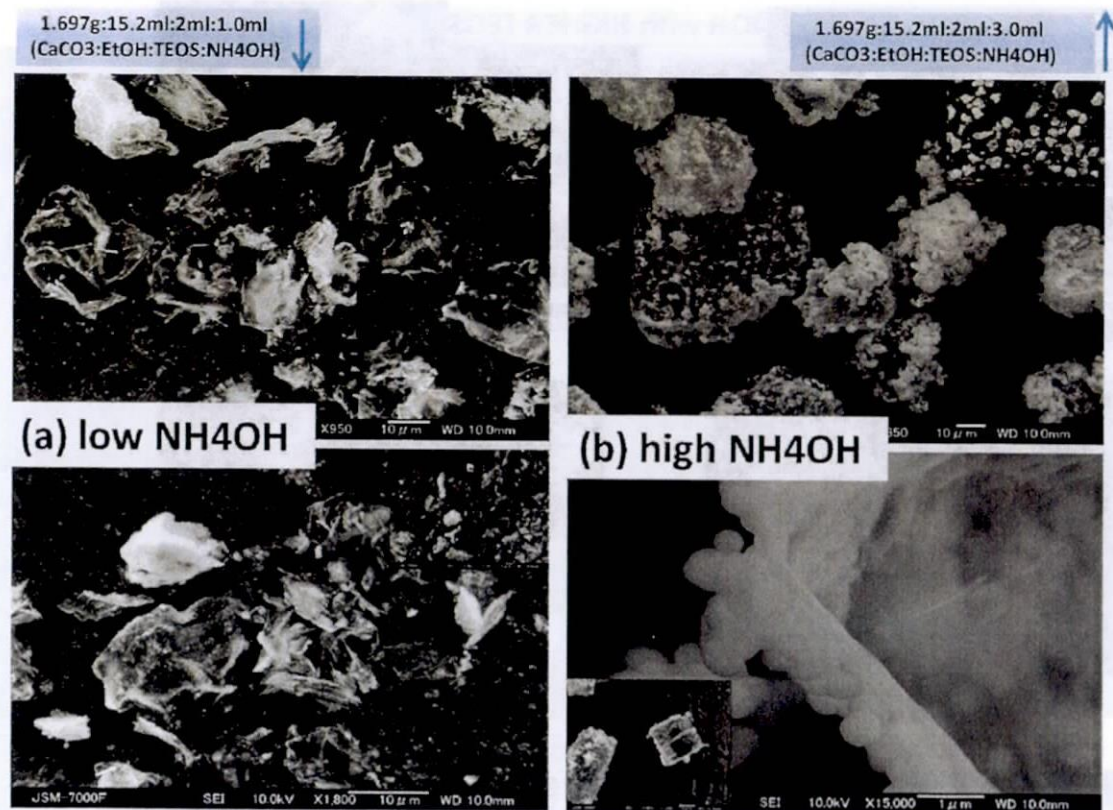


Figure 2.2S. 4 SEM images of anisotropic hollow SiO₂ particles at (a) low ammonia concentration and (b) high concentration of ammonia showing the shell thickness of the amorphous shell with excess silica nanoparticles deposited on the surface shell.

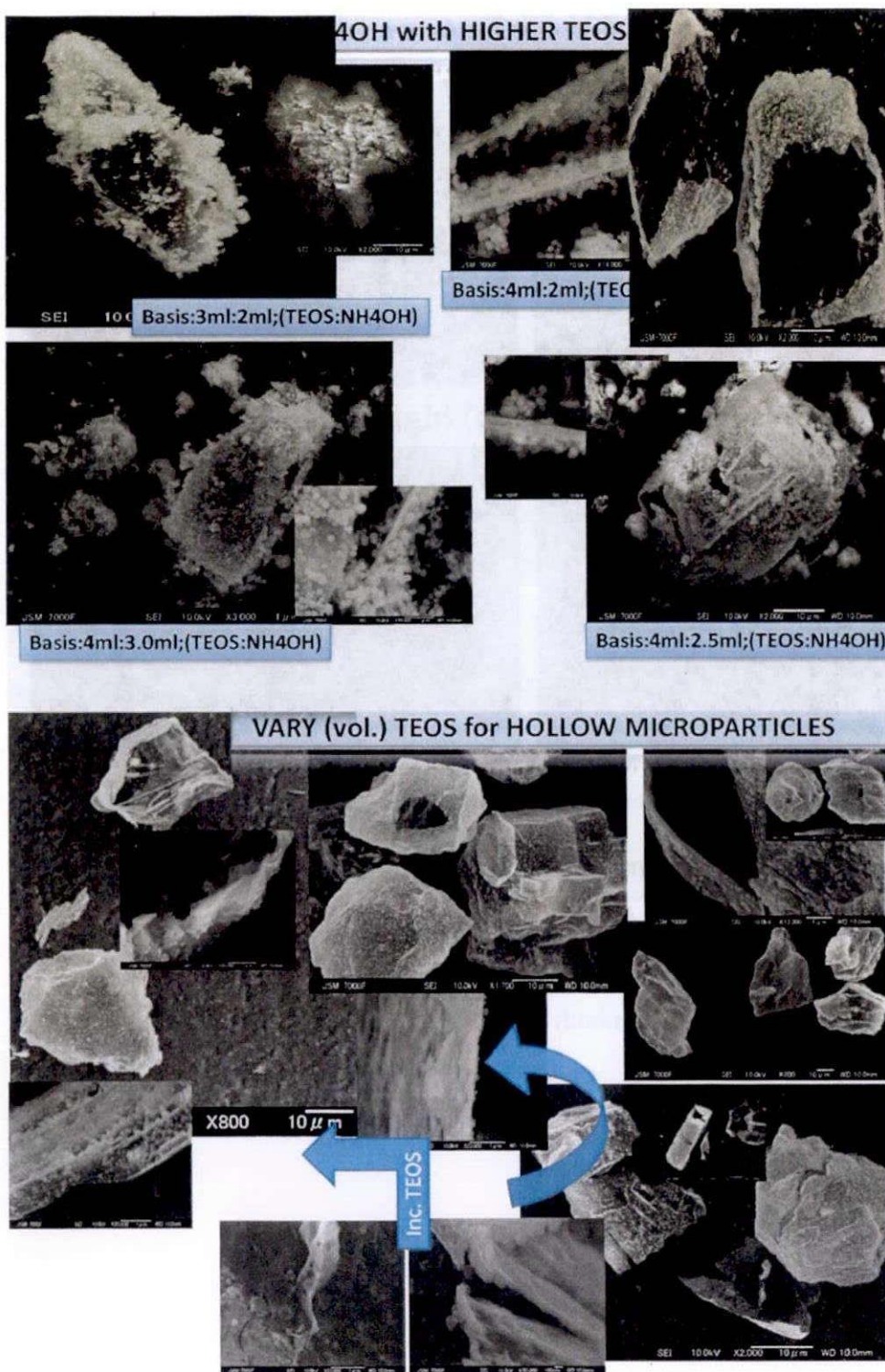


Figure 2.2S. 5 SEM images of anisotropic hollow SiO_2 particles at increasing TEOS concentration and showing the shell thickness of the amorphous shell with excess silica nanoparticles deposited on the surface shell.

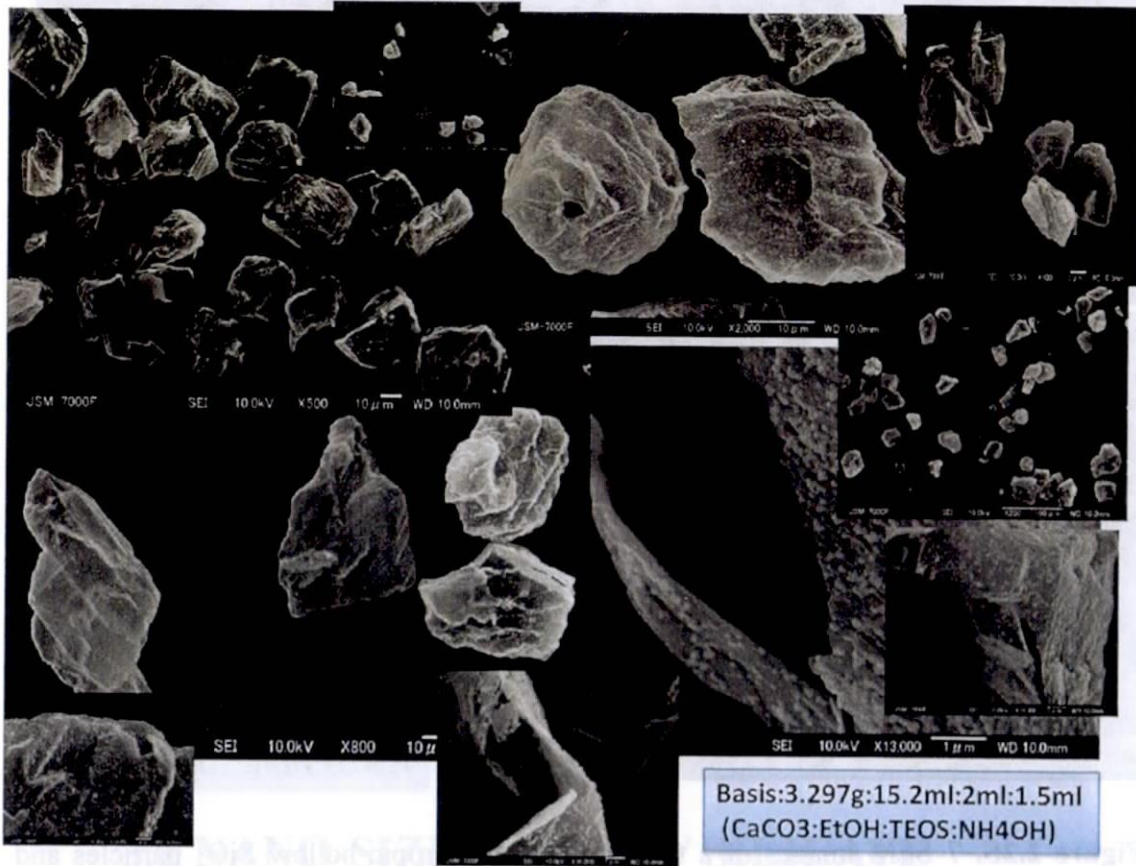


Figure 2.2S. 6 SEM images of a typical ideal anisotropic hollow SiO₂ particles and showing the shell thickness of the amorphous shell

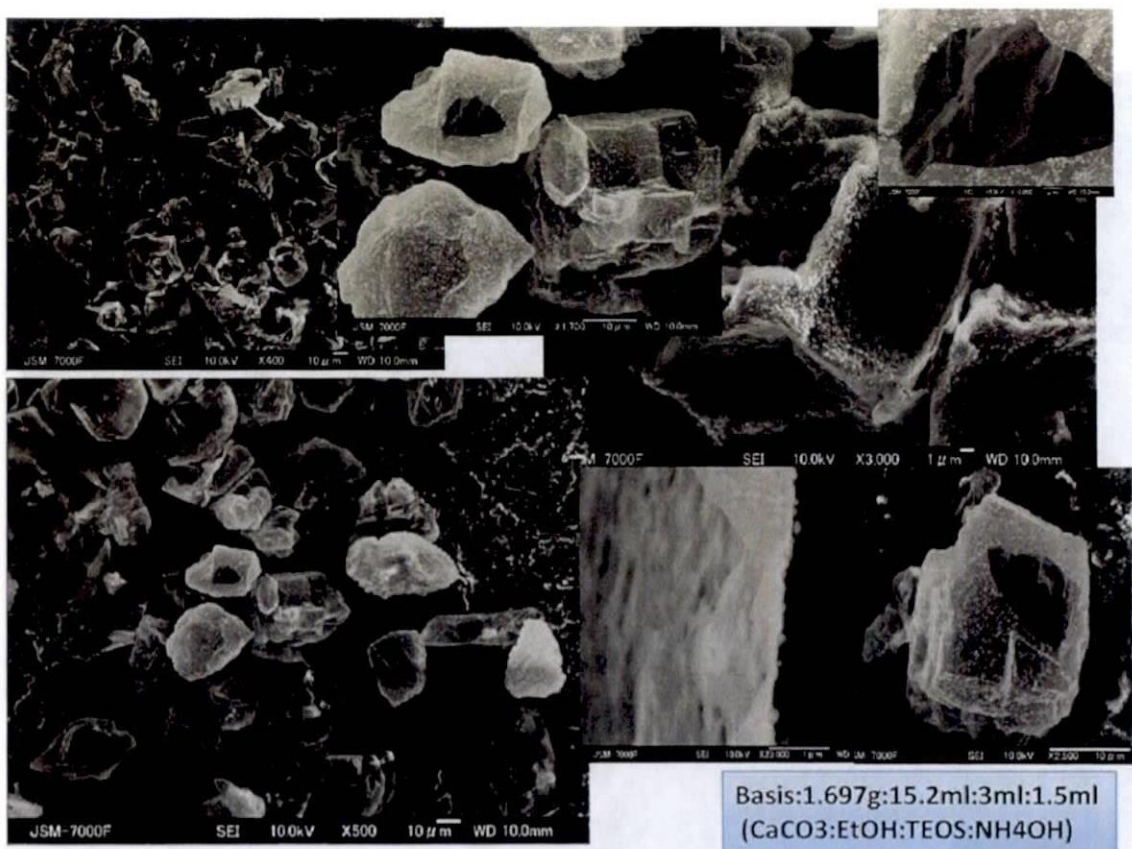


Figure 2.2S. 7 SEM images of a typical ideal anisotropic hollow SiO_2 particles and showing the shell thickness of the amorphous shell at increase TEOS but low in ammonia concentration.

CHAPTER 3

FABRICATION OF POROUS

(MICRO, MESO and MACROPROUS)

AMORPHOUS SHELL HOLLOW

SILICATE PARTICLES

3.1 NANO-SIZE HOLLOW SILICATE

PARTICLES WITH MICRO/MESOPOROUS

AMOPRHOUS SHELL BY DOUBLE

TEMPLATE APPROACH USING CaCO_3 and

CETYLTRIMETHYLAMMONIUM BROMIDE

(CTAB) SURFACTANT MOLECULES

CHAPTER 3

FABRICATION OF POROUS (MICRO, MESO and MACROPOROUS)

AMORPHOUS SHELL HOLLOW SILICATE PARTICLES

3.1 Nano-size hollow silicate particles with micro/mesoporous amorphous shell by double template approach using CaCO_3 nanoparticles and cetyltrimethylammonium bromide (CTAB) surfactant molecules

3.1.1 Introduction

Development of a simple and general method to coat as-synthesized nanoparticles such that the shell surfaces can be hierarchically structured [1, 2] have been exceptionally appealing especially hollow particles with exceptional meso-structured shells (HPMSs). These HPMSs has a unique combination of the characteristics of both macroporous and mesoporous structures in one single piece. The hollow cavity particles can act as storage basin or micro reactor,[3] as the meso-structure shell provides controlled release pathways for encapsulated particles/substances or substantial surface area for reactions.[4] As a results, HPMSs have engrossed strong awareness in a broad range of applications such as separation science, catalysis, sensors and drug delivery.[5] Numerous approaches have been developed in synthesizing HPMSs. Typically, divided into two types based on the template method for the formation of hollow particles. First type involves soft templates consist of block copolymer aggregates,[6] micelles,[7, 8] emulsion,[9, 10] and bubbles (acoustic cavities)[11] have been used to fabricate HPMSs. But, most hollow particles synthesized in the above process usually have non-uniform sizes and difficulty in controlling the morphology of the mesoporous shell. Wherein, commonly reported to be

sensitive to the reaction of the environment, which usually required strict control reaction condition.[12]

While second type, hard templates consist of organic-polymer particles[2, 13-15] and inorganic particles (metal oxides)[16] has been effective in synthesizing well defined hollow size particles with mesoporous shell structure, after the removal of the hard template via calcinations or acid treatment. Base from the cationic surfactant-silicate system,[17] mesoporous silica shell productively deposited on solid cores using cationic surfactant (CTAB (cetyltrimethyl ammonium bromide)) molecules as the structure-directing agent.[18] In previous studies done by Zhao et al., Tan et al. Blas et al. and Qi et al reportedly synthesized HPMSs using some polystyrene latex with cationic surfactant (double template) with tunable size and specific pore-size morphology.[13-15, 19] In addition, several other groups have also fabricated various HPMSs shapes such as an ellipsoidal HPMSs using hematite particles[20] and with diverse surface morphology like raspberry-like mesoporous shells.[21, 22] But, the above process involved the use of some toxic chemicals/ materials with sophisticated route that can be harmful to the environment in order to produce HPMSs.

With this view, CRL, Intelligent processing group (Fuji's laboratory) had been developing a more eco-friendlier approach in fabricating hollow silicate particles using cubic nano-sized CaCO_3 core particles as template.[23] Using the existing method in the Fuji's laboratory and with the addition of CTAB (structure-directing agent), a complex mesoporous structure can be obtained in the amorphous silicate shell. Previous studies done by Le et al group's attempted in utilizing their own synthesized nano-size CaCO_3 particles as core-template with CTAB via double-template method fabricated HPMSs.[24, 25] Although, these studies had done extensive efforts synthesizing hollow

particles with mesoporous shell structure (HPMSs), a facile and scalable high quality HPMSs has yet to be developed. The past reports fall short in maintaining the amorphous silicate shell stability with well defined meso-structure pattern of the HPMSs especially after removal of core template (ex: CaCO_3 or organic/inorganic template).

Here in this chapter reported a simple/modified process in synthesizing non-spherical HPMSs (NSHPMSs) at room temperature (R.T) reaction. The newly synthesized NSHPMSs possess smooth, uniform shell thickness with combined micro/mesoporous wormhole pattern thru modified acid-reflux to removed CaCO_3 core particles and CTAB molecules templates. With controlled particle size, the micro/mesoporous shell thickness can be fined tuned by adjusting the silica source. In this paper, NSHPMSs are investigated with scanning transmission electron microscopy (STEM), transmission electron microscopy (TEM), X-ray Diffraction (XRD in small angle), and nitrogen sorption measurements. Based on the results, a model for the formation of non-spherical hollow silicate with micro/mesomorphous shell (NSHPMSs) is shown in Figure 3.1.1. These specially designed hollow particles covers the different requirements of various nano-science applications.

3.1.2 Starting materials and schematic outline

3.1.2.1 Materials

Nano-cube 60 Calcium carbonate (CaCO_3 , RMHA) (Nittetsu Kogyo) was used as core particles (1st template) while, hexadecyltrimethylammonium bromide (CTAB, 99% Nacalai Tesque, Inc.) as the 2nd template to form a micro/mesoporous shell. Tetraethoxysilane (TEOS, Wako pure chemical) was used as precursor of silica shell.

Ammonia water (NH_4OH , 28% Wako pure chemical) used as catalyst and Ethanol (EtOH , 99% Wako pure chemical) used as a solvent sol gel template reaction.

3.1.2.2 Preparation of $\text{CaCO}_3/\text{CTAB}/\text{SiO}_2$ with micro/mesostructure shell wall

Simpler approached for the fabrication of nano-sized hollow silicate particles with micro / mesoporous shell structure (NSHPMSs) were synthesized base on the previous method done by our laboratory (CRL, NIT) using nano-sized CaCO_3 as 1st template [23, 26] and with additional CTAB as 2nd template (followed the modified synthesis of mesoporous material [27-29]). In this case, CTAB (Cy) was completely dissolved in deionized water (H_2O) by magnetic stirrer at R.T until it becomes clear solution (CTAB solution). Separately, nano-size CaCO_3 mixed with ethanol (EtOH) by magnetic stirrer for about 15 minutes (CaCO_3 solution). Then, CTAB solution and CaCO_3 solution were combined under stirring for 30 minutes at R.T (CTAB+ CaCO_3 solution). Next, NH_4OH (28%) was added to the CTAB+ CaCO_3 solution under vigorous stirring until the solution becomes pH 10-11. After further stirring for 30 minutes, certain amount of TEOS (Tx) was added to the CTAB+ CaCO_3 solution (white milky solution). Then white solution continuously mixed and stirred for 24 h at R.T with the final general molar ratio of $\text{CaCO}_3:\text{EtOH}:\text{TEOS}:\text{H}_2\text{O}:\text{NH}_4\text{OH}:\text{CTAB} = 7:58:1:144:11:0.3$, as synthesized core-shell calcium carbonate / silicate nanoparticles with micro/mesoporous shell structure (CSNSMSs) was prepared. After 24 h continuous stirring, the white gel solution was filtered and washed several times (4X or until becomes neutral) by ethanol. Then, the samples were dried in a vacuum oven to 90 °C for 5 h.

3.1.2.3 Fabrication of hollow silicate nano-size particles with micro/mesostructure shell wall (NSHPMSs)

For complete removal of CaCO₃ core and excess surfactant (CTAB) template, a certain amount of 0.7 g as-synthesized solid sample (CSNSMSs) was carefully refluxed (mixture weak of acid) in a 20 ml (10 mL, 3.0 mol/L, HCl in EtOH : 10 mL, 10% acetic acid in EtOH) acid reflux at 75 °C, stirred for 24 h. After then, filtered and washed several times (4X or until becomes neutral) with distilled H₂O/EtOH mixture. Finally, vacuum dried the obtained sample to 90 °C for 1 d, NSHPMSs was obtained. The schematic process flow for the formation of hollow silicate nanoparticles with micro/mesoporous is shown in Figure 3.1.1.

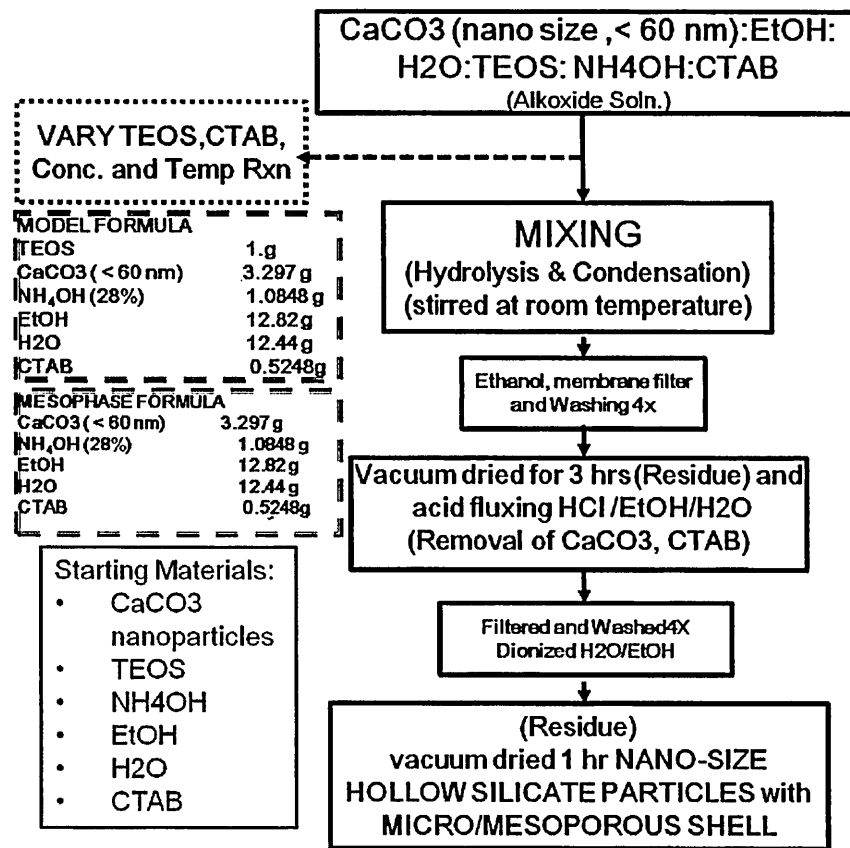


Figure 3.1. 1 Process flow for the fabrication of micro/mesoporous shell wall hollow silicate nanoparticles by double template method (CaCO₃ nanoparticles/CTAB)

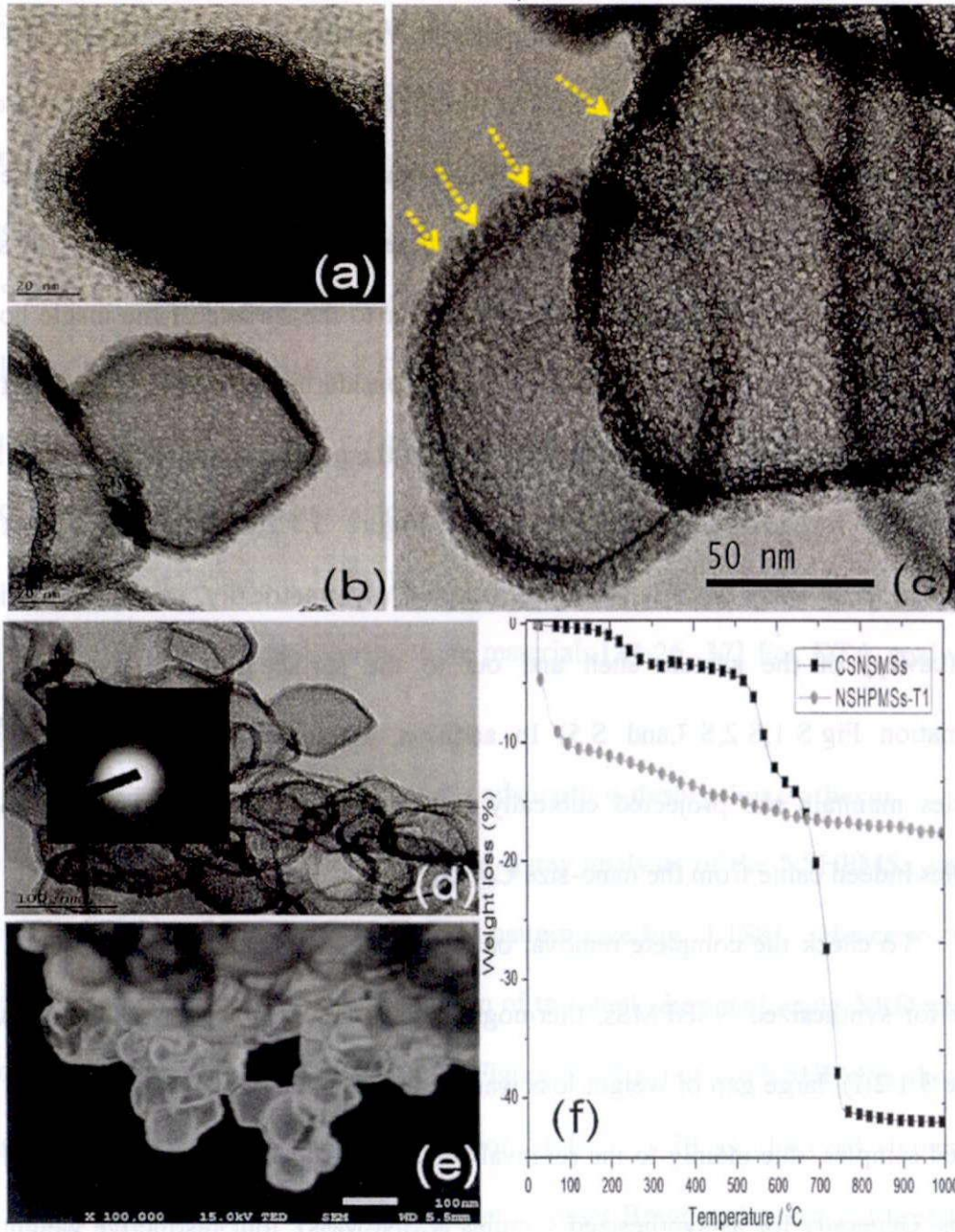
(Note: TEOS ($x = 1$ ml to 4 ml; denoted as NSHPMSs-T x) and CTAB ($y = 0.12$ g to 0.82 g; denoted as NSHPMSs-C y) concentration varied to optimized the fabrication of cubic shape hollow silicate nano-size particles with micro/mesoporous shell. (see Fig.3.1S2 to 3.1S12; supporting Information). Additional inquiry, increase temperature reaction were also investigated which are denoted as NSHPMSs-Z ($Z =$ temperature). For simplicity of this report, the researcher focused on the general results of NSHPMSs-T1 or NSHPMSs-C0.52). Then discussed possible effect upon addition of TEOS, CTAB concentration and elevate temperature reaction in a schematic illustration based on the actual data's

3.1.2.4 Physico-chemical characterization

The product were characterized by X-ray Diffraction (XRD, Model RINT 1100, Rigaku) with Cu K α radiation ($\lambda = 1.54056$ Å), with scanning speed of 0.05° and scanning length of $0.02^\circ/s$ at a small angle (1° to 10° , 2θ) with an operating voltage of 40 kV and emission current 40 mA. Thermal property of the sample was investigated using the Thermogravimetry (TG, TG-8120, Rigaku, Japan) under oxygen atmosphere. Heating rate of the temperature increase at $10^\circ C/min$ with temperature ranged from (22 to 1000) $^\circ C$. Morphology and microstructure of hollow particles were examined using scanning electron microscopy (SEM; JSM-7000F, JEOL) and transmission electron microscopy (TEM, 2000EXII). In STEM and TEM observation, the samples were dispersed in ethanol ultrasonically and were dropped into the copper grid. The specific surface area was calculated by Brunauer-Emmett-Teller (BET) method while pore size distribution of the micro/mesoporous was determined by Barrett-Joyner-Halenda (BJH) method via the automatic surface area analyzer (BELSORP-max) with Nitrogen gas adsorption and desorption isotherm recorded at 77K.

3.1.3. Results and Discussion

3.1.3.1 Morphological observation and Thermal properties



In Figure 3.1.2, STEM (Fig.3.1.2 (e)) and TEM images of non-spherical as-synthesized samples (CSNSMSs) (Fig. 3.1.2(a)) with (cubically) hollow silicate nanoparticles (Fig.3.1.2 (b), (c), (d)) are shown. Visually showed nano-sizes ($\sim < 100$ nm) with an average size of 60 nm hollow particles and uniform shell thickness around (10 to 15) nm. TEM images (Figure 3.1.2(b,c)) observations revealed a wormhole-like pore openings. At the sides of the shell, the pores were directly observed; in some region appeared, aligned parallel and perpendicular to the surface of the inside hollow (cavity) particles (see arrows in Figure 3.1.2(c)). Considering the whole hollow particles, pores (amorphous wormhole pattern) distributed at the perpendicular to the surface shell, producing a ring diffraction pattern (inset: Figure 3.1.2(d)). Indicating that the amorphous pore walls were randomly distributed asymmetrically, started at the inner part (cavity) of the silicate shell and out to the surface.[30-33] (see supporting information Fig.S.1,S.2,S.3,and S.5) In addition, stable nano-sized hollow silicate particles maintain the projected cubically hollow shape, expected shape of hollow particles indeed came from the nano-size CaCO_3 core (1st) template.[23, 26]

To check the complete removal of the templates (CTAB and CaCO_3) via acid reflux for synthesized NSHPMSs, thermogravimetric analysis was used. As shown in Figure 3.1.2(f), large gap of weight loss was observed between as-synthesized and acid-fluxed samples, due mainly to the removal of CaCO_3 , CTAB, organic solvent and OH groups. Generally for as-synthesized samples (CSNSMSs), four distinctive weight loss steps were observed (Figure 3.1.2(f ■)). Step 1 (25 °C to 175 °C) associated with the physically absorbed water [34] (~ 0.32 %) and step 2 (200 °C to 385 °C) related to the decomposition of the organic /CTAB template [35] ($\sim 3.2\%$). Then step 3 (400 °C to 550 °C), directed to the decomposition of OH groups in the $\text{CaCO}_3\text{-SiO}_2$ and the

remaining organic ions [36] (~10%) and step 4 (550 °C to 750 °C) attributed to the complete decomposition of CO₂ and the condensation of silanol groups to form siloxane bonds [34] (~28.9%).

While for acid-refluxed samples (NSHPMSs), three steps were approximately observed in Figure 3.1.2(f ●). In step 1 weight loss (25 °C to 175 °C): also removal of bound water due to the unattached molecular water (~11%). While in step 2 (200 °C to 500 °C): slight weight loss, mainly attributed to some loss of OH⁻ groups (~4.0%); clearly at this point, removal of CTAB molecules was achieved thru acid fluxing. Then in step 3 (above 520 °C): characteristic of structural change (condensation of silanol groups to form siloxane bonds) and decomposition of OH⁻ groups [34](~2.5%). (see supporting information Fig.3.1S7) These results were similar to other studies involving hollow silicate and mesoporous materials.[24-26, 37] For DTA analysis of these samples see Figure 3.1S7.

3.1.3.2 Small-angle X-ray pattern and N₂ adsorption-desorption isotherm

The complete long range powdered X-ray analysis of the NSHPMSs samples predictably exhibited an amorphous silicate pattern (see Fig. 3.1S8). Hence to clearly prove the meso-structure (wormhole) pattern of the shell, the small angle XRD analysis was done. The small-angle X-ray pattern (Figure 3.1.3(a)) of the NSHPMSs showed a strong and broad (100) low angle reflection at (~2.3°) 2θ as observed (typical for MCM-41 wormhole pattern [38]). The absent of other Bragg reflection and broadening of low angle reflections were generally lack of long-range crystallographic order or finite size effect.[31, 39] (see Fig. 3.1S9) By calculation from the d_{100} spacing,[30, 31, 33] the average lattice parameter equals (3.53 to 4.10) nm. By inspection thru TEM images, the calculated results coincide with the observed TEM micrograph.

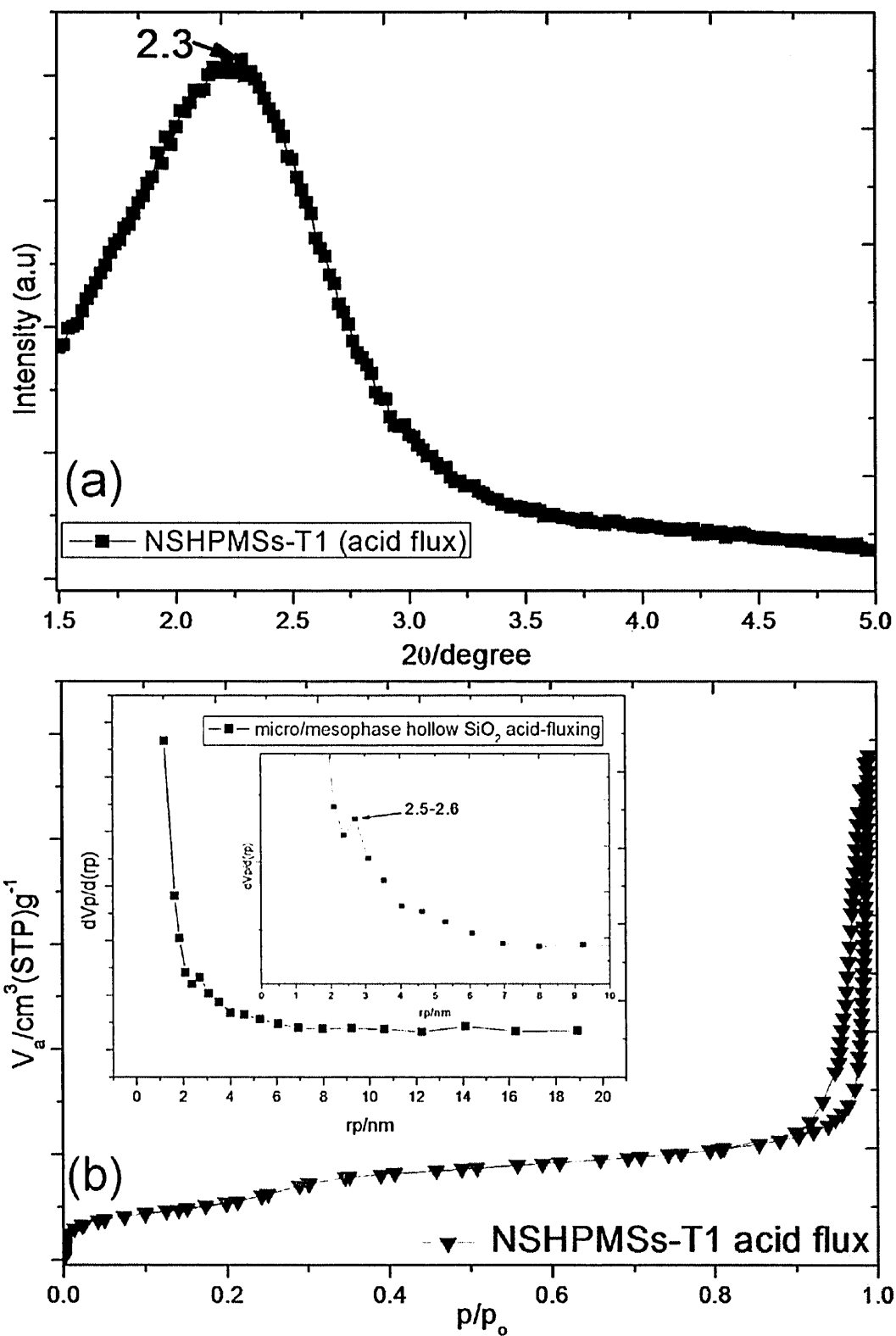


Figure 3.1.3 (a) Small angle XRD pattern and (b) N_2 adsorption-desorption isotherm with pore size distribution (BJH method, inset) of NSHPMSs-T1(acid fluxing)

To establish the distinct micro/mesostructure characteristic of the newly synthesized NSHPMSs, N_2 adsorption-desorption isotherms with (Barrett-Joyner-Halenda) BJH pore size distribution were analyzed as shown in Figure 3.1.3(b). The NSHPMSs samples synthesized at R.T exhibited type IV isotherms (step 1; assigned to 2D hexagonal ($P6mm$) mesostructure, a good agreement to the XRD pattern results). [30, 31, 33] Wherein, the surface area has average results of ~ 2055.5 m^2/g [Brunauer-Emmett-Teller (BET) surface area method] (see Table 3.1S1). Interestingly, the NSHPMSs samples have isotherms displayed with two distinct adsorption steps at the relative pressure. The first step ($0.2 < P/P_o < 0.35$) correspond to nitrogen capillary condensation of the mesoporous like wormhole-like pores, with pore size distribution (BJH) curves in the range of (1.8 to 2.5) nm (See Figure 2 inset). These resulted from the combination of disordered micro/mesoporous shell through CTAB-template shell. While second step ($0.85 < P/P_o < 0.99$) was mainly due to the voids of the nano-sized hollow particles and probably some larger secondary nanopores inside the particles.[40] (see Fig.3.1S10, 3.1S11, and 3.1S12) These showed that both micro/mesoporous with macro-holes pore-size were present in the nano-sized hollow particles, good concurrence with the STEM/TEM observation data. The existence of mesoporous was also in good conformity with the results of small angle XRD pattern data.

3.1.3.3 Effect and Possible scheme upon increasing TEOS, CTAB concentration plus TEMPERATURE reaction

Generally as shown schematically in Figure 3.1.4, which is based on the obtained results, increasing TEOS concentration, CTAB concentration and elevated temperature reaction have greatly influence the physico-chemical properties of the

NSHPMSs materials such as stability, surface morphology, and shell thickness. As observe in Figure 3.1.4A; thickness of the shell increased and low angle reflection (lattice parameters, meso-morphous network pattern) changed upon sufficient increase of TEOS concentration (see Fig.3.1S4, 3.1S9a and 3.1S10 for the actual results). While in Figure 3.1.4B as observed, increasing CTAB concentration surface pore morphology and pore alignment slightly change. (see Fig.3.1S5, 3.1S9b and 3.1S11) Then Figure 3.1.4C, elevate temperature reaction enhance structural stability of the shell and peak of low angle reflection decrease (signify increase of silicate amorphous frame-network [41]). (see Fig. 3.1S6, 3.1S9c and 3.1S12, supplementary information).

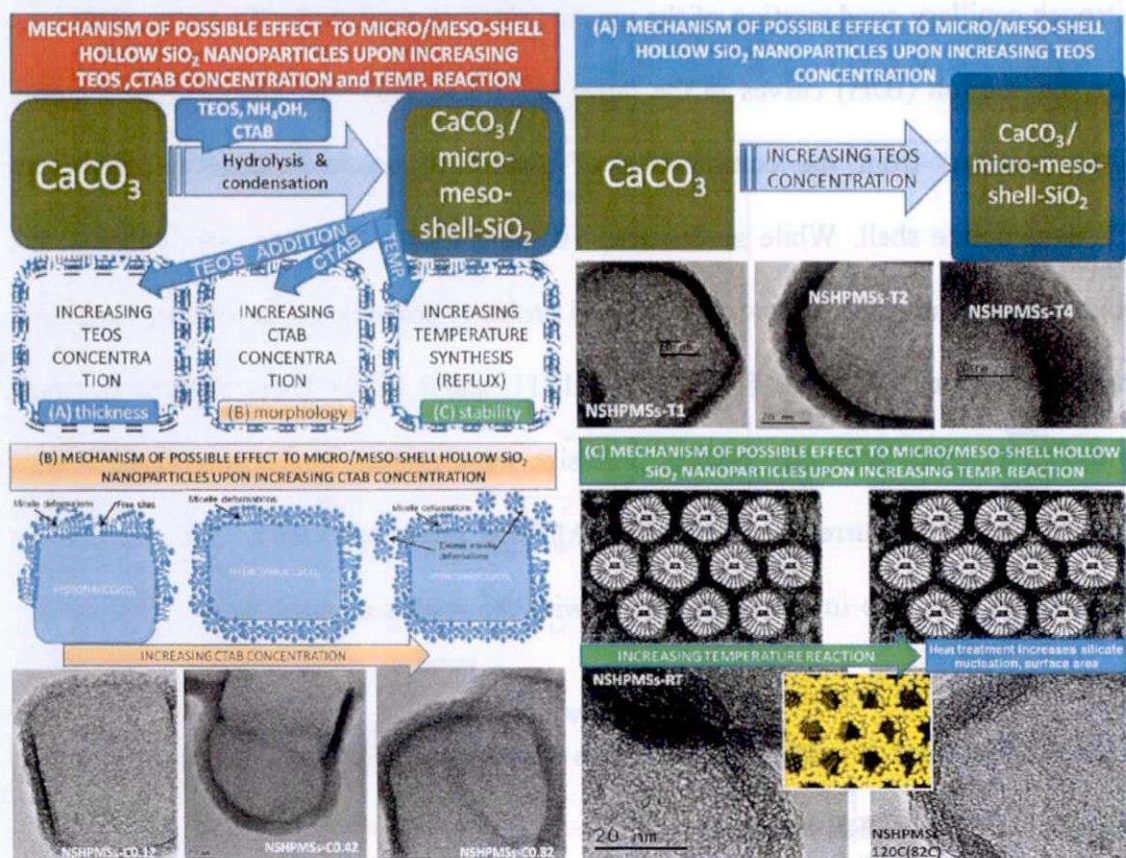


Figure 3.1.4. Schematic illustrations for the possible/reasonable effect upon additional increasing TEOS concentration (A), CTAB concentration (B) and higher temperature reaction (C)

3.1.3.4 General plausible mechanism for the formation of wormhole pattern in NSHPMSs

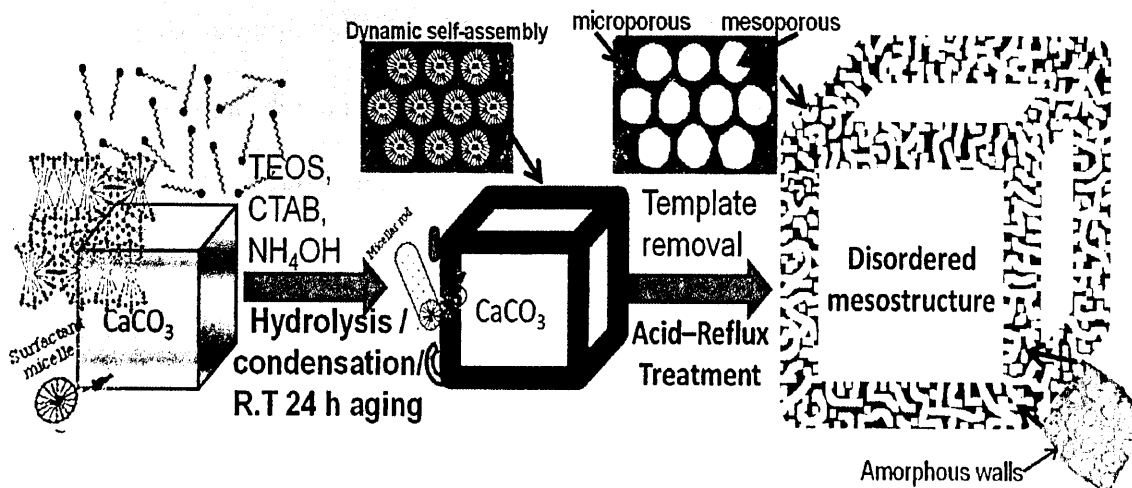


Figure 3.1. 5 Schematic illustration for the formation of NSHPMSs

On the basis of the above results, tentative mechanism was illustrated for the formation of hollow nanoparticles with hierarchically mesomorphous silicate shell (NSHPMSs) as shown in Figure 3.1.4. The newly synthesized NSHPMSs were synthesized in weak basic mixture of ethanol/water solution using cubic nano-size CaCO_3 template. The weak basicity and mixture of ethanol/water allow careful control of the rate of the hydrolysis of TEOS , [4] together with CTAB and nano-size CaCO_3 templates, reduces the possibility of forming solid mesoporous particles as well as fusing them together. Firstly, the nano-sized CaCO_3 particles, (high surface energy) [23], adsorb surfactant CTAB molecules, enriched/coated the surface of CaCO_3 , then form (second) critical micelle concentration. [24, 33] In this case, surfactant CTAB micelles can be perpendicularly deposited in axial direction to the surface of the CaCO_3 , due to weak covalent bond of smaller directionality such as coulombs force and hydrogen bond. [24, 33] Due to the enriched coating of cationic surfactant into the template CaCO_3 and under alkaline condition; silicon source (TEOS) hydrolyzed into silic acid

oligomers can easily bond and interact with the surfactant CTAB. Then, deposited as self-assembly (hexagonally worm-like framework pattern) around CaCO_3 template to generate $\text{CaCO}_3@CTAB/SiO_2$ (CSNSMSs). Finally, stable hollow silicate with amorphous micro/mesoporous shell (NSHPMSs) and with uniquely high surface area was obtained after the removal of templates (CaCO_3 and CTAB) thru weak acid-reflux.

3.1.4 Conclusion.

In summary, this chapter has demonstrated the formation of NSHPMSs with micro/meso-structure shell by means of double templates method [nano-sized CaCO_3 (core-1st template) and CTAB (micelle -2nd template silicate)] via R.T. hydrolysis and condensation reaction. The thickness, micro/mesostructure pattern and stability of the micro/mesophase shell of the modified acid reflux NSHPMSs with stable micro/mesostructure shell can be tuned by adjusting the TEOS, CTAB concentration and elevate temperature reaction (see supporting information data). This is an important for developing hierarchical structured for future nano-science applications. This approach is simple, eco-friendly/versatile, and suitable to the synthesis of composite, hybrid shell and other metal oxide hollow nanoparticles. More importantly, it is believed that micelle-template phase, consist of long hydrophobic chain with polar head group surrounded by silicate network (depended on the temperature reaction [1]), plays a key role during the pore-sized adjustment and formation of new meso-structured silicate shell. Furthermore, size and shape of hollow particles can be adjusted depends on the core-1st template particles.[1, 14] These findings can serve as deeper insight in designing on other CTAB-coated nanostructures and colloids of other dimension and promotes the adoption, modification and translation of various as-synthesized nanoparticles to individualized applications at the concern of the end-user.

References

- [1] Y. Wan, Zhao, On the Controllable Soft-Templating Approach to Mesoporous Silicates, *Chemical Reviews* 107 (7) (2007) 2821-2860.
- [2] Y. Zhao, L. Jiang, Hollow Micro/Nanomaterials with Multilevel Interior Structures, *Advanced Materials* 21 (36) (2009) 3621-3638.
- [3] Y. Li, Y. Zhu, X. Yang, C. Li, Mesoporous Silica Spheres as Microreactors for Performing CdS Nanocrystal Synthesis, *Crystal Growth & Design* 8 (12) (2008) 4494-4498.
- [4] N. Kato, T. Ishii, S. Koumoto, Synthesis of Monodisperse Mesoporous Silica Hollow Microcapsules and Their Release of Loaded Materials, *Langmuir* 26 (17) (2010) 14334-14344.
- [5] X.W. Lou, L.A. Archer, Z. Yang, Hollow Micro-/Nanostructures: Synthesis and Applications, *Advanced Materials* 20 (21) (2008) 3987-4019.
- [6] Y. Li, X. Li, Y. Li, H. Liu, S. Wang, H. Gan, J. Li, N. Wang, X. He, D. Zhu, Controlled Self-Assembly Behavior of an Amphiphilic Bisporphyrin–Bipyridinium–Palladium Complex: From Multilayer Vesicles to Hollow Capsules, *Angewandte Chemie International Edition* 45 (22) (2006) 3639-3643.
- [7] D.H.W. Hubert, M. Jung, P.M. Frederik, P.H.H. Bomans, J. Meuldijk, A.L. German, Vesicle-Directed Growth of Silica, *Advanced Materials* 12 (17) (2000) 1286-1290.
- [8] H. Xu, W. Wang, Template Synthesis of Multishelled Cu₂O Hollow Spheres with a Single-Crystalline Shell Wall, *Angewandte Chemie International Edition* 46 (9) (2007) 1489-1492.
- [9] C.E. Fowler, D. Khushalani, S. Mann, Interfacial synthesis of hollow microspheres of mesostructured silica, *Chemical Communications* (19) (2001) 2028-2029.
- [10] M. Fujiwara, K. Shiokawa, I. Sakakura, Y. Nakahara, Silica Hollow Spheres with Nano-Macroholes Like Diatomaceous Earth, *Nano Letters* 6 (12) (2006) 2925-2928.
- [11] Y. Cai, H. Pan, X. Xu, Q. Hu, L. Li, R. Tang, Ultrasonic Controlled Morphology Transformation of Hollow Calcium Phosphate Nanospheres: A Smart and Biocompatible Drug Release System, *Chemistry of Materials* 19 (13) (2007) 3081-3083.

- [12] D. Lootens, C. Vautrin, H. Van Damme, T. Zemb, Facetted hollow silica vesicles made by templating cationic surfactant vesicles, *Journal of Materials Chemistry* 13 (9) (2003) 2072-2074.
- [13] Y. Zhao, H. Wang, Y. Liu, J. Ye, S. Shen, Hollow MCM-41 microspheres derived from P(St-MMA)/MCM-41 core/shell composite particles, *Materials Letters* 62 (27) (2008) 4254-4256.
- [14] B. Tan, S.E. Rankin, Dual Latex/Surfactant Templating of Hollow Spherical Silica Particles with Ordered Mesoporous Shells, *Langmuir* 21 (18) (2005) 8180-8187.
- [15] H.I.n. Blas, M. Save, P. Pasetto, C.d. Boissière, C.m. Sanchez, B. Charleux, Elaboration of Monodisperse Spherical Hollow Particles with Ordered Mesoporous Silica Shells via Dual Latex/Surfactant Templating: Radial Orientation of Mesopore Channels, *Langmuir* 24 (22) (2008) 13132-13137.
- [16] R.M. Anisur, J. Shin, H.H. Choi, K.M. Yeo, E.J. Kang, I.S. Lee, Hollow silica nanosphere having functionalized interior surface with thin manganese oxide layer: nanoreactor framework for size-selective Lewis acid catalysis, *Journal of Materials Chemistry* 20 (47) (2010) 10615-10621.
- [17] C.T. Kresge, M.E. Leonowicz, W.J. Roth, J.C. Vartuli, J.S. Beck, Ordered mesoporous molecular sieves synthesized by a liquid-crystal template mechanism, *Nature* 359 (6397) (1992) 710-712.
- [18] S.B. Yoon, J.-Y. Kim, J.H. Kim, Y.J. Park, K.R. Yoon, S.-K. Park, J.-S. Yu, Synthesis of monodisperse spherical silica particles with solid core and mesoporous shell: mesopore channels perpendicular to the surface, *Journal of Materials Chemistry* 17 (18) (2007) 1758-1761.
- [19] G. Qi, Y. Wang, L. Estevez, A.K. Switzer, X. Duan, X. Yang, E.P. Giannelis, Facile and Scalable Synthesis of Monodispersed Spherical Capsules with a Mesoporous Shell, *Chemistry of Materials* 22 (9) (2010) 2693-2695.
- [20] W. Zhao, M. Lang, Y. Li, L. Li, J. Shi, Fabrication of uniform hollow mesoporous silica spheres and ellipsoids of tunable size through a facile hard-templating route, *Journal of Materials Chemistry* 19 (18) (2009) 2778-2783.

- [21] X.W. Lou, C. Yuan, L.A. Archer, Shell-by-Shell Synthesis of Tin Oxide Hollow Colloids with Nanoarchitected Walls: Cavity Size Tuning and Functionalization, *Small* 3 (2) (2007) 261-265.
- [22] I. Gorelikov, N. Matsuura, Single-Step Coating of Mesoporous Silica on Cetyltrimethyl Ammonium Bromide-Capped Nanoparticles, *Nano Letters* 8 (1) (2007) 369-373.
- [23] M. Fuji, C. Takai, Y. Tarutani, T. Takei, M. Takahashi, Surface properties of nanosize hollow silica particles on the molecular level, *Advanced Powder Technology* 18 (2007) 81-91.
- [24] Y. Le, J.-F. Chen, J.-X. Wang, L. Shao, W.-C. Wang, A novel pathway for synthesis of silica hollow spheres with mesostructured walls, *Materials Letters* 58 (15) (2004) 2105-2108.
- [25] Y. Le, M. Pu, J.-f. Chen, Theoretical and experimental studies on molecular spectra of the silica hollow spheres, *Materials Research Bulletin* 41 (9) (2006) 1714-1719.
- [26] R.V.R. Virtudazo, H. Watanabe, M. Fuji, M. Takahashi, A Simple Approach to form Hydrothermally Stable Templated Hollow Silica Nanoparticles, in: *Characterization and Control of Interfaces for High Quality Advanced Materials III*, John Wiley & Sons, Inc., 2010, pp. 91-97.
- [27] S. Liu, P. Cool, O. Collart, P. Van Der Voort, E.F. Vansant, O.I. Lebedev, G. Van Tendeloo, M. Jiang, The Influence of the Alcohol Concentration on the Structural Ordering of Mesoporous Silica: Cosurfactant versus Cosolvent, *The Journal of Physical Chemistry B* 107 (38) (2003) 10405-10411.
- [28] R.V. Rivera-Virtudazo, A.K.G. Tapia, J.F.B. Valenzuela, L.D. Cruz, H.D. Mendoza, E.V. Castriciones, Lacunarity Analysis of TEM Images of Heat-Treated Hybrid Organosilica Materials, in: B. Şener (Ed.) *Innovations in Chemical Biology*, Springer Netherlands, 2009, pp. 397-403.
- [29] L.X. Zhang, P.C. Li, X.H. Liu, L.W. Du, E.K. Wang, The Effect of Template Phase on the Structures of As-Synthesized Silica Nanoparticles with Fragile Didodecyldimethylammonium Bromide Vesicles as Templates, *Advanced Materials* 19 (23) (2007) 4279-4283.

- [30] Y. Guo, A. Mylonakis, Z. Zhang, G. Yang, P.I. Lelkes, S. Che, Q. Lu, Y. Wei, Templated Synthesis of Electroactive Periodic Mesoporous Organosilica Bridged with Oligoaniline, *Chemistry – A European Journal* 14 (9) (2008) 2909-2917.
- [31] X. Guo, Y. Deng, B. Tu, D. Zhao, Facile Synthesis of Hierarchically Mesoporous Silica Particles with Controllable Cavity in Their Surfaces, *Langmuir* 26 (2) (2009) 702-708.
- [32] B. Pauwels, G. Van Tendeloo, C. Thoelen, W. Van Rhijn, P.A. Jacobs, Structure Determination of Spherical MCM-41 Particles, *Advanced Materials* 13 (17) (2001) 1317-1320.
- [33] X. Guo, Y. Deng, D. Gu, R. Che, D. Zhao, Synthesis and microwave absorption of uniform hematite nanoparticles and their core-shell mesoporous silica nanocomposites, *Journal of Materials Chemistry* 19 (37) (2009) 6706-6712.
- [34] J.-A. Kim, J.-K. Suh, S.-Y. Jeong, J.-M. Lee, S.-K. Ryu, Hydration reaction in synthesis of crystalline-layered sodium silicate, *Journal of Industrial and Engineering Chemistry* 6 (4) (2000) 219-225.
- [35] M. Yang, G. Wang, Z. Yang, Synthesis of hollow spheres with mesoporous silica nanoparticles shell, *Materials Chemistry and Physics* 111 (1) (2008) 5-8.
- [36] E.T. Stepkowska, Z. Sulek, J.L. Perez-Rodriguez, A. Justo, C. Maqueda, Thermal and microstructural studies on mud with additives, *Journal of Thermal Analysis* 37 (1991) 1497-1511.
- [37] J.-F. Chen, H.-M. Ding, J.-X. Wang, L. Shao, Preparation and characterization of porous hollow silica nanoparticles for drug delivery application, *Biomaterials* 25 (4) (2004) 723-727.
- [38] B. Shi, J. Ren, A. Wang, X. Liu, Y. Wang, Synthesis and characterization of wormhole-like mesostructured polyaniline, *Journal of Materials Science* 44 (24) (2009) 6498-6504.
- [39] C.E. Fowler, D. Khushalani, B. Lebeau, S. Mann, Nanoscale Materials with Mesostructured Interiors, *Advanced Materials* 13 (9) (2001) 649-652.
- [40] J.-G. Wang, H.-J. Zhou, P.-C. Sun, D.-T. Ding, T.-H. Chen, Hollow Carved Single-Crystal Mesoporous Silica Templated by Mesomorphous

Polyelectrolyte–Surfactant Complexes, *Chemistry of Materials* 22 (13) (2010) 3829-3831.

[41] J.-H. Sun, M.-O. Coppens, A hydrothermal post-synthesis route for the preparation of high quality MCM-48 silica with a tailored pore size, *Journal of Materials Chemistry* 12 (10) (2002) 3016-3020.

CHAPTER 3.1

Supporting Information

Simple Template Approach a Room-Temperature Synthesis of Non-spherical Nano-sized Hollow Silicate with Micro/Mesoporous Shell

Results

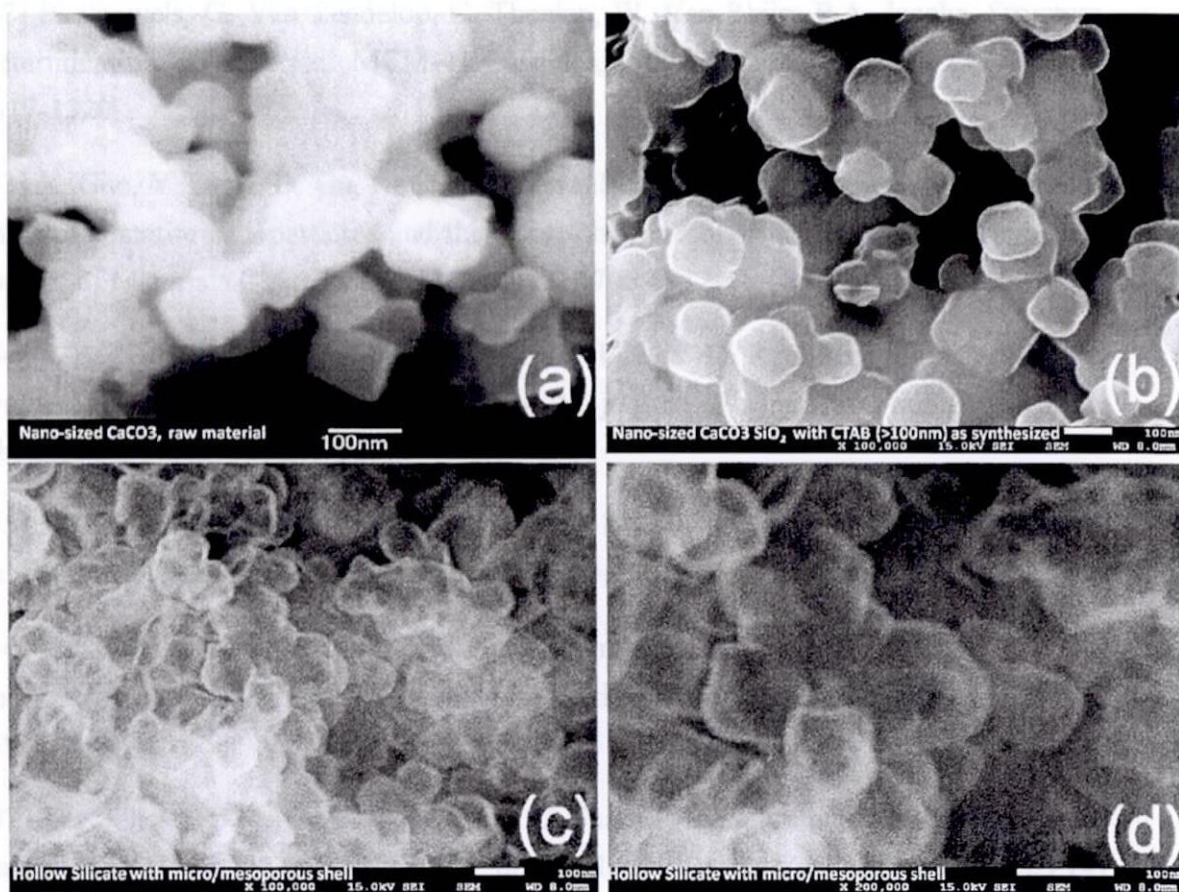


Fig.3.1S 1 SEM images: (a) Nano-size CaCO₃ particles (raw), (b) (x100000) CaCO₃ coated with SiO₂ @ CTAB as-synthesized (CSNSMSs) and nano-size hollow silicate with micro/mesoporous shell (NSHPMSs) with different magnification at (c) x100000, (d) x200000.

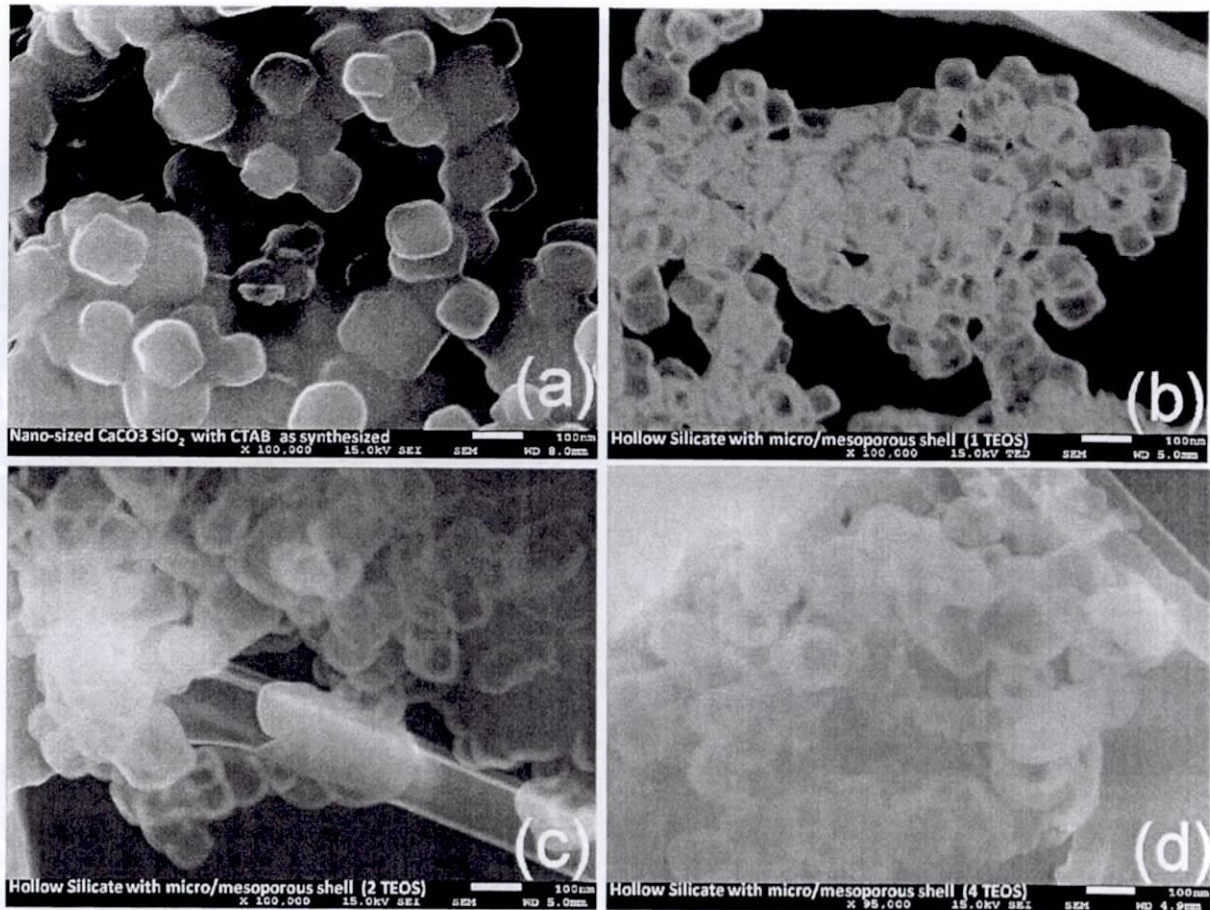


Fig.3.1S 2 (a) SEM images of CaCO_3 coated with SiO_2 @CTAB as synthesized (CSNSMSs) and STEM images of nano-size hollow silicate with micro/mesoporous shell (NSHPMSs) at increasing TEOS (vol) namely (b)NSHPMSs-T1;1 mL TEOS, (c) NSHPMSs-T2; 2mL TEOS and (c) NSHPMSs-T4;4 mL TEOS.

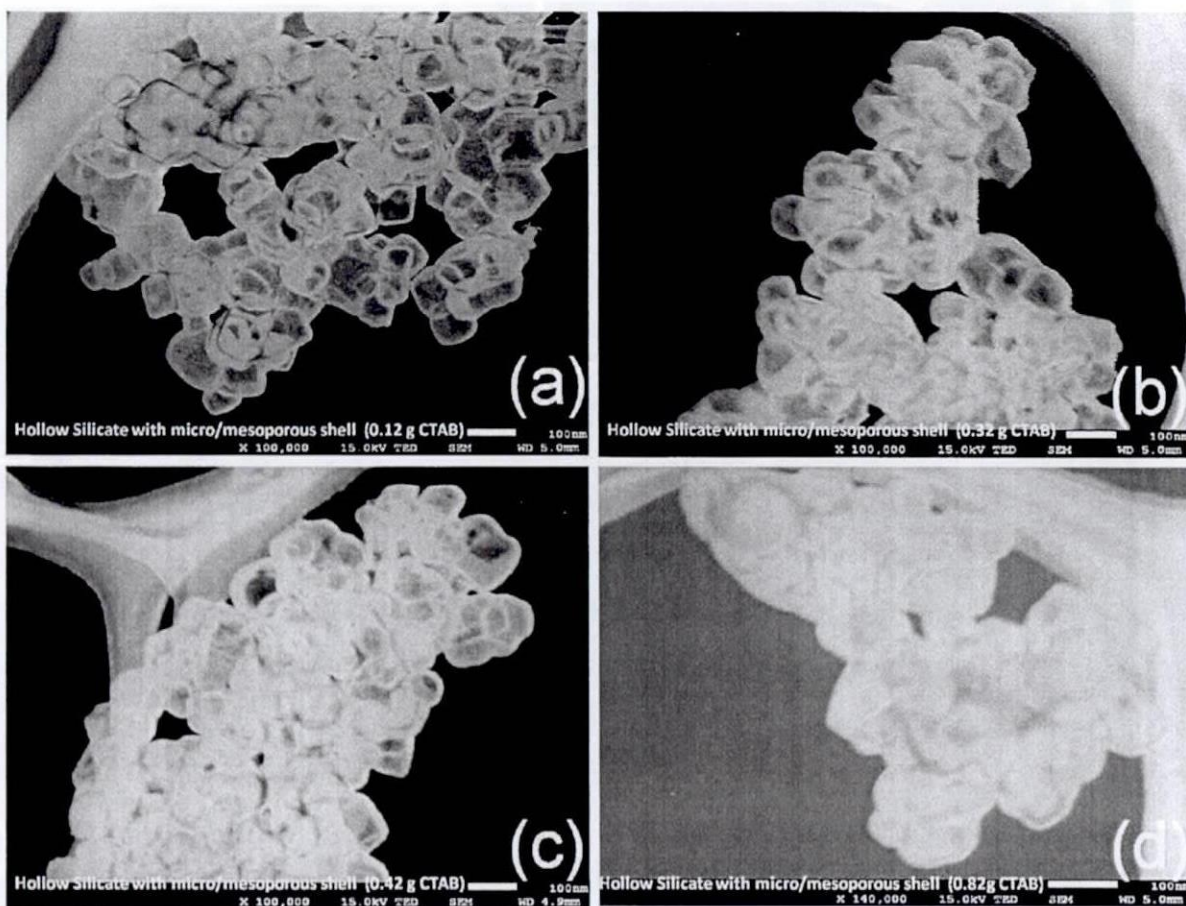


Fig.3.1S 3 STEM images: After acid reflux, hollow silicate with micro/mesoporous shell (NSHPMSs) at increasing CTAB (wt.) (a) NSHPMSs-C0.12; 0.12 g , (b) NSHPMSs -C0.32; 0.32 g , (c) NSHPMSs-C0.42; 0.42 g and (d) NSHPMSs -C0.82; 0.82 g.

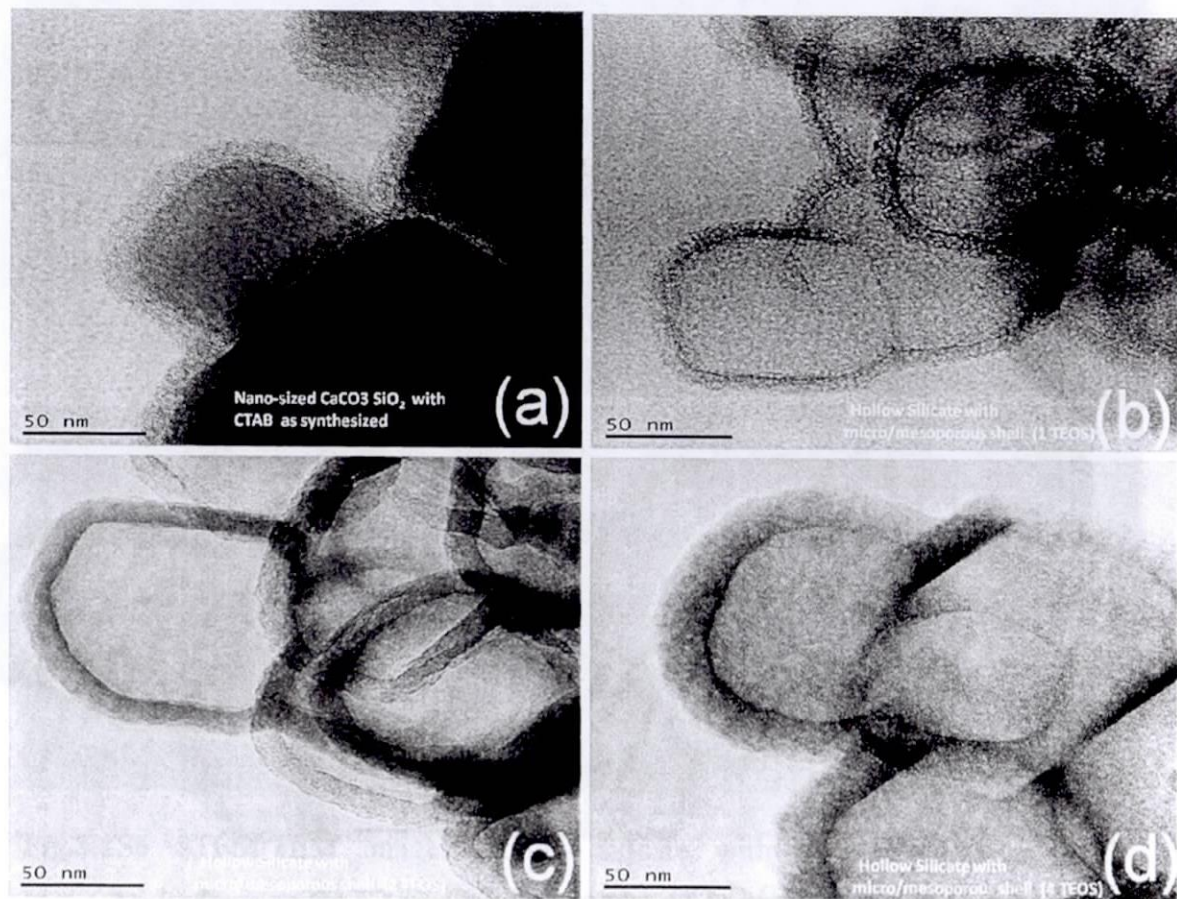


Fig.3.1S 4 TEM images: (a) CaCO_3 coated with SiO_2 @CTAB as-synthesized (CSNSMSs) and after acid reflux, hollow silicate with micro/mesoporous shell (NSHPMSs) at increasing TEOS (vol) (b) NSHPMSs-T1, (c) NSHPMSs-T2 and (c) NSHPMSs-T4.

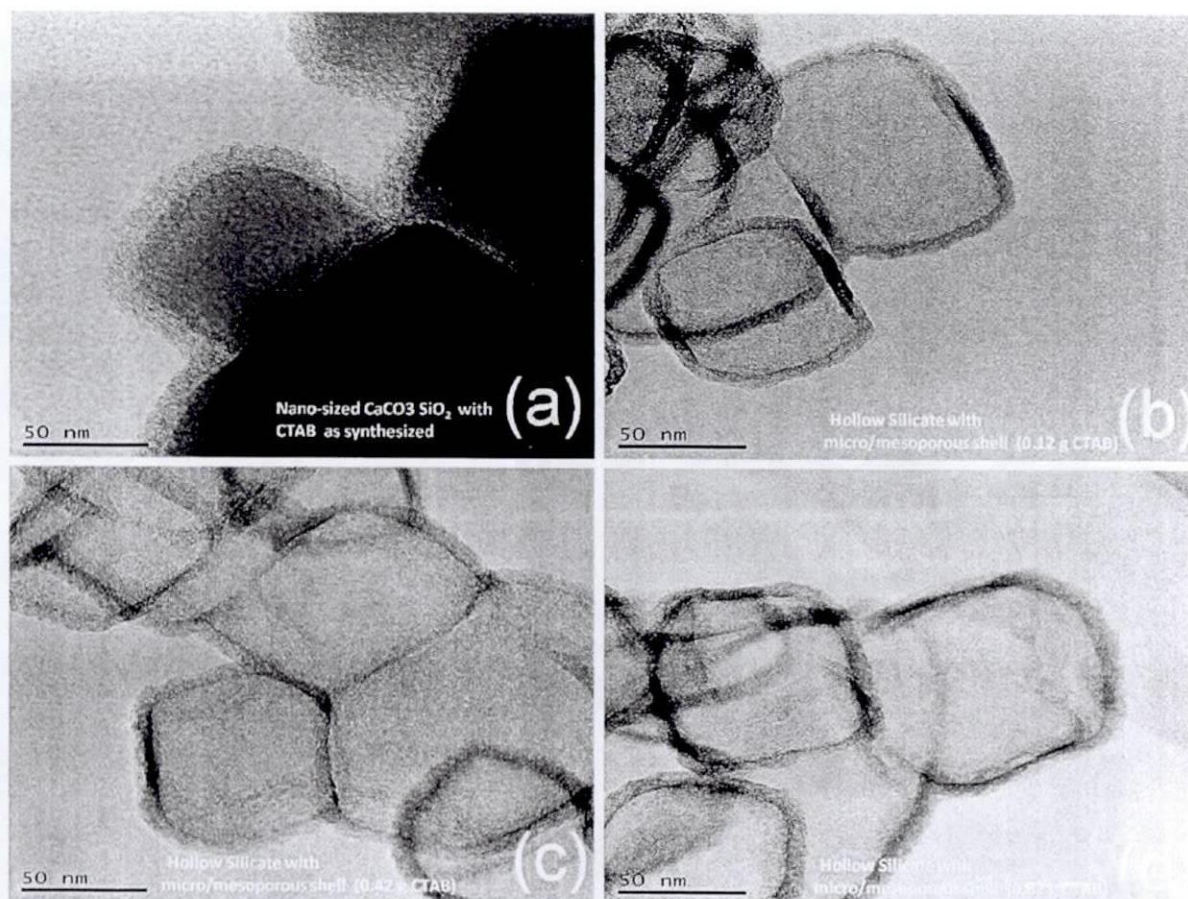


Fig.3.1S 5 TEM images: (a) CaCO_3 coated with SiO_2 @ CTAB as-synthesized (CSNSMSs) and after acid reflux, hollow silicate with micro/mesoporous shell (NSHPMSs) at increasing CTAB (wt.) (b)NSHPMSs –C0.12, (c) NSHPMSs–C0.42 and (d) NSHPMSs –C0.82.

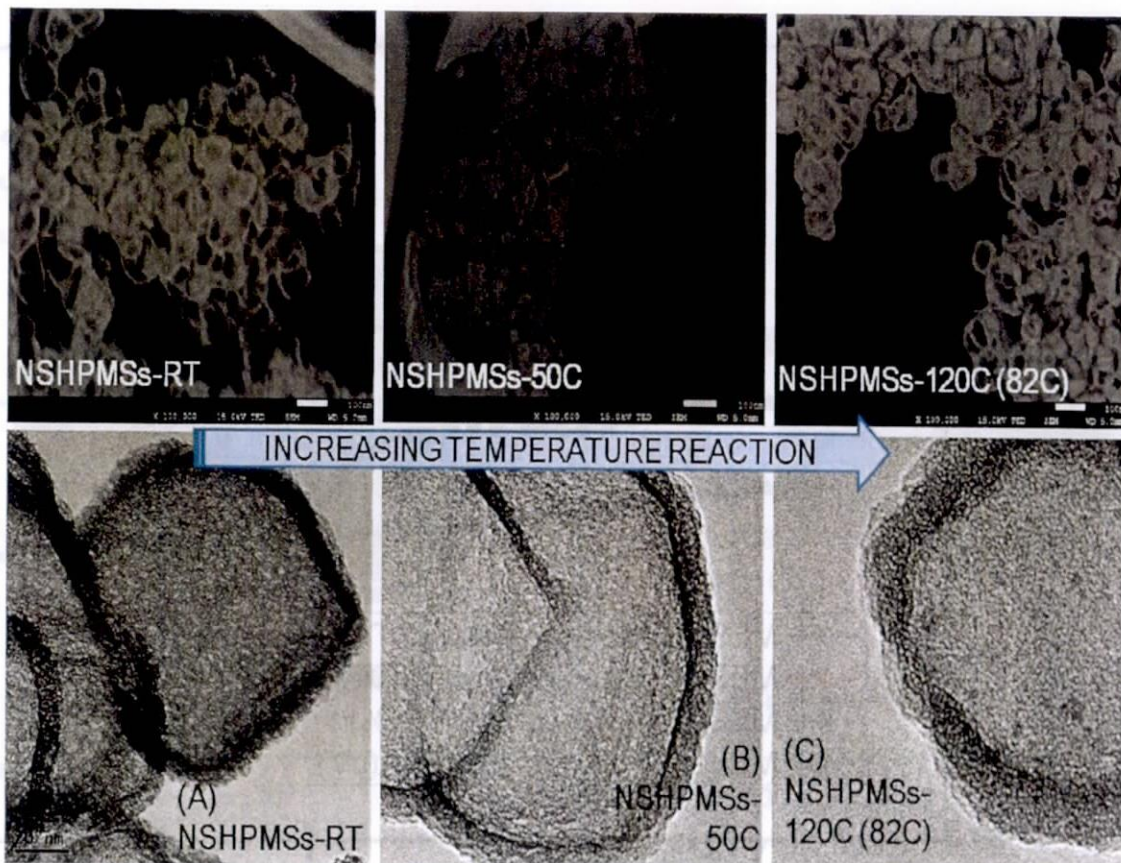


Fig.3.1S6 STEM/TEM images: hollow silicate with micro/mesoporous shell (NSHPMSs) at increasing temperature reaction (A) NSHPMSs-RT, (B) NSHPMSs-50 °C and (c) NSHPMSs-120°C (82°C).

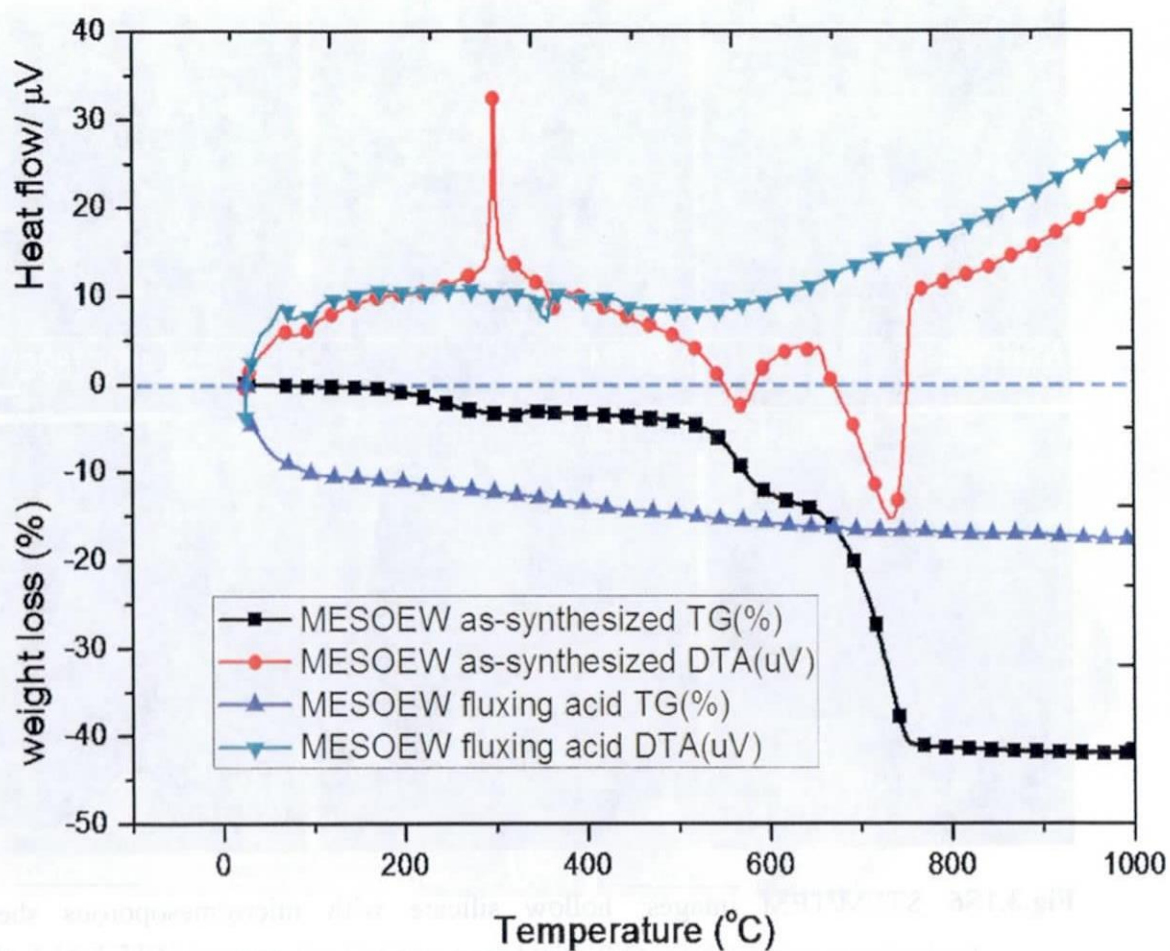


Fig.3.1S 7 Thermogram (TG) and Differential Thermal Analysis (DTA) data of as-synthesized MESOEW (CSNSMSs; ■ TG; ● DTA) with acid-reflux hollow silicate with micro/mesoporous shell MESOEW (NSHPMSs; ▲ TG; ▼ DTA)

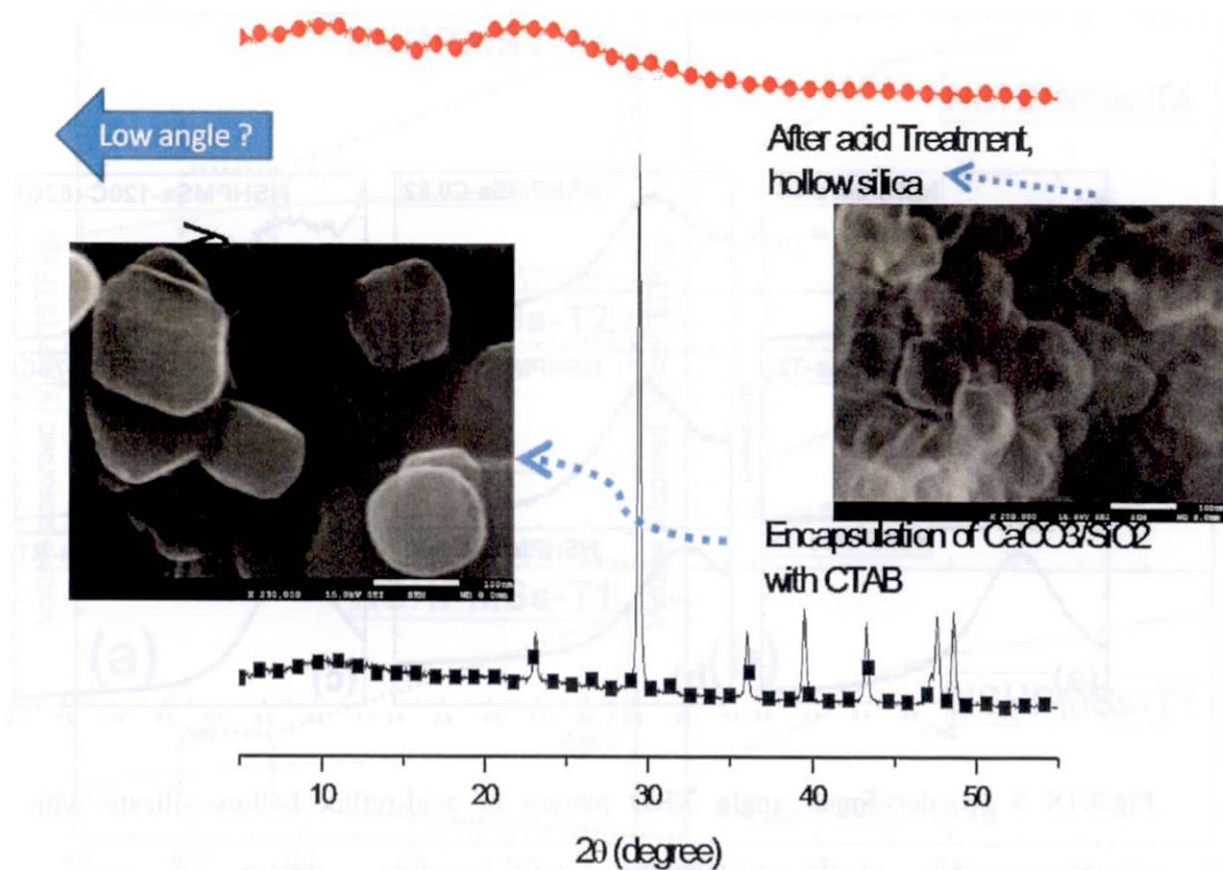


Fig.3.1S 8 Powder XRD pattern of as-synthesized CSNSMS (■; inset SEM image of CSNSMS-encapsulation of CaCO₃/SiO₂ with CTAB) with acid-reflux hollow silicate with micro/mesoporous shell NSHPMSs (●; inset SEM image of amorphous NSHPMSs.)

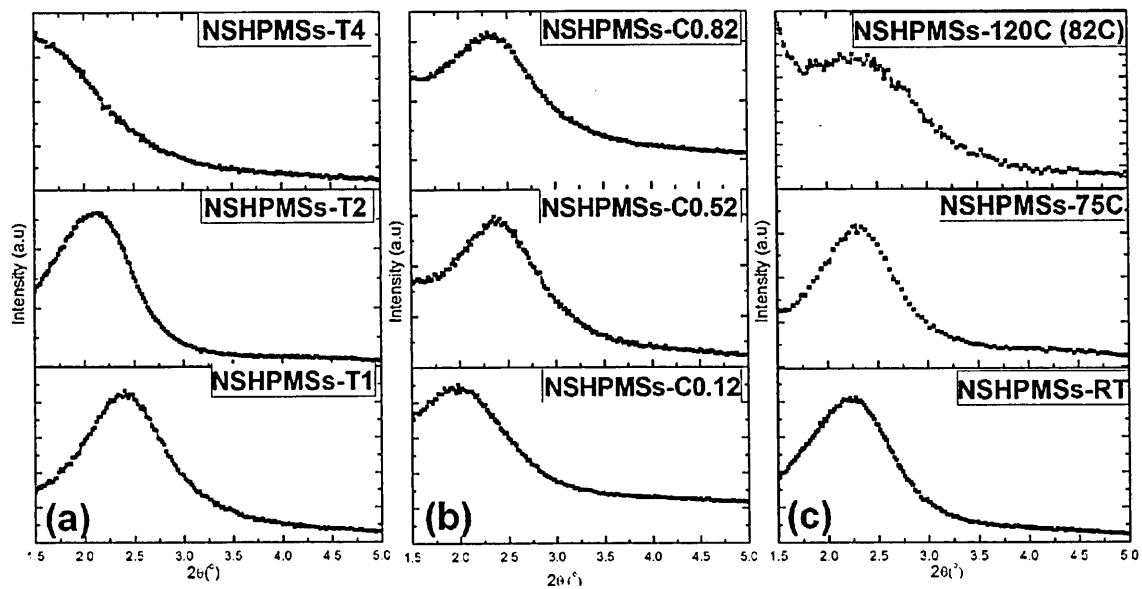


Fig.3.1S 9 Powder Small angle XRD pattern of acid-reflux hollow silicate with micro/mesoporous shell (NSHPMSs); (a) increasing TEOS concentration (NSHPMSs-T1, NSHPMSs-T2 and NSHPMSs-T4); (b) increasing CTAB concentration (NSHPMSs C0.12, NSHPMSs-C0.52 and NSHPMSs-C0.82); (c) elevate temperature reaction (NSHPMSs-RT, NSHPMSs-75°C and NSHPMSs-120°C (82°C))

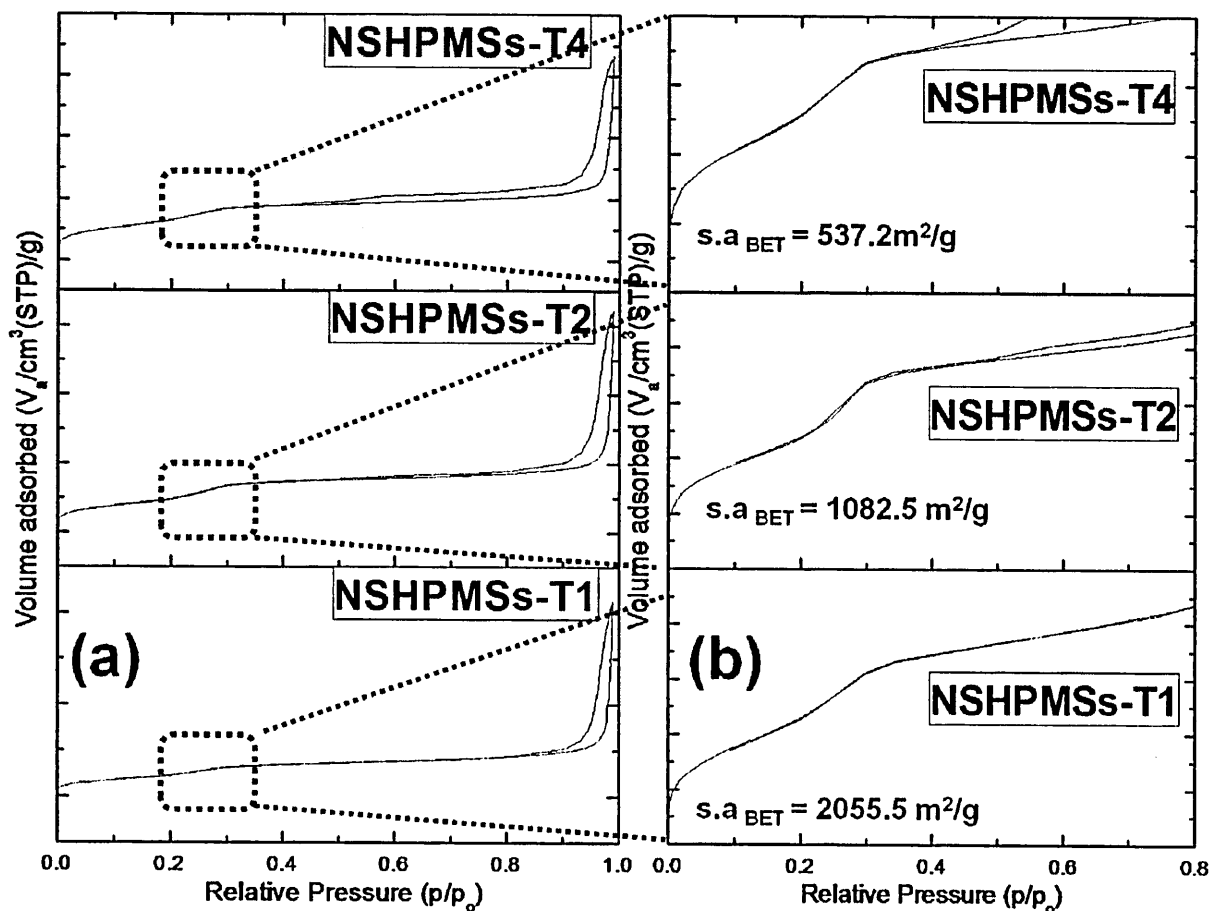


Fig.3.1S 10 Nitrogen adsorption-desorption isotherms (with enlarge view), hollow silicate with micro/mesoporous shell (NSHPMSs) at increasing TEOS (vol) (NSHPMSs-T1, NSHPMSs-T2 and NSHPMSs-T4)

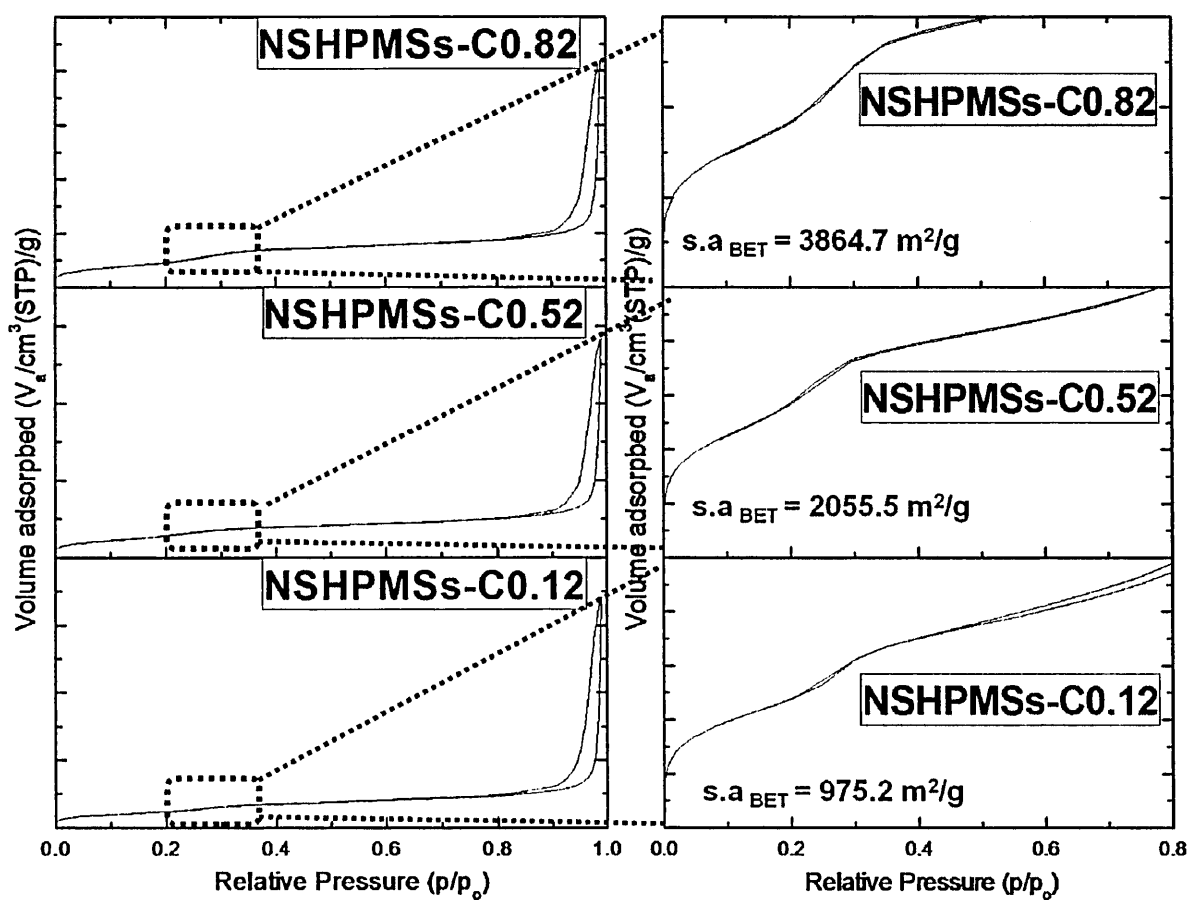


Fig.3.1S 11 Nitrogen adsorption-desorption isotherms (with enlarge view), hollow silicate with micro/mesoporous shell (NSHPMSs) at increasing CTAB concentration (NSHPMSs-C0.12, NSHPMSs-C0.52 and NSHPMSs-C0.82)

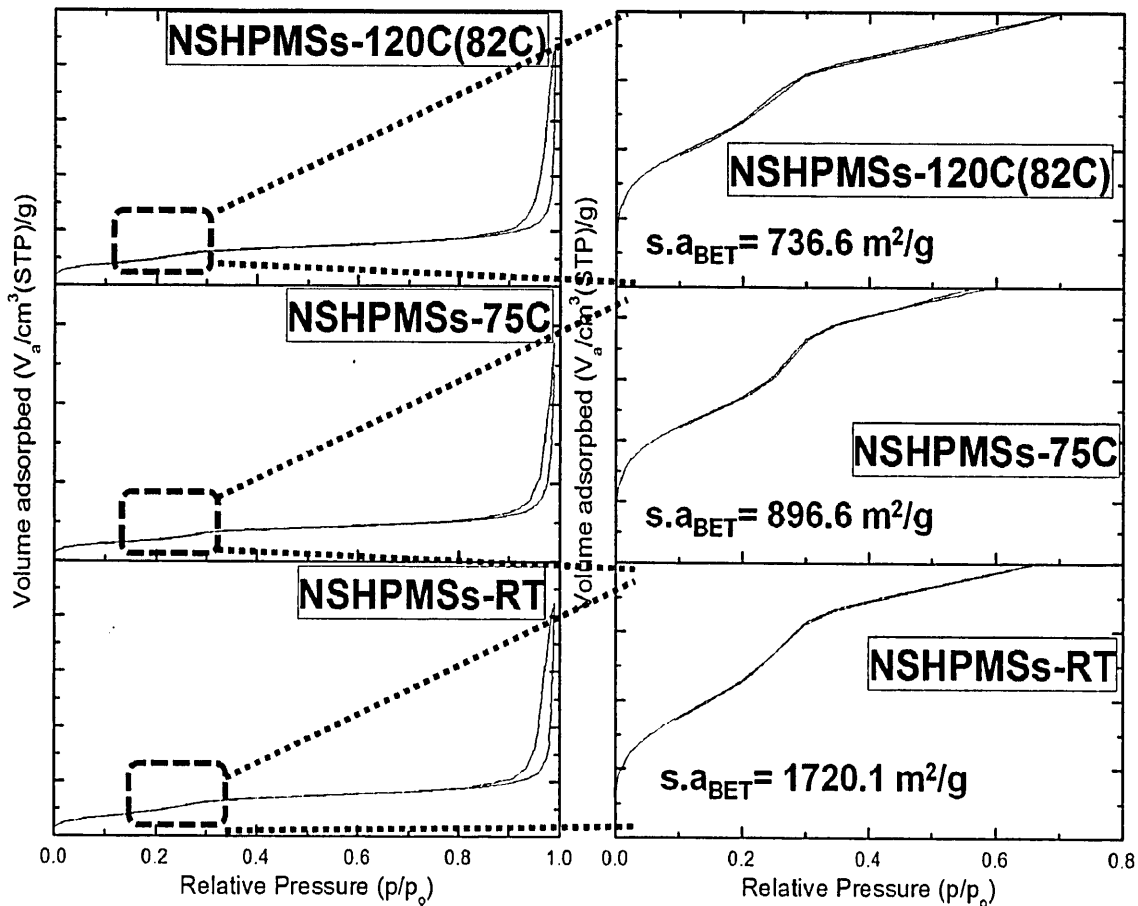


Fig.3.1S 12 Nitrogen adsorption-desorption isotherms (with enlarge view), hollow silicate with micro/mesoporous shell (NSHPMSs) at increasing temperature reaction (NSHPMSs-RT, NSHPMSs-75°C and NSHPMSs-120°C (82°C))

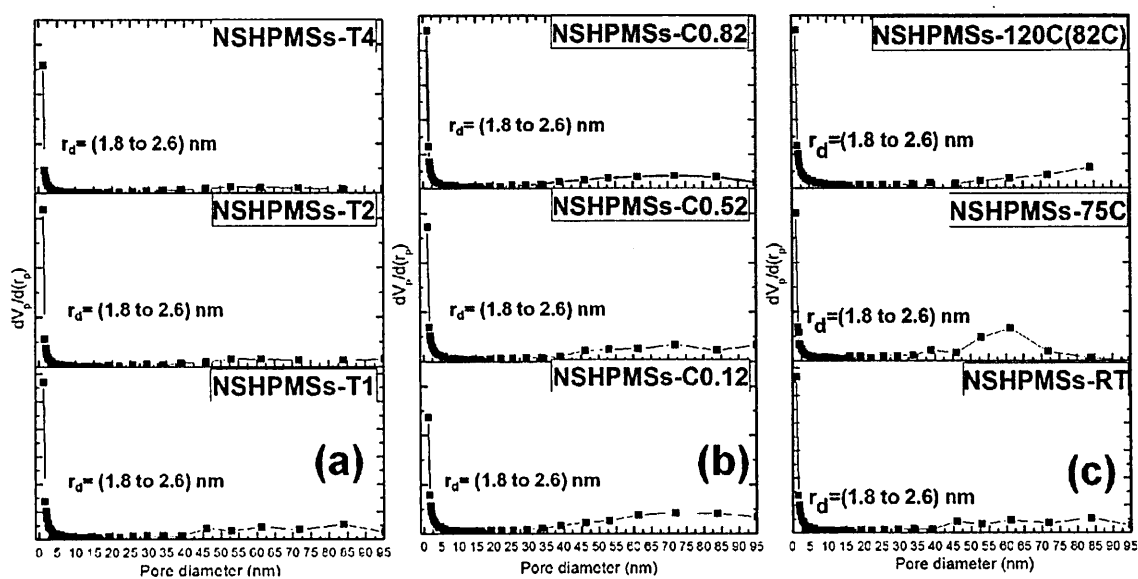


Fig.3.1S 13 Pore size distribution (PSD) curves of acid-reflux hollow silicate with micro/mesoporous shell (NSHPMSs); (a) increasing TEOS concentration (NSHPMSs-T1, NSHPMSs-T2 and NSHPMSs-T4); (b) increasing CTAB concentration (NSHPMSs-C0.12, NSHPMSs-C0.52 and NSHPMSs-C0.82); (c) elevate temperature reaction (NSHPMSs-RT, NSHPMSs-75°C and NSHPMSs-120°C (82°C))

Table 3.1 S1. Characterization of NSHPMSs

S a m p l e	BET surface area (m²/g)^a	Pore volume (cm³/g)^a	Pore size (nm)^a
NSHPMS_s-T1*	2055.5	6.59	1.8 to 2.6
NSHPMS_s-T2	1082.5	2.45	1.8 to 2.6
NSHPMS_s-T4	537.2	1.0	1.8 to 2.6
NSHPMS_s-C0.12	975.2	5.21	1.8 to 2.6
NSHPMS_s-C0.52*	2055.5	6.59	1.8 to 2.6
NSHPMS_s-C0.82	3864.7	13.0	1.8 to 2.6
HSNP**	309.4	2.75	Not applicable
NSHPMS_s-RT	1720.1	6.50	1.8 to 2.6
NSHPMS_s-50°C	1116.2	3.95	1.8 to 2.6
NSHPMS_s-75°C	896.5	3.35	1.8 to 2.6
NSHPMS_s-120°C	736.6	2.66	1.8 to 2.6

[a] measured by N₂ adsorption at 77K with BJH method curve estimation

[*] NSHPMS_s-T1 and NSHPMS_s-C0.52 are the same sample (for discussion purposed only)

[**] HSNP= hollow silicate nanoparticles without CTAB

CHAPTER 3

FABRICATION OF POROUS

(MICRO, MESO and MACROPOROUS)

AMORPHOUS SHELL HOLLOW

SILICATE PARTICLES

3.2 MICRO-SIZE HOLLOW SILICATE

PARTICLES WITH MESO/MACROPOROUS

SHELL BY DOUBLE EMULSION APPROACH

WITH ADDITION OF SODIUM

POLYMETHACRYLATE (NA-PA)

(WATER-SOLUBLE POLYMER)

3.2 Micro-size hollow silicate particles with meso/macroporous shell wall by double emulsion approach with addition of sodium polymethacrylate (Na-PA, water-soluble polymer)

3.2.1 Introduction

Design and fabrication of porous hollow inorganic microspheres with unique structure morphologies have received significant importance because of the potential application in catalysis, anode materials, low-dielectric materials, gas sensors, protection for biological active agent, encapsulation and controlled release for various substances [1-4]. In conventional procedures, silica spheres have been obtained using surfactant, block copolymers and using colloidal suspensions.[5] Usually polymers and some surfactants (such as Tween 80 and Span 80) are used to synthesizing hollow micro spheres particles. Preparation of micro-size hollow spheres with meso/macroporous shell wall using surfactant (Tween 80, Span 80) and water-soluble polymer (sodium polymethacrylate) have been successfully reported.[6-8] Wherein, the tween 80's chemical name is Poly oxy ethylene sorbitan mono oleate or Sorbitan monooleate ethoxylate and Span 80's chemical name is Sorbitan oleate or Sorbitan (Z)-mono 9-octadecenoate while sodium polymethacrylate is a good example for a water soluble polymer. As reported, this is a simple pathway for synthesizing hollow silica microspheres with meso/macroporous shell wall. As simple chemical method that produces silica hollow particles with macoholes in their shell walls, the orphologies are analogous to diatomaceous earth. The key point of this preparation was the addition of suitable water-soluble polymer into the water phase one. [6, 7] Lately, macro-porous hollow silicates have been investigated extensively as promising

electrode materials in lithium-ions [9-11]. The basic explanation for lead acid battery failure to obtain high specific energies; majority of active material in both positive and negative electrode were not fully discharged which delimit the reaction especially at higher discharge rates [9]. Previous studies reported that porous hollow silicate-glass microspheres (PHSM) can allow more electrolyte storage and enhance high rate energy storage for lead acid batteries [9, 10]. Then several techniques have been developed, but most of those routes have complex approach that needs long reaction time and often resulted to breakage of silica shell [12, 13]. Alternatively, using double emulsion process is one of the simple-practical / economical-way in producing hollow microspheres. However there were some problems involved in this method such as broad size distribution, poor size control, reproducible droplet size and low entrapment yield [14, 15]. Here in this section, it was able to minimize this problems by following the works of Fujiwara (water₁/oil/water₂) [7, 8] with our modified (set-up) pressurized N₂ filtration and calcination. Then, hollow silicate microspheres with macroporous shell were successfully prepared.

3.2.2 Starting materials and schematic outline

3.2.2.1 Materials

All chemicals used in this work were commercially available and were used without further purification. Aqueous sodium polymethacrylate average Mw ~9,500 (Na-PA; Sigma-Aldrich, USA), sodium silicate solution Na₂SiO₃ (SiO₂ 30 %; Kishira Chemical.co.Ltd, Japan), ammonium carbonate NH₄HCO₃ (Kanto Chemical Co.Ltd, Japan), n-hexane (Kanto Chemical Co.Ltd, Japan), Tween 80/ Span 80 (Kanto Chemical Co.Ltd, Japan) and Ethanol (EtOH, 99% Wako pure chemical)

3.2.2.2 Synthesis of microsphere hollow silicate particles

In this study, the researcher followed the similar preparation of Fujiwara group's[6] except that the obtained powder samples were set-up by our modified filtration (pressurized with N_2) and then sintered the microspheres. In this typical procedure, PHSM were obtained by double emulsion system (interfacial reaction). There were basically three solution namely sodium silicate solution with or without water soluble polymer (W_1P-X) as water phase one, n-hexane with surfactant (Tween 80/ Span 80) solution (O) as Oil phase one and ammonium bicarbonate solution (W_2) as water phase two. Initially, aqueous sodium polymethacrylate (Na-PA; X) solution (10.0 g of 30 %; Na-PA solution with average Mw $\sim 9,500$) was mixed with sodium silicate solution (30.0 g, SiO_2 30 %), then addition of (deionized) water fixed at 36 mL. This water phase (first phase solution) with polymer (W_1P-10 ; $\sim W_1P-X$) was added to oil phase (O; second phase solution) composed of n-hexane (72 mL) with Tween 80 (1.0 g) and Span 80 (0.50 g). The resulting two phase solution (W_1P-10/O) was emulsified by homogenizer (As One Co., Japan ; Model no. Auto cell Master CM 200 with ~ 8200 rpm) for 1 min. Then (W_1P-10/O) solution immediately poured into the third phase aqueous (W_2) solution (2 mol/L; 250 mL) of ammonium carbonate (NH_4HCO_3). After 2 h stirring at 35 °C, filtered the mix solution (N_2 pressure filtration, membrane [1.0 μm] filter type), washed (water /ethanol), dried at 100 °C for 1 d and then the white powder sintered at 700 °C (10 °C /min). To simplify this report, only the amount of Na-PA was varied at 0.0 g, 8.0 g, 10.0 g, 12 g, and 13 g designated as ($W_1P-0/O/W_2$, $W_1P-8/O/W_2$, $W_1P-10/O/W_2$, $W_1P-12/O/W_2$, and $W_1P-13/O/W_2$ respectively). A schematic process flow is illustrated in Figure 3.2.1.

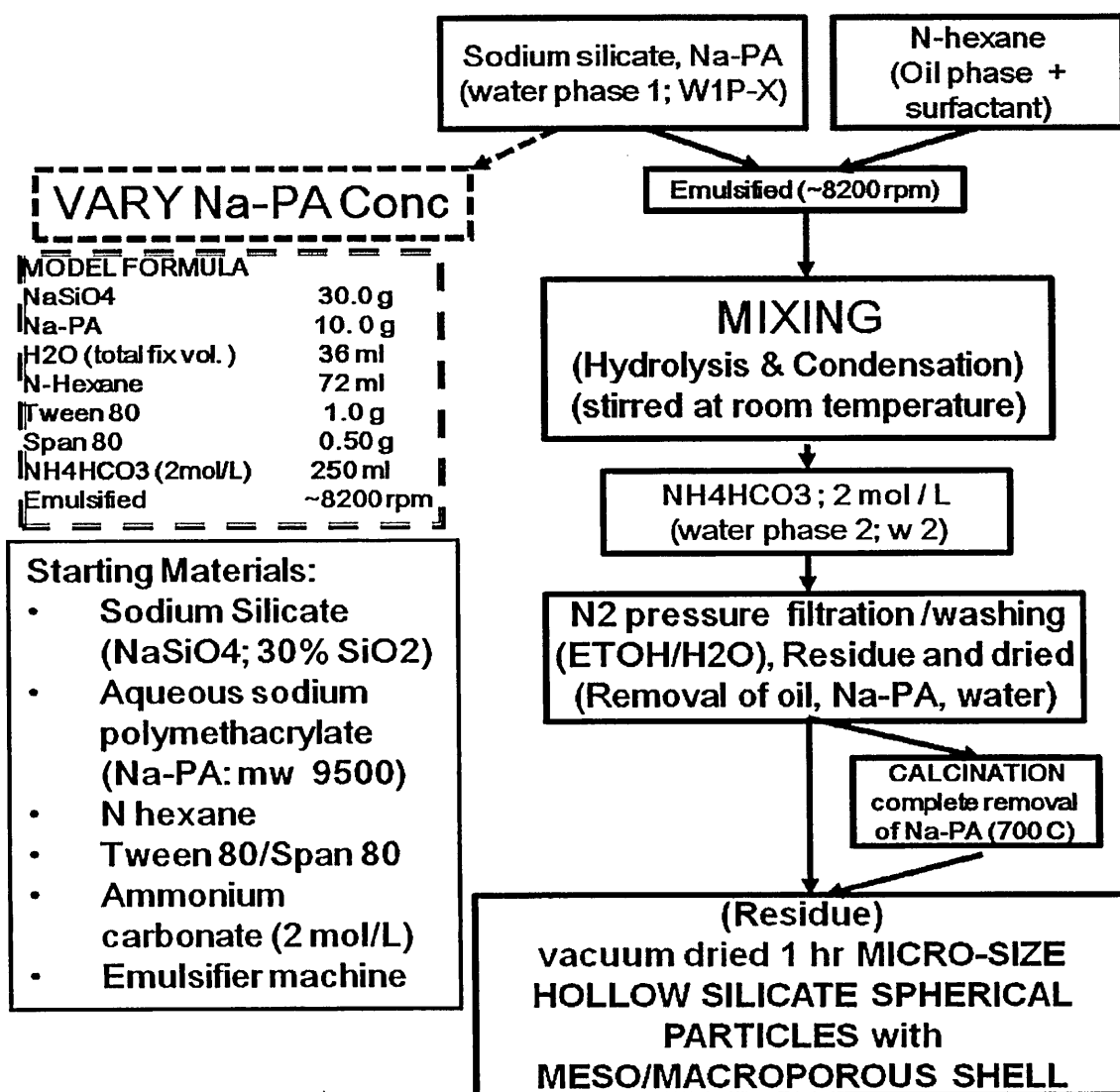


Figure 3.2.1 Process flow for the preparation/fabrication of the meso/macroporous shell wall by double emulsion method with the addition of sodium polymethacrylate (Na-PA)

3.2.2.3 Physico-chemical characterization

PHSM samples were characterized by X-ray diffraction (XRD; Model RINT 1100, Rigaku Corp., Cu K α), thermogravimetry (TG; TG-8120, Rigaku Corp., O₂ condition), scanning electron microscopy (SEM; JSM-7000F, JEOL) with optical digital microscopy

(ODM; VHX series, Keyence Corp.), and particle size distribution (PSD; MICROTRAC MT3000II series, Nikkiso Co. Ltd.). Then specific surface area (s.a) calculated by Brunauer-Emmett-Teller (BET) method and pore size distribution determined by Barrett-Joyner-Halenda (BJH) method via the automatic surface area analyzer (BELSORP-max, BEL Japan Inc., 77 K).

3.2.3 Results and discussion

3.2.3.1 Morphological observation and Particle size distribution (PSD) analysis

As shown in Figure 3.2.2, optical microscopy (ODM; Fig. 3.2.2a) and SEM (Fig. 3.2.2b) images reveal that calcined PHSM were successfully prepared by $W_1P-X/O/W_2$ method. With the continuous addition of Na-PA, macroporous surface morphologies gradually formed with thickness of about less than $1\mu\text{m}$. While in PSD (Fig. 3.2.3), particles exhibited highly disperse (inset SEM images in Fig.3.2.3) and peak particle size estimated at (7 to 12) μm . Based from the previous reported data, [6, 8, 16] the researcher monitored the research works parameters to these following such as volume ratio of W_1P-X to O to W_2 , weight ratio of surfactant, homogenize rotation (~ 8200 rpm), and concentration of sodium silicate (W_1P-X) in order to maintain the size of spheres especially for precipitant NH_4HCO_3 . Fujiwara et al. reported that if another precipitant (such as NH_4Cl) or other parameters, homogenous hollow micro size sphere particles will not be achieved. (Detailed explanation can be furtherly explain by their research works [6, 7]). This imply that when preparation conditions (such as volume ratio, emulsification rotation, and sodium silicate) were appropriate, formation of silica precipitate along the outer interface of the ($\text{water}_1/\text{oil}/\text{water}_2$) emulsion system (see Fig. 3.2.6) and appeared

homogenous micro-size particles (Fig.3.2.3). The hollow structure of silicate (PHSM) was formed spontaneously and no core compound was needed. Then with sufficient amount of Na-PA (easily attachable to silicate solution and simply washed-up by filtration and calcination) generated a unique hierarchical macroporous shell wall hollow silicate particles. For more details of the results see supporting data's in Figure 3.2S1 to 3.2S8.

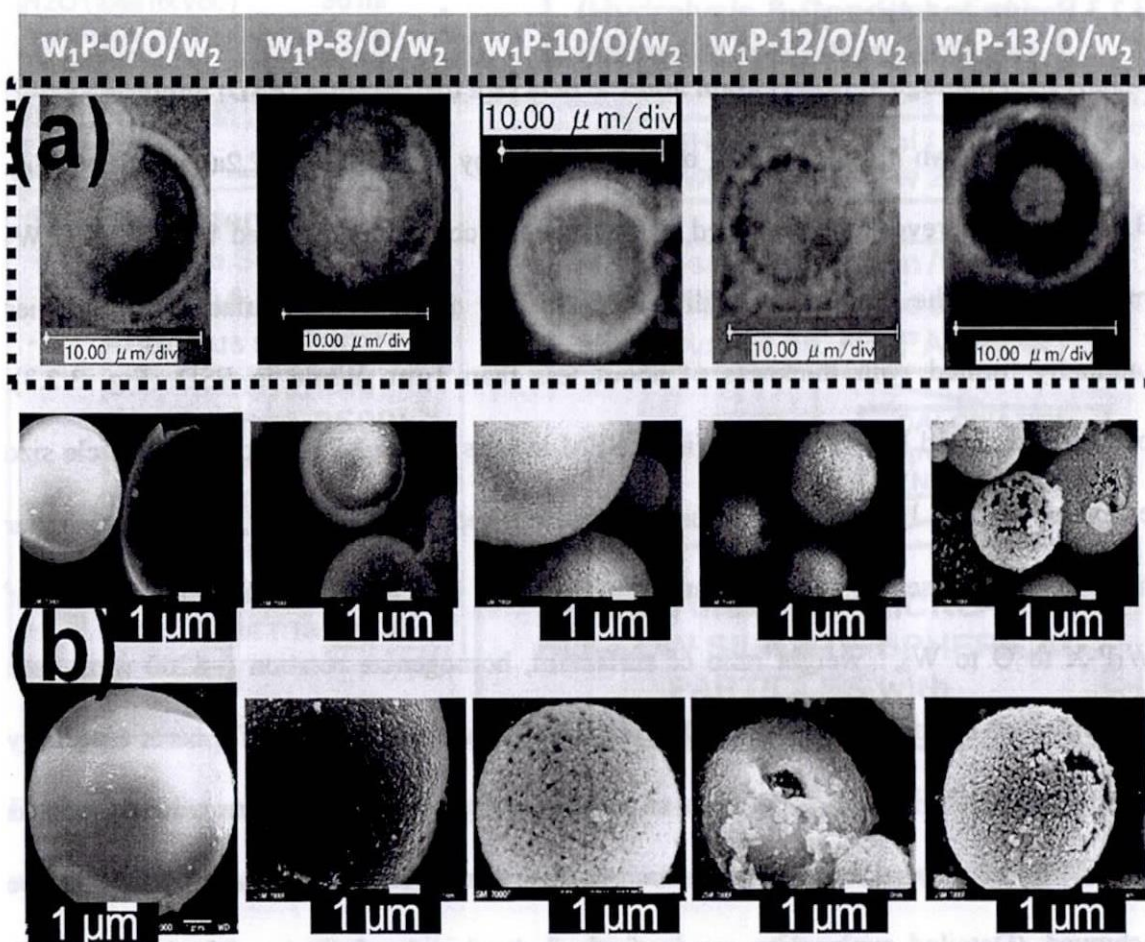


Figure 3.2.2 (a) ODM images, (b) SEM images calcined PSHM prepared by $W_1P-X/O/W_2$ at increasing Na-PA

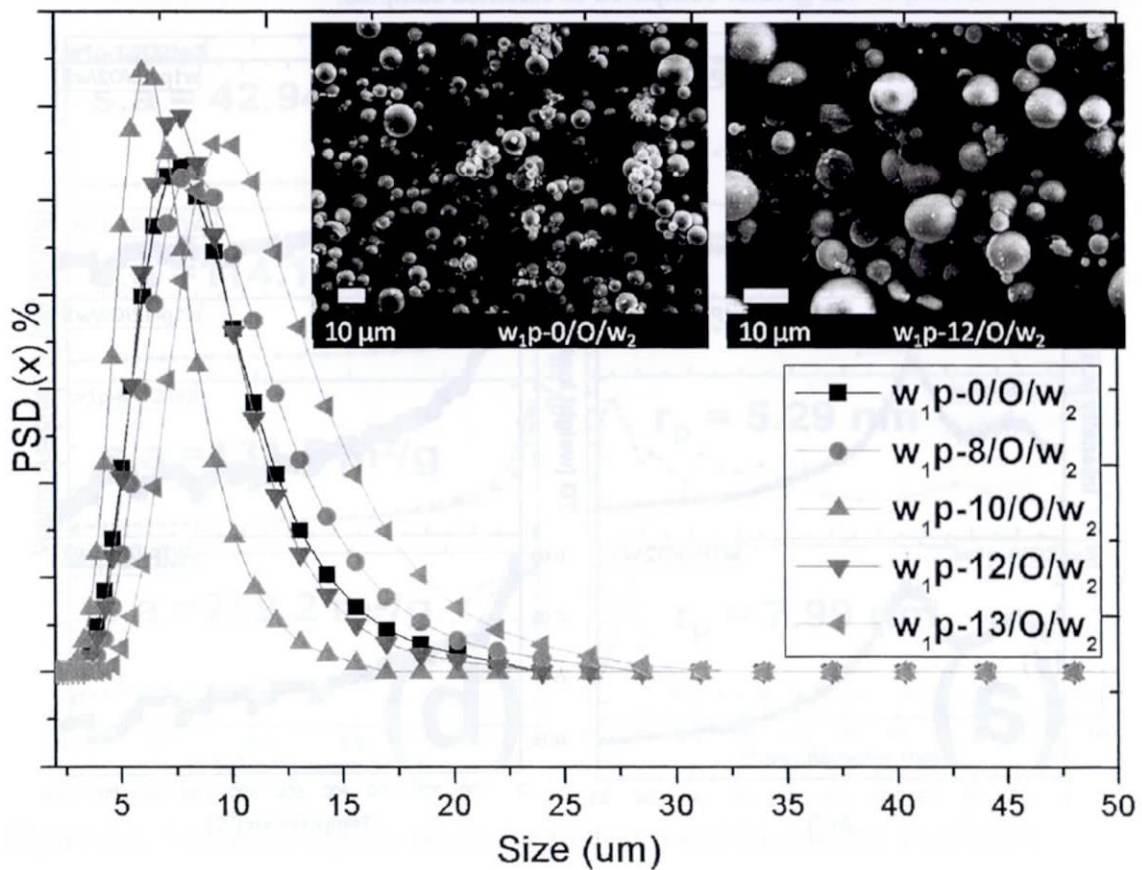
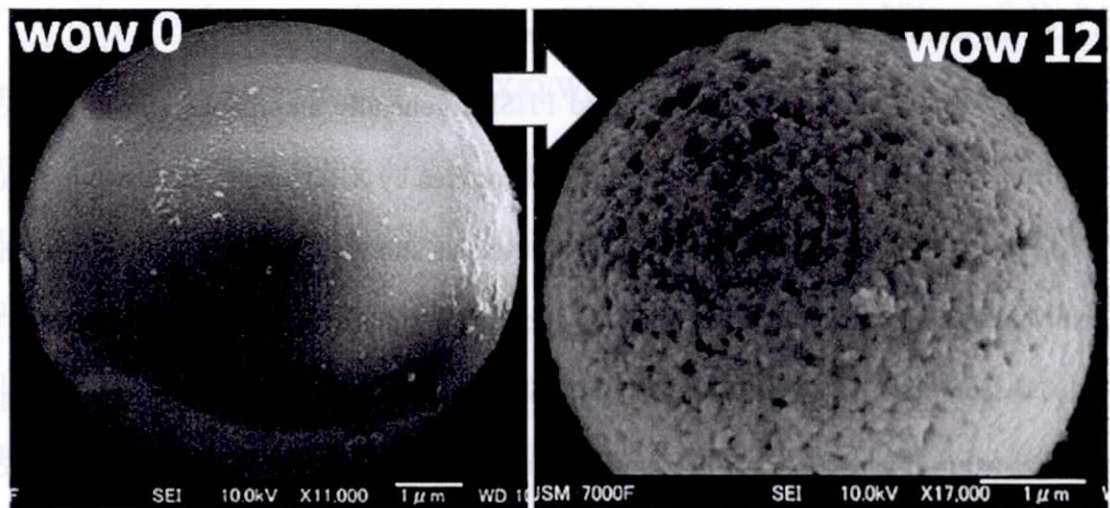


Figure 3.2.3 PSD graph with inset SEM images of calcined PSHM prepared by $W_1P-X/O/W_2$ at increasing Na-PA

3.2.3.2 Crystallographic and Thermal properties

Wherein shell walls of calcined PHSM, generally amorphous silicate network free from additive Na-PA (polymer) was clearly proven by XRD pattern as shown in Figure 3.2.4a [8, 17]. This also confirmed by TG analysis as shown in Figure 3.2.4b, all calcined PHSM showed less than 4 % weight loss, typical for sintered hollow silicate particles [4, 18]. The complete XRD pattern with TGDTA analysis of uncalcined and calcined sample can be seen in Figure 3.2S.9 which is compared. Obviously, TG/DTA analysis weight loss of uncalcined sample was greater compared to calcined samples.

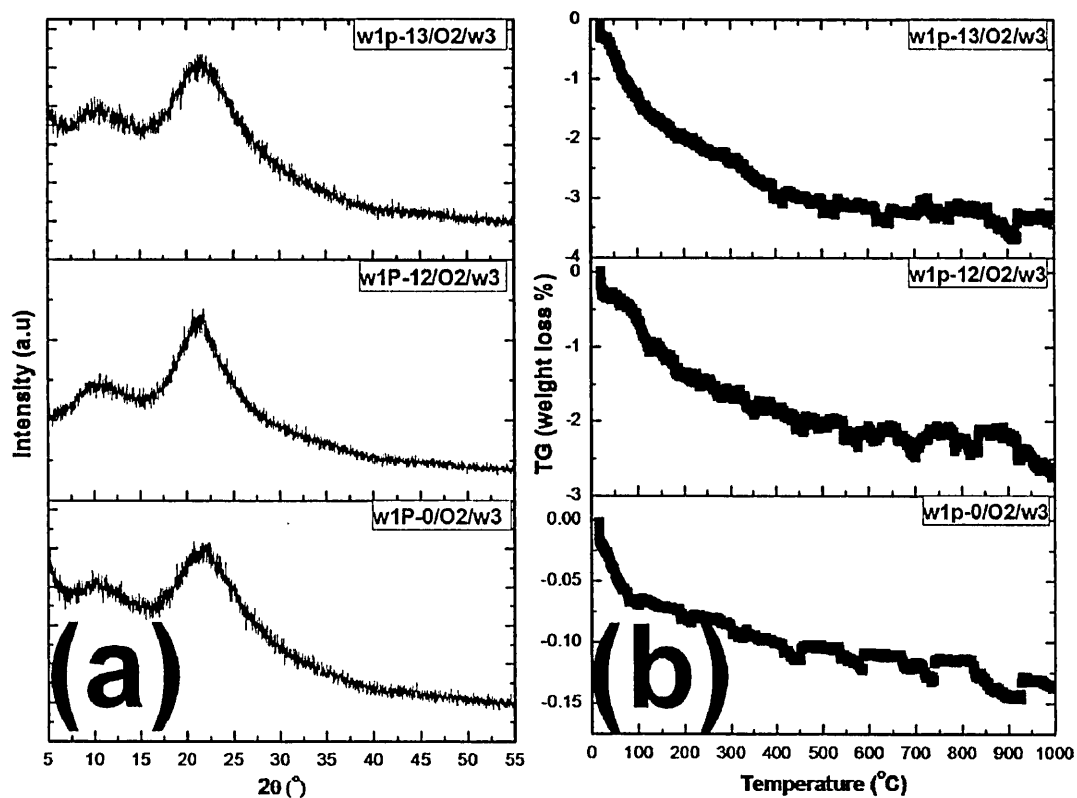


Figure 3.2. 4 (a) Amorphous XRD pattern and (b) TG traces calcined PHSM prepared by $W_1P-X/O/W_2$ method at increasing Na-PA

The weight loss and exothermic peaks increase as the addition of Na-PA concentration maximize onto the $W_1P-X/O/W_2$ solution proximately around ~30% at exothermic peaks temperature around 250-250°C to 350°C. This occurred due to the dissociation of remaining organic Na-PA molecules attached onto the silicate shell during emulsion process especially if uncalcined. But calcined and uncalcined both exhibited amorphous silicate phase. This signifies that washing during filtration was not enough to wash-off organic substances and calcination will enhance more silicate stability of the shell.

3.2.3.3 N_2 adsorption/desorption properties

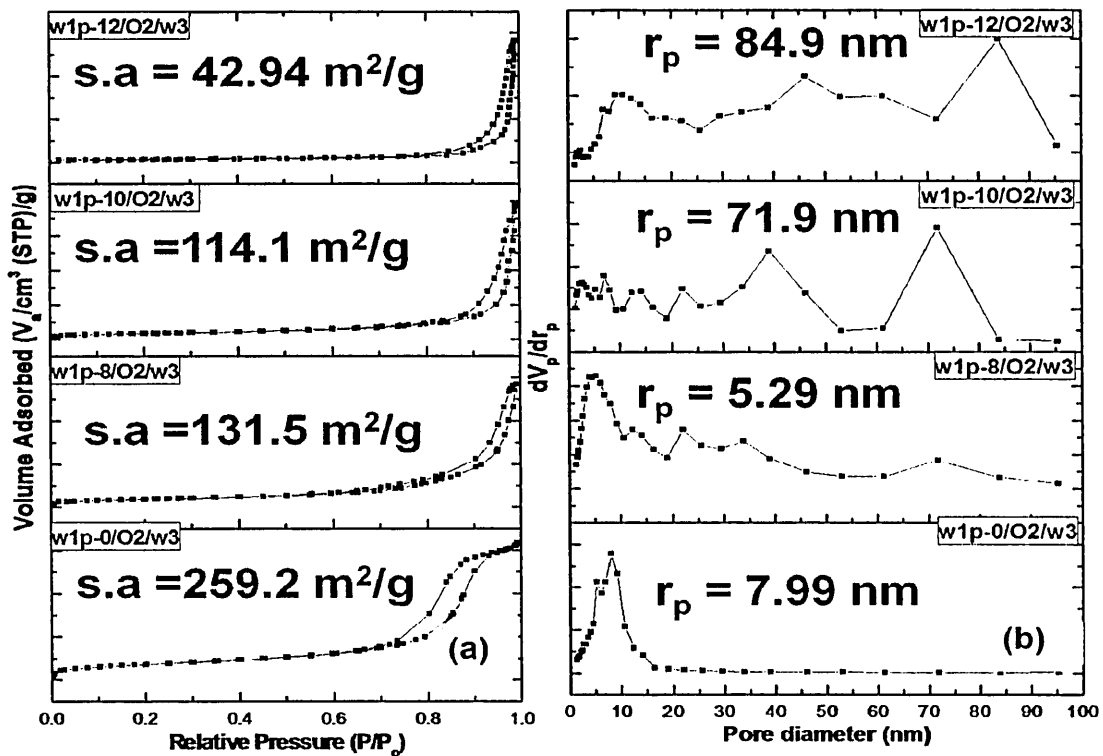


Figure 3.2. 5 (a) N_2 adsorption- desorption isotherms and (b) pore size distribution calculated by BJH method of calcined PHSM prepared by $W_1P-X/O/W_2$ method at increasing Na-PA

In Figure 3.2.5 (a and b), N_2 adsorption-desorption isotherms of calcined PSHM samples with increasing Na-PA (Fig. 3.2.5a) and BJH plots (Fig. 3.2.5b) were shown (type IV isotherm (IUPAC) [19]). These demonstrated a significant influence of Na-PA on the porosity properties of PSHM sample such as the relative pressure (P/P_0) in capillary condensation of N_2 shifted toward higher values from 0.6 to 0.9. In which the specific surface area (s.a), decreased remarkably from 259.2 m^2/g to 42.94 m^2/g and mesopore shell enlarged to macropore (r_p ; pore size distribution) estimated from 7.99 nm to 84.9 nm upon the addition of Na-PA. (Note: small surface area is associated with large pore diameters wherein the large flow rate is proportional to the fourth power of diameter. Hence in general, an inverse relationship between pore size and specific surface area can be attained[20]) This correlates with the SEM images (Fig.3.2.2b and Figure 3.2.3), macropore spaces greater than 100 nm were observed.

3.2.3.4 Probable mechanism for the formation of hierarchical porous hollow silicate micro-size spheres via double emulsion method

Detailed gradual formation and orientations of hierarchical mesoporous to macroporous structure into the shell wall were shown in Fig.3.2.2 (b) and Fig.3.2.3 (inset: SEM images of hierarchical porous surface) respectively. It is anticipated that hierarchical mesopore in $W_1P-0/O/W_2$ expanded to macro-holes as interspatial empty space between nanoparticles at the shell wall (see Fig.3.2.3 and 3.3.6) after addition of Na-PA (water-soluble polymer). These formations were also the same idea of some cage-like (diatom-like) particle [4, 7, 21, 22]. From these findings, scheme for the development of calcined PSHM with amorphous shells is illustrated in Figure 3.2.6. As illustrated, mixing

the W_1P-X and O along the interface of the $W_1P-X/O/W_2$ emulsion produced silicate matrices. At suitable amount of Na-PA (water-soluble polymer) present in the W_1P-X solution with silica nanoparticles are instantly produced at the interface (Fig 3.2.6 inset). Then silica nanoparticles along with Na-PA are aligned along the $W_1P-X/O/W_2$ interface forming amorphous network silicate shells; then filtered (N_2 pressure) /washed/dried to obtain dried white powder. Finally sintering the PHSM (completely removed water-soluble polymers) produced more steady silicate shell wall with hierarchical architecture. Detailed investigations on the effects of water-soluble other sodium-polymers on silicate solution and different sintering condition in inert gas are under investigation.

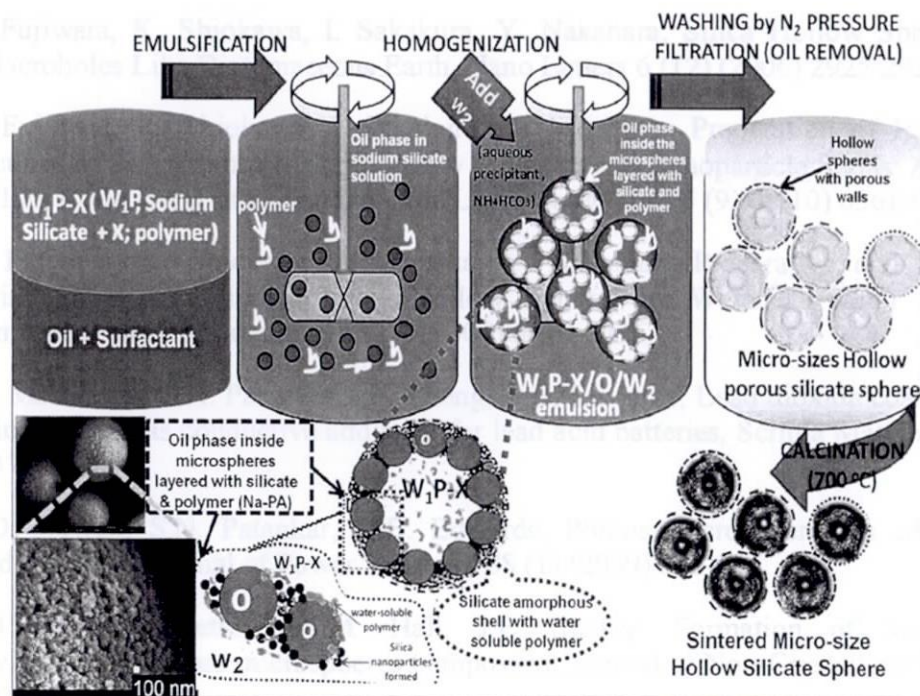


Figure 3.2.6 Conceptual scheme of the porous hollow silicate microsphere by $W_1P-X/O/W_2$ interfacial reaction upon addition of Na-PA and calcinations. Inset: SEM images of the hierarchical surface structure hollow microsphere particles ($W_1P-12/O/W_2$).

3.2.4 Conclusion

In summary, this section reported a faster route combining double emulsion with N_2 pressure filtration were developed for preparing calcined PHSM. The effect of addition of Na-PA (polymer) to sodium silicate solution (W_1P-X , inner water phase) of $W_1P-X/O/W_2$ emulsion produced macro-hole (r_p ; 84.9 nm) from the original mesopore (r_p ; 7.99 nm) shell wall of amorphous PHSM. We believe that this could be compatible for future controlled-release system especially with the inclusion/addition/functionalization of inorganic elements (electrode materials for lead batteries) and large variety of organic molecules.

References

- [1] F. Caruso, Hollow Capsule Processing through Colloidal Templating and Self-Assembly, *Chemistry – A European Journal* 6 (3) (2000) 413-419.
- [2] A.P.R. Johnston, B.J. Battersby, G.A. Lawrie, M. Trau, Porous functionalized silica particles: a potential platform for biomolecular screening, *Chemical Communication* (2005) 848-850.
- [3] W.H. Suh, A.R. Jang, Y.H. Suh, K.S. Suslick, Porous, Hollow, and Ball-in-Ball Metal Oxide Microspheres: Preparation, Endocytosis, and Cytotoxicity, *Advanced Materials* 18 (14) (2006) 1832-1837.
- [4] Y. Zhao, L. Jiang, Hollow Micro/Nanomaterials with Multilevel Interior Structures, *Advanced Materials* 21 (36) (2009) 3621-3638.
- [5] A.S. Angelatos, K. Katagiri, F. Caruso, Bioinspired colloidal systems via layer-by-layer assembly, *Soft Matter* 2 (1) (2006) 18-23.
- [6] M. Fujiwara, K. Shiokawa, I. Sakakura, Y. Nakahara, Silica Hollow Spheres with Nano-Macroholes Like Diatomaceous Earth, *Nano Letters* 6 (12) (2006) 2925-2928.
- [7] M. Fujiwara, K. Shiokawa, I. Sakakura, Y. Nakahara, Preparation of Hierarchical Architectures of Silica Particles with Hollow Structure and Nanoparticle Shells: A Material for the High Reflectivity of UV and Visible Light, *Langmuir* 26 (9) (2010) 6561-6567.
- [8] M. Fujiwara, K. Shiokawa, Y. Tanaka, Y. Nakahara, Preparation and Formation Mechanism of Silica Microcapsules (Hollow Sphere) by Water/Oil/Water Interfacial Reaction, *Chemistry of Materials* 16 (25) (2004) 5420-5426.
- [9] S.D. McAllister, S.N. Patankar, I.F. Cheng, D.B. Edwards, Lead dioxide coated hollow glass microspheres as conductive additives for lead acid batteries, *Scripta Materialia* 61 (4) (2009) 375-378.
- [10] J.D. Newell, S.N. Patankar, D.B. Edwards, Porous microspheres as additives in lead-acid batteries, *Journal of Power Sources* 188 (1) (2009) 292-295.
- [11] M.M. Ashton-Patton, M.M. Hall, J.E. Shelby, Formation of low density polyethylene/hollow glass microspheres composites, *Journal of Non-Crystalline Solids* 352 (6-7) (2006) 615-619.
- [12] L. Qi, Colloidal chemical approaches to inorganic micro- and nanostructures with controlled morphologies and patterns, *Coordination Chemistry Reviews* 254 (9-10) (2010) 1054-1071.

- [13] E. Pouget, E. Dujardin, A. Cavalier, A. Moreac, C. Valery, V. Marchi-Artzner, T. Weiss, A. Renault, M. Paternostre, F. Artzner, Hierarchical architectures by synergy between dynamical template self-assembly and biomineralization, *Nat Mater* 6 (6) (2007) 434-439.
- [14] K. Pays, J. Giermanska-Kahn, B. Pouligny, J. Bibette, F. Leal-Calderon, Double emulsions: how does release occur?, *Journal of Controlled Release* 79 (1-3) (2002) 193-205.
- [15] M.F. Ficheux, L. Bonakdar, F. Leal-Calderon, J. Bibette, Some Stability Criteria for Double Emulsions, *Langmuir* 14 (10) (1998) 2702-2706.
- [16] M.A. Aravand, M.A. Semsarzadeh, Particle Formation by Emulsion Inversion Method: Effect of the Stirring Speed on Inversion and Formation of Spherical Particles, *Macromolecular Symposia* 274 (1) (2008) 141-147.
- [17] D.S. Andreyev, E.A. Arriaga, Fabrication of perforated sub-micron silica shells, *Scripta Materialia* 57 (10) (2007) 957-959.
- [18] J.-A. Kim, J.-K. Suh, S.-Y. Jeong, J.-M. Lee, S.-K. Ryu, Hydration reaction in synthesis of crystalline-layered sodium silicate, *Journal of Industrial and Engineering Chemistry* 6 (4) (2000) 219-225.
- [19] K.S.W. Sing, Physisorption of nitrogen by porous materials, *Journal of Porous Materials* 2 (1995) 5-8.
- [20] M. du Plessis, Relationship between specific surface area and pore dimension of high porosity nanoporous silicon – Model and experiment, *physica status solidi (a)* 204 (7) (2007) 2319-2328.
- [21] C. Takai, T. Hotta, S. Shiozaki, Y. Boonsongrit, H. Abe, Unique porous microspheres with dense core and a porous layer prepared by a novel S/O/W emulsion technique, *Chemical Communications* (37) (2009) 5533-5535.
- [22] C. Takai, T. Hotta, S. Shiozaki, S. Matsumoto, T. Fukui, Key techniques to control porous microsphere morphology in S/O/W emulsion system, *Colloids and Surfaces A: Physicochemical and Engineering Aspects* 373 (1-3) (2011) 152-157.

CHAPTER 3.2

Supporting Information

FABRICATION OF CALCINED HIERARCHICAL POROUS HOLLOW SILICATE MICRO-SIZE SPHERES VIA DOUBLE EMULSION PROCESS

RESULTS:

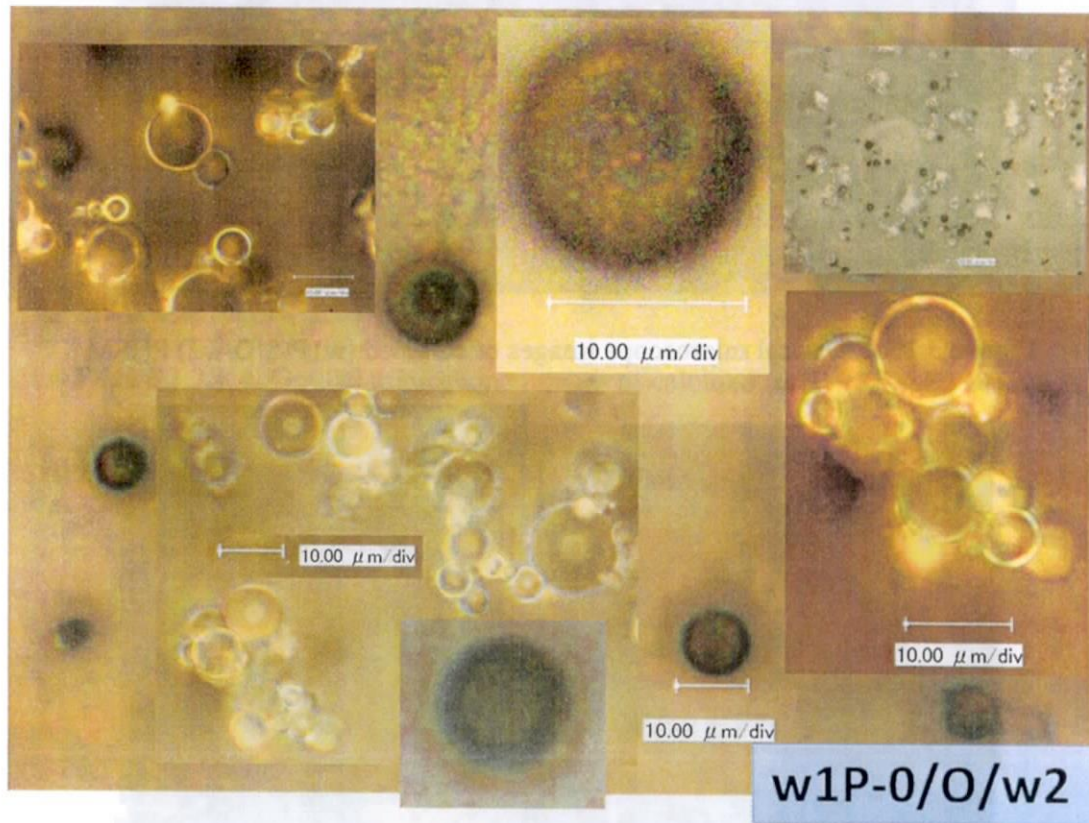


Figure 3.2S. 1 Optical microscope images of calcined (w1P-0/O/w2) PHSM

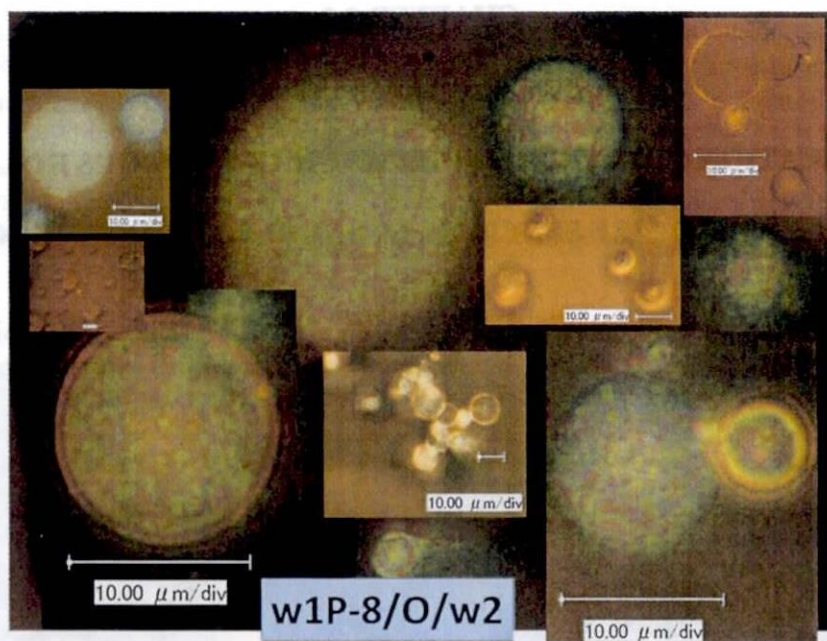


Figure 3.2S. 2 Optical microscope images of calcined (w1P-8/O/w2) PHSM

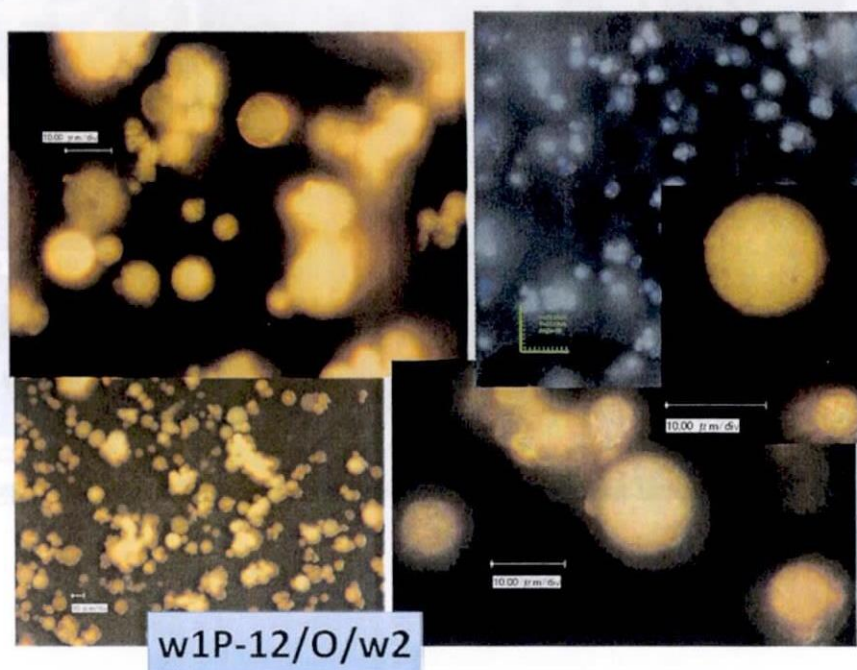


Figure 3.2S. 3 Optical microscope images of calcined (w1P-12/O/w2) PHSM

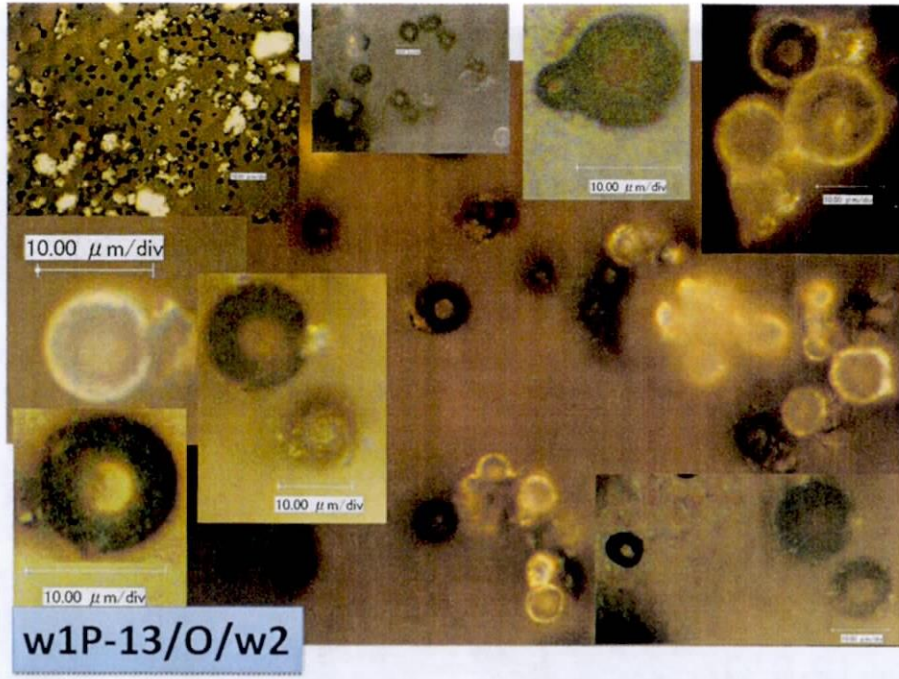


Figure 3.2S. 4. Optical microscope images of calcined (w1P-13/O/w2) PHSM

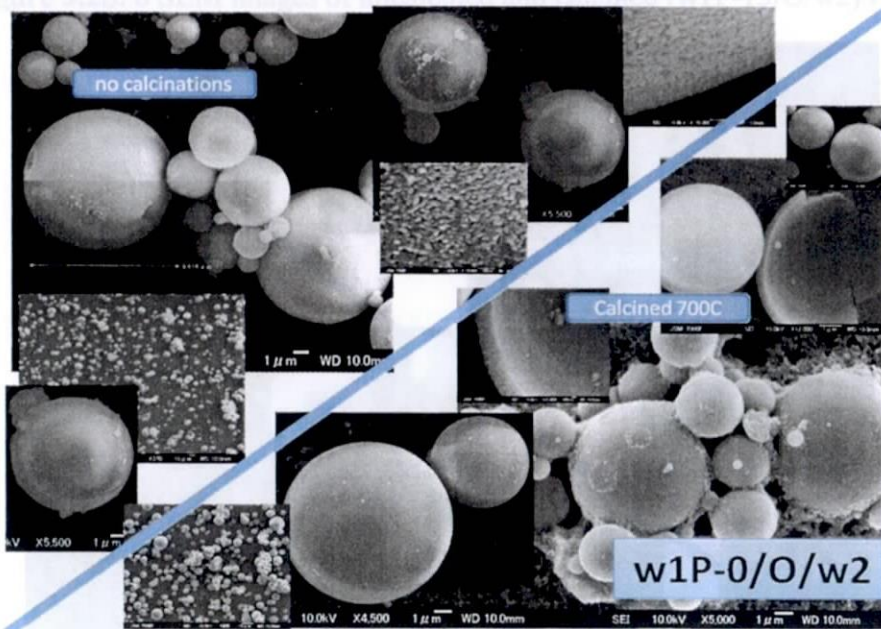


Figure 3.2S. 5 SEM images of uncalcined and calcined (w1P-0/O/w2) PHSM

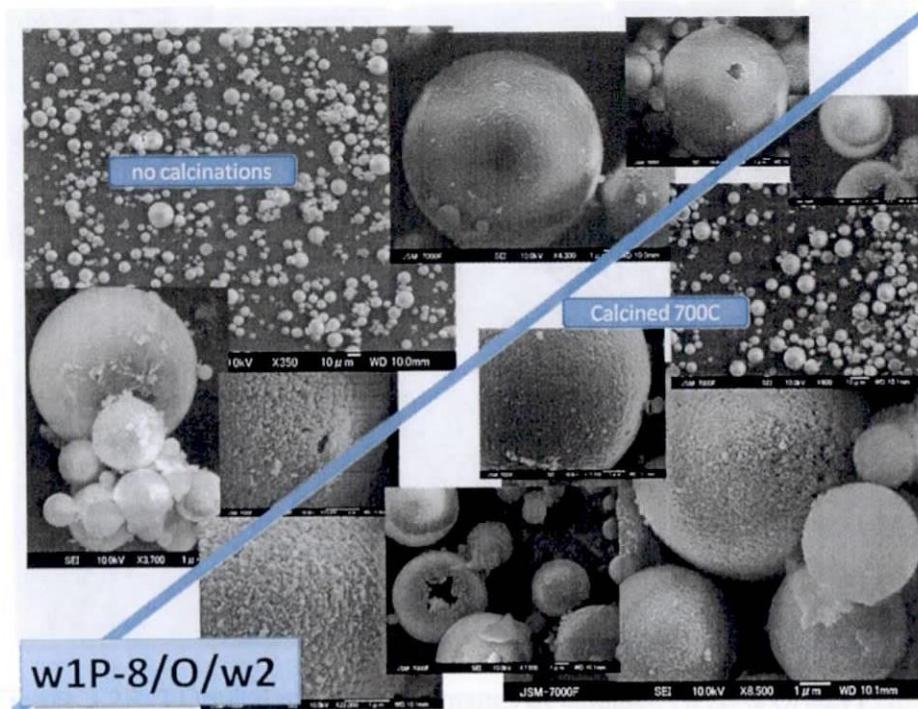


Figure 3.2S. 6 SEM images of uncalcined and calcined (w1P-8/O/w2) PHSM

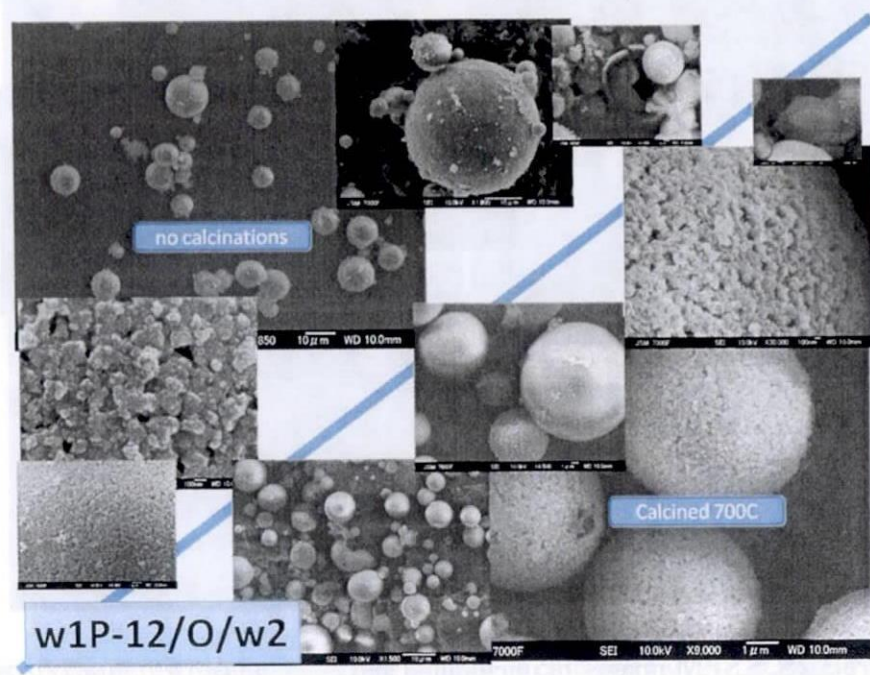


Figure 3.2S. 7 SEM images of uncalcined and calcined (w1P-12/O/w2) PHSM

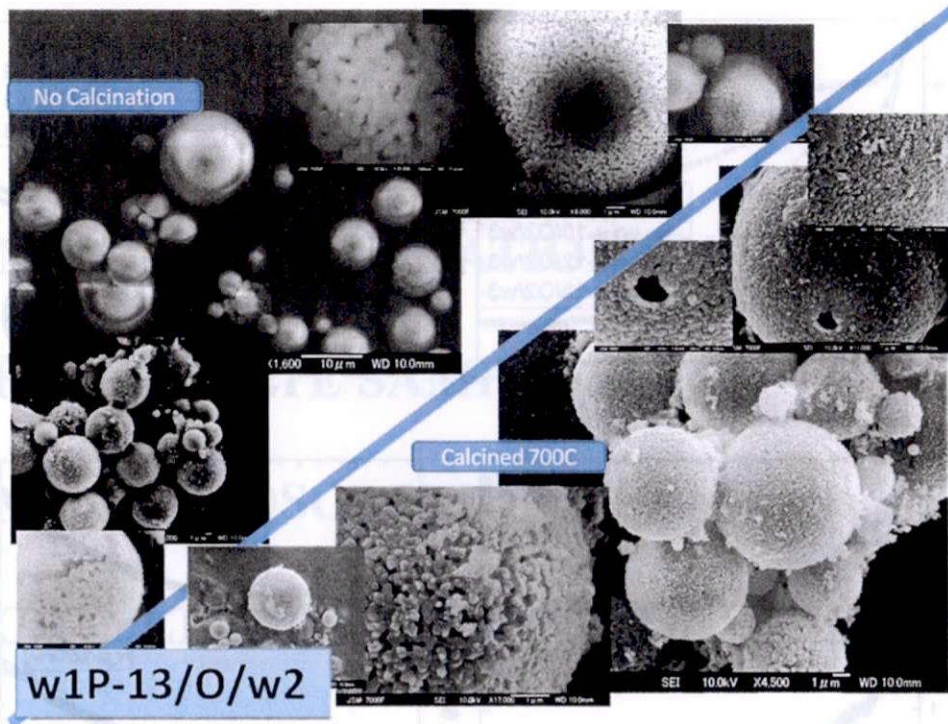


Figure 3.2S. 8 SEM images of uncalcined and calcined (w1P-13/O/w2) PHSM

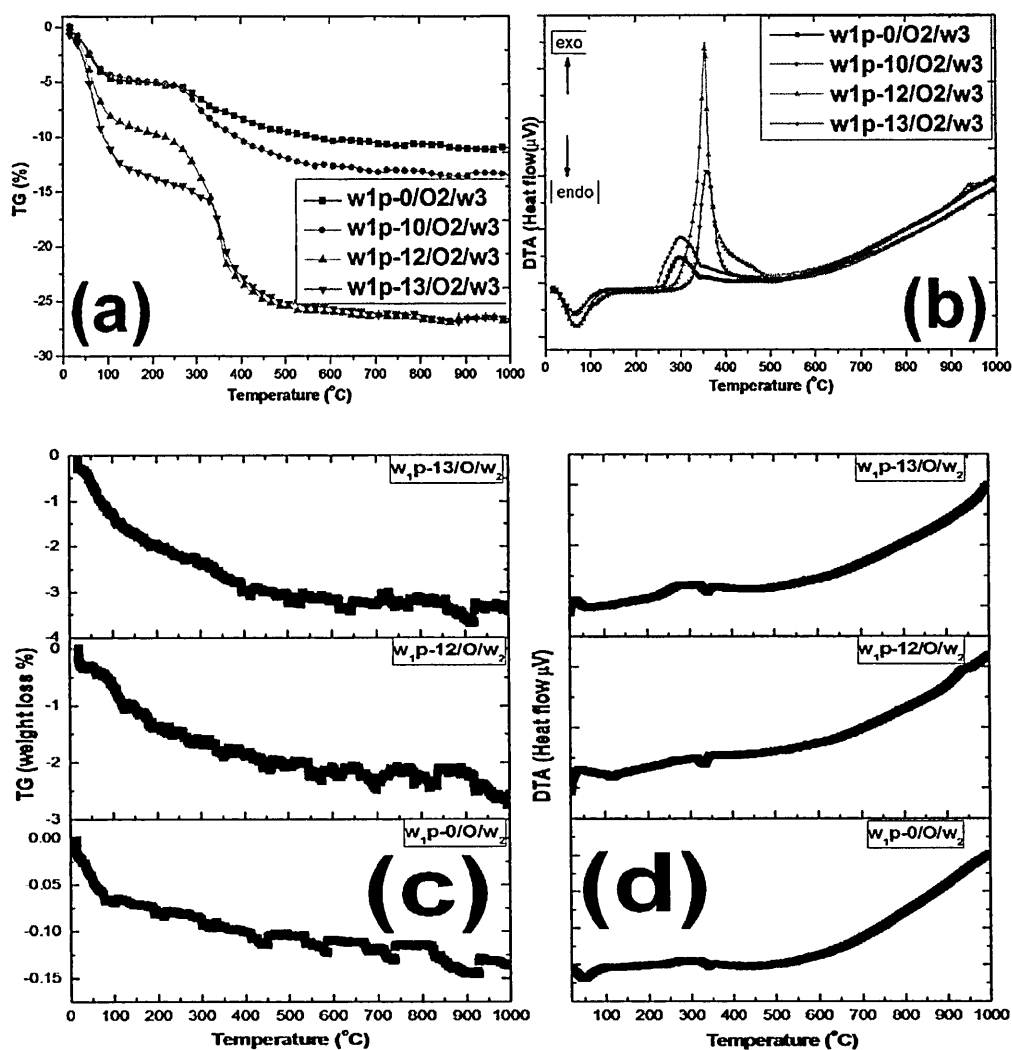


Figure 3.2S. 9 TG/DTA micrograph of uncalcined (a,b) and calcined (c,d) PHSM samples